

Electronic Theses and Dissertations, 2004-2019

2014

Performance Evaluation of Two Silt Fence Geosynthetic Fabrics During and After Rainfall Event

Gregg Dubinsky
University of Central Florida

 Part of the [Environmental Engineering Commons](#)
Find similar works at: <https://stars.library.ucf.edu/etd>
University of Central Florida Libraries <http://library.ucf.edu>

This Masters Thesis (Open Access) is brought to you for free and open access by STARS. It has been accepted for inclusion in Electronic Theses and Dissertations, 2004-2019 by an authorized administrator of STARS. For more information, please contact STARS@ucf.edu.

STARS Citation

Dubinsky, Gregg, "Performance Evaluation of Two Silt Fence Geosynthetic Fabrics During and After Rainfall Event" (2014). *Electronic Theses and Dissertations, 2004-2019*. 4715.
<https://stars.library.ucf.edu/etd/4715>

PERFORMANCE EVALUATION OF TWO SILT FENCE GEOSYNTHETIC FABRICS
DURING AND AFTER RAINFALL EVENT

by

GREGG STEVEN DUBINSKY, E.I.
B.S. University of Central Florida, 2012

A thesis submitted in partial fulfillment of the requirements
for the degree of Masters of Science in Environmental Engineering
in the Department of Civil, Environmental, Construction Engineering
in the College of Engineering & Computer Science
at the University of Central Florida
Orlando, Florida

Spring Term
2014

Major Professor: Manoj Chopra

© 2014 Gregg Steven Dubinsky

ABSTRACT

Silt fence is one of the most widely used perimeter control devices and is considered an industry standard for use in the control of sediment transport from construction sites. Numerous research studies have been conducted on the use of silt fence as a perimeter control, including a number of studies involving controlled laboratory flume tests and outdoor tests performed in the field on construction sites with actual monitored storm events. In field tests, due to the random and uncontrollable nature of real storm events and field conditions, studies have shown difficulty in evaluating silt fence performance. These field studies have shown the need for performance testing of silt fence in a more controlled environment, which can also simulate the actual use and performance in the field. This research, which is a continuation of ongoing research on silt fence fabrics at UCF Stormwater and Management Academy, was conducted in order to evaluate silt fence performance under simulated field conditions. Presented in this thesis are evaluation of two silt fence fabrics, a woven (ASR 1400) fabric and nonwoven (BSRF) fabric. Both fabrics were installed separately on a tilted test bed filled with a silty-sand soil and subjected to simulated rainfall.

Previous field studies on the performance of silt fence fabrics have evaluated the turbidity and sediment removal efficiencies only after the rain event, with the assumption that the efficiency values represent the true overall performance of silt fence. The results of this study revealed that the turbidity and suspended sediment performance efficiencies of silt fence were significantly affected by the time of sampling. The performance efficiencies during rainfall remained less than 55 percent, however, after the rainfall event ended, the performance efficiencies increased over time, reaching performance efficiency upwards of 90 percent. The

increase in efficiency after rainfall was due to the constant or decreasing ponding depth behind the silt fence, increased filtration due to fabric clogging, and sedimentation of suspended particles.

The nonwoven fabric was found to achieve higher removal efficiencies and flow-through rates both during and after the rain event when compared with the woven fabric. However, over the entire test duration (during and after rainfall combined), the projected overall efficiencies of both fabrics were similar. The projected overall average turbidity performance efficiencies of the woven and nonwoven silt fence fabrics was 80 and 78 percent, respectively. Both fabric types also achieved comparable overall average suspended sediment concentration efficiencies of 79 percent.

This result leads to the conclusion that silt fence performance in the field is dependent on three main processes: filtration efficiency occurring during the rain event, filtration and sedimentation efficiency occurring after the rainfall event, and flow-through rate of the silt fence fabrics. Decreases in the flow-through rate lead to increases in the overall efficiency. This thesis quantifies the different mechanisms by which these processes contribute to the overall efficiency of the silt fence system and shows how these processes are affected by different conditions such as the degree of embankment slope and rainfall intensity.

Dedicated to my family and friends, in memory of my father, Leon

ACKNOWLEDGMENTS

The author would like to express his gratefulness to his major advisor Dr. Manoj Chopra for his encouragement and overall guidance throughout his graduate education at the University of Central Florida. In addition, he would also like to thank Dr. Ikiensinma Gogo-Abite for his contribution to the research through helpful discussion and advice and for serving on his graduate thesis committee. The author further extends gratitude to Dr. Andrew Randall and Dr. Dingbao Wang for also serving on his graduate thesis committee.

The author would like to express thanks to the staff and students of the Stormwater Management Academy. In particular, he would like to thank Mike Hardin, Christopher Hickson, Mario Samson, and Sean Ram.

TABLE OF CONTENTS

LIST OF FIGURES	ix
LIST OF TABLES	xi
ABBREVIATIONS	xiii
CHAPTER 1: INTRODUCTION	15
Problem Statement.....	15
Objective.....	17
Thesis Organization	18
CHAPTER 2: LITERATURE REVIEW	20
Introduction.....	20
Geotextile Characterization	22
Geotextile Index Testing.....	22
Sediment Removal Mechanisms of Silt Fence	25
Sedimentation Theory.....	25
Filtering Theory	28
Previous Silt Fence Research.....	32
Flume Studies.....	32
Field Testing	34
Bench Scale Testing.....	35
Field Scale Testing.....	36
Summary.....	37
CHAPTER 3: METHODOLOGY	39
Introduction.....	39
Soil Characteristics	39
Soil Classification and Particle Size Distribution.....	39
Proctor (Laboratory) Compaction Test.....	42
Permeability Test	43
Silt Fence Geotextiles	43
Test Bed Preparation and Setup.....	46
Field Scale Testing Procedure	50
Limitations of Field Scale Testing.....	54
CHAPTER 4: RESULTS AND DISCUSSION.....	55
Introduction.....	55
Fabric Performance during Rain Events.....	59
Fabric Reduction Efficiency during Rain Events	59
Flow-through rate during the Rain Event	73
Silt Fence Failure	85
Fabric Performance following Rain Events.....	88
Fabric Reduction Efficiency following Rain Events	88
Flow-through rate after the Rainfall Event	99
Overall Performance Efficiency (Collected): Both During and After Rain events	103
Overall Performance Efficiency (Projected).....	110
CHAPTER 5: CONCLUSION	119

APPENDIX A: ANALYSES OF SOIL TESTING	122
Soil Particle Distribution	123
Compaction Testing.....	124
Constant Head Permeability Testing	126
APPENDIX B: STATISTICAL ANALYSES OF PERFORMANCE EFFICIENCY	127
Statistical Difference between Initial and Repeat Tests	128
Statistical Analysis of woven fabric performance efficiency verse nonwoven fabric performance efficiency	129
Performance Efficiency Based on Embankment Slope	131
Performance Efficiency Change of Test 1 to Test 2	132
Change in Efficiency from During Rainfall to After Rainfall	134
APPENDIX C: STATISTICAL ANALYSES OF FLOW-THROUGH RATE	135
Change in Flow Through Rate with Change in Embankment Slope	136
Change in Flow Through Rate from Test 1 to Test 2	137
Change in Flow-Through Rate due to Change in Rainfall Intensity	138
Change in Flow Through Rate from During Rainfall to After Rainfall	139
APPENDIX D: MISCELLANEOUS	140
Time Dependent Efficiency and Flow Rate Results	141
Change in Performance Efficiency and Discharge Concentration with Time	152
LIST OF REFERENCES	155

LIST OF FIGURES

Figure 1 Mechanism of particle accumulation: (a) All pipes are opened (series filtration), (b) Few pipes are obstructed (series and parallel filtration), (c) Filter cake formation above completely obstructed pipes (Faure et al. 2006)	29
Figure 2 Particle size distribution curve	41
Figure 3 Woven (ASR 1400) silt fence installed on a tilted test bed (Gogo-Abite 2012) ...	44
Figure 4 Nonwoven (BSRF) silt fence installed on a tilted test bed	45
Figure 5 Pictures of test bed modifications (a) plywood for depth, and (b) visqueen to protect plywood (Gogo-Abite 2012).....	47
Figure 6 Test bed setup (a) woven fabric, rain gages, and meter stick installed, (b) test bed compaction, (c) rainfall simulator and tilted test bed with nonwoven fabric installed	49
Figure 7 Sample field test matrix for 10 percent slope (repeated for 33 and 10 percent slopes).....	50
Figure 8 Field scale testing: Downstream collection system.....	52
Figure 9 Woven fabric volume-weighted mean turbidity performance efficiency with embankment slope	65
Figure 10 Woven fabric volume-weighted mean SSC performance efficiency with embankment slope	65
Figure 11 Nonwoven fabric volume-weighted mean turbidity performance efficiency with embankment slope	67
Figure 12 Nonwoven fabric volume-weighted mean SSC performance efficiency with embankment slope	67
Figure 13 Trend of decreasing flow-through rate with increasing upstream SSC for both woven and nonwoven fabrics	77
Figure 14 Nonwoven fabric change in flow rate with change in ponding depth between Test 1 and Test 2 on a 33 percent slope	81
Figure 15 Filter cake formation on nonwoven (a) untested fabric (b) cake formation after completion of Test 1 (c) cake formation after completion of Test 2	83
Figure 16 Silt fence failures: (a) pullout of fabric from middle stake on 33% slope (b) overtopping on 33% slope (c) corner stake failure on 33% slope (d) corner stake tear on 25% slope	86
Figure 17 Time dependent average turbidity reduction efficiency and downstream value on 10 percent slope	94
Figure 18 Woven fabric time dependent efficiency values and ponding depth on 25 percent slope and 25 mm/h rainfall intensity	96
Figure 19 Conceptual example of how the concentration gradient in ponding volume may change over time after rainfall ends	98
Figure 22 Maximum dry unit weight of silty-sand soil	124
Figure 23 Time dependent average turbidity performance efficiency and downstream value on 25 percent slope.....	152
Figure 24 Time dependent average turbidity performance efficiency and downstream value on 33 percent slope.....	153

Figure 25 Time dependent average SSC performance efficiency and downstream value on 10 percent slope.....	153
Figure 26 Time dependent average SSC performance efficiency and downstream value on 25 percent slope.....	154
Figure 27 Time dependent average SSC performance efficiency and downstream value on 33 percent slope.....	154

LIST OF TABLES

Table 1 ASTM Specifications for Silt Fence Fabrics	23
Table 2 Summary of soil particle classification analyses	40
Table 3 Comparison of woven and nonwoven fabrics.....	45
Table 4 Woven fabric test volume-weighted mean turbidity and SSC results during the rain event.....	61
Table 5 Nonwoven fabric test volume-weighted mean turbidity and SSC results during the rain event.....	62
Table 6 Woven fabric turbidity and SCC performance efficiency from Test 1 to Test 2	70
Table 7 Nonwoven fabric turbidity and SSC performance efficiency from Test 1 to Test 2	72
Table 8 Summary results for flow-through rate of woven and nonwoven fabrics during the rain event.....	74
Table 9 Average flow-through rate occurring during the rain event between Test 1 and Test 2 for both woven and nonwoven fabrics	79
Table 10 Woven fabric test volume-weighted mean turbidity and SSC results after the rain event.....	90
Table 11 Nonwoven fabric test volume-weighted mean turbidity and SSC results after the rain event.....	91
Table 12 Average flow-through rates during and after rain events	100
Table 13 Estimated average hydraulic detention time of the ponding volume	101
Table 14 Overall performance efficiency of woven silt fence (collected samples)	105
Table 15 Overall performance efficiency of nonwoven silt fence (collected samples)	106
Table 16 Summary of volume-weighted mean turbidity and SCC performance efficiency	108
Table 18 Projected overall woven fabric performance efficiency	112
Table 19 Projected overall nonwoven fabric performance efficiency	113
Table 20 Summary of overall projected performance efficiency	115
Table 21 Discharge water volume both during and after rainfall	117
Table 22 Materials finer than 75- μ m by washing analysis	123
Table 23 Sieve analysis.....	123
Table 24 Hydrometer analysis	123
Table 25 Maximum dry unit weight for silty-sand	125
Table 26 Silty-sand soil permeability	126
Table 27 Wilcoxon rank sum test: Woven fabric significant p-values between initial and repeat tests.....	128
Table 28 Wilcoxon rank sum test: Nonwoven fabric significant p-values between initial and repeat tests.....	128
Table 29 Wilcoxon rank sum test: Significant p-values for nonwoven fabric having greater performance efficiency than woven fabric during the rain event	129
Table 30 Wilcoxon rank sum test: Significant p-values for nonwoven fabric having greater performance efficiency than woven fabric after the rain event.....	129

Table 31 Wilcoxon rank sum test: Significant p-values for nonwoven fabric having an overall greater performance efficiency than woven fabric.....	129
Table 32 Wilcoxon rank sum test: Significant p-values for woven and nonwoven fabric having significantly different projected overall performance efficiency.....	130
Table 33 Single factor ANOVA: Woven fabric statistical difference of volume-weighted mean efficiency between different slopes	131
Table 34 Single Factor ANOVA: Nonwoven fabric statistical difference of volume-weighted mean efficiency between different slopes	131
Table 35 Wilcoxon rank sum test: Woven fabric statistical difference of turbidity performance efficiency between Test 1 and Test 2.....	132
Table 36 Wilcoxon rank sum test: Woven fabric statistical difference of sediment performance efficiency between Test 1 and Test 2.....	132
Table 37 Wilcoxon rank sum test: Nonwoven fabric statistical difference of turbidity performance efficiency between Test 1 and Test 2.....	133
Table 38 Wilcoxon rank sum test: Nonwoven fabric statistical difference of sediment performance efficiency between Test 1 and Test 2.....	133
Table 39 Wilcoxon rank sum test: Woven fabric statistical difference of performance efficiency during and after rainfall	134
Table 40 Wilcoxon rank sum test: Nonwoven fabric statistical difference of performance efficiency from during rainfall to after rainfall	134
Table 41 Wilcoxon rank sum test: Woven fabric statistical difference for flow through rate between slopes	136
Table 42 Wilcoxon rank sum test: Nonwoven fabric statistical difference for flow through rate between slopes	136
Table 43 Wilcoxon rank sum test: Statistical difference of flow-through rate between Test 1 and Test 2.....	137
Table 44 Single factor ANOVA: Woven fabric statistical difference of flow-through rate based on different rainfall intensities	138
Table 45 Single factor ANOVA: Nonwoven fabric statistical difference of flow through rate based on different rainfall intensities	138
Table 46 Wilcoxon rank sum test: Statistical difference of flow through rate between during and after the rain event.....	139
Table 47 Woven fabric time dependent efficiency and flow-through rate results on 10% slope	141
Table 48 Woven fabric time dependent efficiency and flow-through rate results on 25% slope	143
Table 49 Woven fabric time dependent efficiency and flow-through rate results on 33% slope	144
Table 50 Nonwoven fabric time dependent efficiency and flow-through rate results on 10% slope	146
Table 51 Nonwoven fabric time dependent efficiency and flow-through rate results on 25% slope	148
Table 52 Nonwoven fabric time dependent efficiency and flow-through rate results on 33% slope	150

ABBREVIATIONS

AOS = apparent opening size (mm)
AR = after rainfall
 b_{TB} = test bed width (m)
 d_p = particle diameter (m)
DR = during rainfall
E = efficiency (%)
EFF = effluent
g = gravitational constant (m/s^2)
INF = influent
K = hydraulic conductivity (cm/s)
mg/L = milligrams per liter
 n = number of samples taken during the rain event
NTU = nephelometric turbidity unit
 m = number of samples taken after the rain event
PD = ponding depth at face of silt fence (cm)
 q = flow-through rate of silt fence ($L/m^2/h$)
S = embankment slope (%)
SSC = suspended sediment concentration (mg/L)
 t = time (h)
T = turbidity (NTU)
TS = total solids (mg/L)
V = volume of water (L)
 v_c = critical settling velocity (cm/min)
 v_s = particle settling velocity (m/s)
WMEC = weighted mean influent concentration (mg/L)
WMET = weighted mean effluent turbidity (NTU)
WMIC = weighted mean influent concentration (mg/L)
WMIT = weighted mean influent turbidity (NTU)
 ρ = density (kg/m^3)
 τ = hydraulic detention time (min)

μ = dynamic viscosity (kg/m/s)

CHAPTER 1: INTRODUCTION

Problem Statement

According to the United States Environmental Protection Agency (USEPA 2012), soil erosion is the largest contributor to nonpoint source pollution in the United States. It is estimated that over 4 billion tons of sediment are discharged into ponds, rivers, and lakes in the United States each year and approximately 10 percent of this amount is due to erosion occurring from land undergoing construction activities or land development (FDEP 2008). Eroded sediment can cause a number of environmental and economic problems. Eroded sediments that carry nutrients such as phosphorus and nitrogen can lead to the development of algal blooms and lake eutrophication. If the eroded sediments are small and remain suspended in the water body, they can block sunlight from penetrating the water body, disrupting photosynthesis. If, however, the eroded sediments are large, they may settle to the bottom of the water body, reducing its storage capacity and possibly increasing its flood frequency (Harbor 1999).

On construction sites, the erosion rate and the potential for sediment discharge are greatest during the active construction phase of the project (Owens et al. 2000). Active construction causes increase in the erosion rates when compared to the pre- and post-construction conditions due to the loss of protective vegetative cover. Due to large erosion rates during active construction, the soil loss from these sites over even a short period can rival losses that would have taken decades to erode naturally (EPA 2007). For this reason it is important to limit the sediment load that has the potential to be discharged from the construction site during the active phase. A number of technologies including both erosion and perimeter control are

used for this purpose. However, silt fence in particular, is considered an industry standard for use on construction sites (Faucette et al. 2008)

Numerous research studies have been conducted on the use of silt fence as a perimeter sediment control. Majority of studies involve controlled laboratory flume tests (Britton et al. 2000, Farias et al. 2006, Risse et al. 2008) and outdoor tests performed in the field on construction sites with real monitored storm events (Barrett et al. 1995, Faucette et al. 2008). Although flume studies have shown that silt fence performs well in removing sediment from concentrated flows, these tests do not correctly simulate the field conditions of the use and performance of silt fence. In the field, the composition of the eroded soil is different from the parent soil and will contain more silt and less sand particles due to the higher erosion rate of these particles in comparison to sand particles (FDEP 2008). Rainfall collision with the ponding volume upstream of the silt fence will also disrupt settling within the pond during rainfall. These difference between the flume tests and actual field conditions lead to an overestimation of the silt fence performance.

The field studies evaluated the discharge concentration through the silt fence by comparing either to the known erosion rate of the soil or to the upstream concentration in the ponding volume after the rain event. Evaluating silt fence on a time dependent basis during rainfall however is not possible during these tests. For this reason, and due to the random and uncontrollable nature of real storm events and field conditions, it has been difficult to evaluate silt fence performance in the field. Both flume and field studies have shown the need to further evaluate silt fence in conditions which cannot only simulate the actual use and performance of silt fence in the field but can do so in a controlled environment.

Objective

The research presented in this thesis has been conducted in order to evaluate silt fence performance under varying field conditions. The study was performed on a tilted test bed filled with a silty-sand soil (AASHTO classification type A-2-4) set to different degrees of slope and subjected to varying intensities of simulated rainfall. The research is a continuation of previous research project conducted by Gogo-Abite and Chopra (2013) at UCF Stormwater Laboratory. Performance evaluation was completed on two silt fence fabrics, a woven (ASR 1400) fabric and a nonwoven (BSRF) fabric. These silt fence fabrics were installed separately on the tilted test bed and subjected to simulated rainfall events of 27, 76, and 127 mm/h (1, 3, 5 in/h) and to differing embankment slopes of 10, 25, and 33 percent.

The objective of this study is to evaluate the performance of both silt fence fabrics under field conditions and to quantify the turbidity and suspended solids performance efficiency as well as the flow-through rates of the fabrics under different embankment slope and rainfall intensity. Additional objective will also be to compare the performance of both silt fence fabrics. The woven fabric used in this study is the traditional monofilament geosynthetic typically used on construction sites. Previous studies on this fence have shown its inability to achieve required water quality performance targets (Barrett et al. 1995, Faucette et al. 2008, Gogo-Abite and Chopra 2013). The nonwoven fabric was designed to reduce turbidity and suspended solids and permit a greater flow-through rate of the fabric than the traditional woven monofilament silt fence (Risse et al. 2008). The performance efficiency of the nonwoven fabric should be greater than the woven fabric due to the pore sizes of both fabrics. Previous studies by Gogo-Abite and Chopra (2013) show that the apparent opening sizes (AOS) of the woven and nonwoven fabrics

are 0.70 mm and 0.21 mm, respectively. This thesis aims to study if the difference in AOS between the silt fence materials causes a significant difference in the performance efficiency. It is also of interest to see if any removal occurs by filtration at all with the woven fabric, as the AOS of this fabric is actually larger than 100 percent of the soil particle sizes used in the study.

The study further seeks to evaluate silt fence on a time dependent basis and determine if a difference in performance exists between removal encountered during and after rainfall. It will be interesting to see if changes in the embankment slope and rainfall intensity affect the removal mechanisms occurring for each of these processes over the entire duration of treatment.

Thesis Organization

The research was conducted in order to investigate the performance of silt fence materials under field scale conditions and to quantify the differences in performance occurring both during and after rainfall events. In order to present the research, an introduction is presented in Chapter 1 that discusses the significance of the study, objectives of the research, and the thesis organization.

Provided in Chapter 2 is a review of literature related to silt fence. The review discusses index properties of geotextiles that are relevant to silt fence, the theory that forms the basis for the types of filtration and sedimentation that occurs in silt fence treatment, and a review of previous flume, field, bench-scale, and field-scale studies that have been completed on silt fence.

After the literature review, the methodology is discussed in Chapter 3. In this chapter, details of the properties of the soil type, the properties of the silt fence, the field scale testing procedure, and the limitations of this testing procedure are presented.

Following the methodology, the results of the field scale performance testing of silt fence fabrics is presented in Chapter 4. The chapter is divided into three main sections; discussions on the performance evaluation of silt fence during the rain event, after the rain event, and over the entire duration of treatment.

The fifth and final chapter presents summary, conclusions, and recommendations of the field scale results of the study.

CHAPTER 2: LITERATURE REVIEW

Introduction

Erosion and soil losses from unprotected construction sites are one of the leading sources of sediments found in water bodies across the U.S. (Hayes et al. 2005). Due to the natural vegetative cover being removed from the soil, it is not uncommon for these sites to have soil erosion rates as high as 2 to 40,000 times greater than the preconstruction conditions (Harbor 1999). The increase in erosion has led to approximately 80 million tons per year of sediment being deposited to lakes, rivers and waterways in the United States due in part to inadequate preventive measures during the construction phase (Harbor 1999).

To control sediment transfer from construction sites, the prevention of erosion should be the primary focus. The common erosion control practices are temporary seeding, mulching, geotextile matting, chemical stabilization, and many other erosion control practices (USEPA 2011). These practices are the first line of defense in controlling sediment detachment from the exposed soil in construction sites by preventing erosion. The last line of defense in controlling sediment emissions from leaving the construction site are perimeter controls. These devices are used on the perimeters of construction sites and are used to intercept concentrated runoff water and remove its sediment. Thus, retaining the sediments on site and keeping them from entering offsite areas such as water bodies, roadways, and storm drains. Some of the sediment control measures include silt fence, filter socks, temporary diversion berms, temporary fill diversions, temporary slope drains, and floating turbidity barriers (FDEP 2008).

Of the perimeter control devices, silt fence is considered the current industry standard for perimeter control on construction sites (Faucette et al. 2008). Silt fence is defined as, “a temporary sediment barrier consisting of a filter fabric stretched across and attached to supporting posts and entrenched” (FDEP 2008). The supporting posts are usually made of wood, at least 2.5 x 5.0 centimeter (1 x 2 inch) in cross sectional area, and are a minimum of 0.9 meter (3 feet) in length. The posts are buried a minimum of 0.3 meter (1 foot) into the ground, but they may not exceed 0.9 meter (3 feet) in height above the surface. This maximum height requirement is because larger fence heights may cause the silt fence to impound a volume of water great enough to cause the stakes to fail. The stake posts are then installed at a maximum of 3 meter (10 feet) apart if the fence is used without a wire support. If no wire support is used, then the stakes are spaced a maximum of 1.8 meter (6 feet) apart.

In most cases, silt fence is installed around the perimeter of the construction site so that it can intercept all runoff water which has the potential to flow off of the site. The silt fence works by first acting as a physical barrier that reduces the velocity of the runoff water. Then, depending on the type of silt fence geotextile and the soil characteristics, the silt fence filters the sediment from the concentrated runoff water. As the silt fence starts to filter the sediment, the particles begin to clog the fabric, decreasing the ability of the silt fence to transmit water. When the flow-through rate of the silt fence starts to decrease, the runoff water starts to pond upstream of the silt fence, creating a ponding volume of accumulated runoff. Then, depending on the flow-through rate of the fabric, the suspended particles within the ponding volume may settle out of suspension before the water is discharged through silt fence. Thus, silt fence removes

sediment by two mechanisms, filtration through the fabric and sedimentation of suspended particles.

The remainder of this literature review discusses the types and properties of geotextiles used in silt fence applications, the theory of the sediment removal mechanisms of silt fence, and previous research which has been completed on silt fence.

Geotextile Characterization

ASTM (1987) defines geotextile as “any permeable textile used with foundation, soil, rock, or any other geotechnical engineering related material as an integral part of a manmade product, structure, or system.” Silt fence therefore qualifies as a geotextile. These permeable textiles can be categorized as either woven or nonwoven. The woven geotextiles have relatively uniform rectangular openings and are manufactured by weaving synthetic fibers into flexible and porous fabrics (Koerner 2012). The fibers are interwoven perpendicular to each other; the horizontal elements are referred to as weft fibers and the longitudinal elements are referred to as warp fibers (Zhang et al. 2013). Unlike woven fabrics, which have relatively uniform openings, the pore structure and morphology of nonwoven geotextiles can be highly complex (Rawal and Saraswat 2011). These geotextiles are manufactured by needle punching or melt bonding (Lamy et al. 2013) with their fibers oriented in multidirectional and random arrangements (Fisher and Jarrett 1984).

Geotextile Index Testing

With the broad use of silt fence geotextiles in the industry, it is necessary to determine the properties of individual fabrics in reference to other fabrics and to recommended values. In

this regard ASTM D6461 (2007) has provided a list of current standard test methods in order to determine the index properties of silt fence fabrics. These index properties which are of interest in silt fence are: grab-tensile strength, ultraviolet (UV) stability, apparent opening size (AOS), and fabric permittivity. The recommended specifications for these index properties for silt fence are listed in Table 1. The details of these tests were not discussed in this thesis, however, a brief discussion of how these parameters affect silt fence performance in the field is discussed below.

TABLE 1 ASTM SPECIFICATIONS FOR SILT FENCE FABRICS

Property	Direction	ASTM Test Methods	Units	ASTM D6461
Grab strength	Machine	D 4632	N	400
	X-Machine			400
Permittivity		D 4491	sec ⁻¹	0.05
AOS		D 451	mm	0.6
Ultraviolet stability		D 4355	% Retained strength	70% after 500 h of exposure

Permittivity is an indicator of the amount of water that can pass through a geotextile and is defined as the “volumetric flow rate of water per unit cross sectional area per unit head under laminar flow conditions, in the normal direction through a geotextile” (ASTM D4491 2009). Permittivity has been shown to be a good indicator of the clogging potential for nonwoven geotextiles where less clogging of the geotextile is observed with increasing permittivity (Aydilek and Edil 2003). However, permittivity is not a good indicator of the potential flow-through rate of the geotextile that will be encountered in the field (Weggel and Ward 2012). In the field, the permittivity of silt fence has been shown to decrease due to the impingement of sediment on the fabric.

The AOS of the fabric is a measure of the largest pore sizes of the fabric. AOS is found by running beads of a certain diameter through the fabric; and the AOS is the bead size for which 5% or less of the beads pass through. AOS may give an indication of the particle size that can be removed through filtration by the fabric. However in the field, pressure brought on by ponding water induces tensile strain on the silt fence that can result in larger pore openings (Gogo-Abite and Chopra 2013). Since AOS has been shown to have a proportional linear relationship to tensile strain (Wu et al. 2008), AOS may not give an accurate representation of the sediment removal potential of silt fence fabrics in the field.

UV stability is a very important property for silt fence. It is not uncommon for silt fence to remain on construction sites for long periods of time. Sunlight has been shown to be a dominant degradation factor for many geotextiles (Suits and Hsuan 2003), and as such, solar radiation has the potential to degrade silt fence, reducing its ability to function properly. Solar radiation, in the form of photons, has energies, which range from 300 to 390 kJ/mol. Making them sufficiently strong enough to degrade polymer carbon (C-C) and hydrogen (C-H) bonds of the silt fence fabric, which range from 340 to 420 kJ/mol (Suits and Hsuan 2003). For this reason, UV stabilizers are added to protect polymers and prolong their lifetimes when they are used in exposed applications. In silt fence, ultraviolet ray inhibitors and stabilizers are used, and must be designed to provide a minimum of 6 months solar radiation protection (FDEP 2008). Even when silt fences are UV stabilized, it has still been shown that their tensile strength and strain at break continue to decrease with exposure to UV, however, the rate of degradation is greatly reduced (Dierickx and Van Den Berghe 2004).

Sediment Removal Mechanisms of Silt Fence

The two major mechanisms of sediment removal by silt fence occurs by particle sedimentation by gravity and by filtration of particles through the fabric. Knowledge of both sedimentation and filtration theory is necessary in order to understand the mechanisms of sediment removal by silt fence. Discussed in the following two sections is the basic theory behind these mechanisms.

Sedimentation Theory

One of the most important, cost effective, and widespread treatments of suspended solids removal from water is by sedimentation (Barrett et al. 1995). Sedimentation during silt fence treatment occurs due to the formation of a ponding water volume caused by the flow rate of runoff water being greater than the flow rate of water through the silt fence. The ponding water volume, which is concentrated with eroded sediments, acts as a small dynamic sedimentation pond. Sedimentation will occur if the suspended particles in the pond are large and dense enough to settle out by gravitational forces in a time that is less than the critical settling velocity of the system (Howe et al. 2012). The critical particle settling velocity is related to both the ponding depth and the hydraulic detention time and is given by the following expressions in Equations 1 and 2:

$$v_c = \frac{PD}{\tau} \quad (1)$$

$$\tau = \frac{3(10^4)*PD}{q*S} \quad (2)$$

where v_c is the critical settling velocity (cm/min); PD is the ponding depth at the fence face (cm); τ is the hydraulic detention time (min); q is the flow-through rate of the fence (L/m²-hr); and S is the slope percent of the ground which is in contact with the ponding water volume (%). The hydraulic detention time refers to the amount of time it would take for the entire ponding volume to flow through the silt fence.

In order for sedimentation to occur, the particle settling velocity must be greater than the critical settling velocity. The particle settling velocity is dependent on a number of factors, one of which is the type of particle suspension within the pond. In total, there are four particle suspension classifications, however only two are relevant to silt fence. They are, Type I (Discrete) particle settling and Type III (Hindered) settling.

Type I Particle Settling

Type I particle settling occurs in dilute solutions where individual particles do not interact with each other. Under these conditions each individual particle settles based on their own size and density (Howe et al. 2012). Assuming laminar flow conditions, the settling velocity is given by Stokes' Law as

$$v_s = \frac{g*d_p^2*(\rho_p - \rho_w)}{18*\mu} \quad (3)$$

where v_s is the particle settling velocity (m/s); g is the gravitational constant (m/s²); d_p is the particle diameter (m); ρ_p is the density of particle (kg/m³); ρ_w is the density of water (kg/m³); and μ is the dynamic viscosity (kg/m-s). Based on Equation 3, settling velocity is proportional to both the particle diameter and density. For this reason it is unlikely that very small particles such

as silts and clays will be removed by settling in silt fence applications due to their low settling velocities (Arjunan et al. 2006).

Type III Settling

In the literature it is common for Stokes law to be referred to in discussions on silt fence in conjunction with sedimentation mechanisms even when the solids concentrations are large. Under high concentrations however, solutions are not dilute enough, and particle interactions restrict the settling potential of the solution. Under these conditions, Type 1 settling and Stokes law are not justified, and the governing settling mechanism is instead Type III, or hindered settling.

In type III settling, the settling velocities of particles are affected by the presence of other particles due to particle collisions and frictional forces (Howe et al. 2012). During this type of settling, a blanket of particles forms with a distinct interface due to particle aggregation (Howe et al. 2012). This causes the settling velocity of larger particles to be reduced, however the settling velocity of smaller particles, such as silts and clays, are likely to be increased if they are caught within the settling blanket. Under Type III settling, the settling velocity is also dependent on the soil type and the solids concentration. As the solids concentration increases, the settling velocity decreases (Howe et al. 2012). Therefore, as the solids concentration increases, the potential removal by sedimentation will decrease. However, a larger solids concentration will increase the potential for removal by filtration.

Filtering Theory

An understanding of the basic theory of filtration and how it applies to silt fence applications is presented in this section. The discussion is broken up into three parts; how the filtration mechanism occurs in geotextiles, how filtration of the fabric affects the flow-through rate of the geotextile, and a brief discussion on different types of geotextile/soil interactions.

Filtration Mechanism

A discussion on the mechanics of filtration in geotextile applications is described by Faure et al. (2006), a summary of this discussion is presented below.

In a silt fence fabric, small openings in the fabric act as small pipes. Many of these openings in the fabric make up a pipe network where water and fine particles can flow through. The flow-through rate of this system is equal to the sum of the flow-through rates in each individual pipe in the network. Depending on the geotextile properties such as pore opening size and fabric thickness, as well as soil characteristics of the slurry, particles in suspension may settle or be caught within the individual pipes. Filtering of this nature is referred to as parallel filtering (Figure 1a). Different pipes will undergo parallel filtration at different rates depending on the properties of each pipe. Some pipes may experience an excessive amount of parallel filtration and become obstructed; causing additional particles to pile up in the pipe. This is called series filtration (Figure 1b). If series filtration causes a pipe to become entirely filled with particles, additional particles will start to accumulate on the outside of the fabric and will form a filter cake (Figure 1c).

As particles continue to be filtered by the fabric, the impinged particles reduce the pore sizes of the pipes. The reduction in pore size limits the ease with which water can flow through the fabric and also increases the filtration ability of the fabric. These mechanisms are discussed in more detail in the following sections.

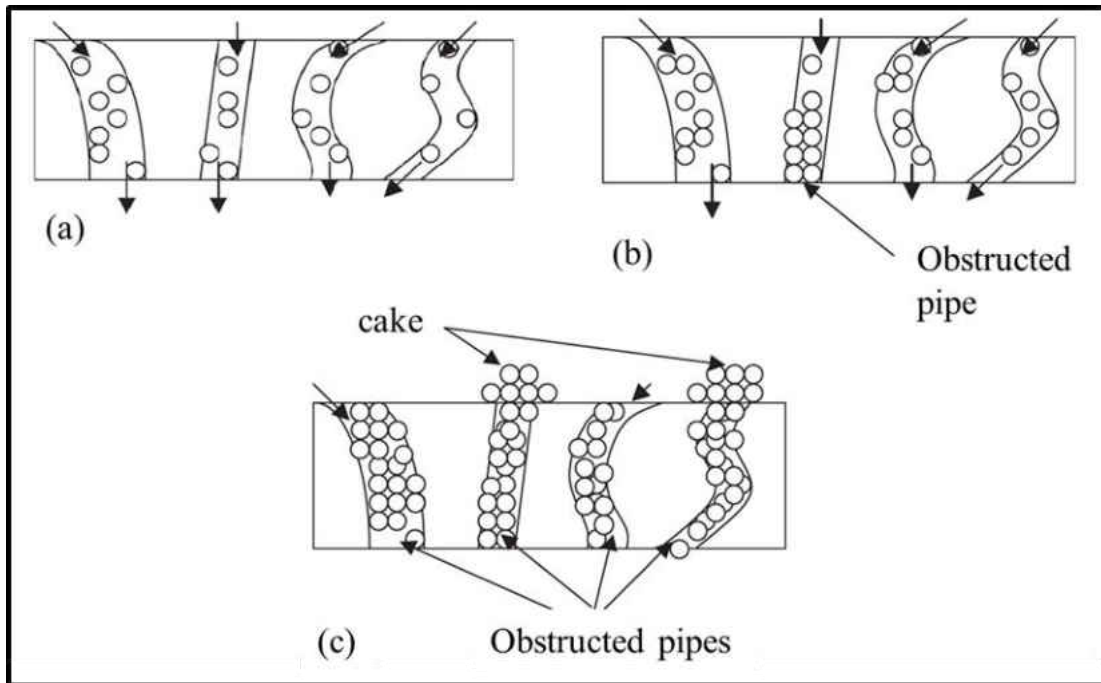


FIGURE 1 MECHANISM OF PARTICLE ACCUMULATION: (A) ALL PIPES ARE OPENED (SERIES FILTRATION), (B) FEW PIPES ARE OBSTRUCTED (SERIES AND PARALLEL FILTRATION), (C) FILTER CAKE FORMATION ABOVE COMPLETELY OBSTRUCTED PIPES (FAURE ET AL. 2006)

Effect of Filtration on Flow Rate

The purpose of silt fence is to remove soil particles from a concentrated slurry, while still permitting the flow of water through it. However, as soil particles accumulate both within and on the fabric, both the pore sizes of the fabric and the ability of the fabric to transmit water are reduced (Fisher and Jarrett 1984, Britton et al. 2000, Risse et al. 2008). The decrease in flow-through rate causes an increase in the accumulation of ponding water upstream of the silt

fence. Although this will increase the hydraulic detention time of the system, allowing additional time for the sedimentation mechanism to take place, excessive ponding could also cause the ponding water to overtop the silt fence (Farias et al. 2006). The additional pressure brought on by large ponding depths could also cause the silt fence to fail. For these reason silt fence must be prevented from becoming clogged with sediment and there must exist a compromise between the fabrics ability to retain soil and its ability to transmit water (Fisher and Jarrett 1984).

Sansone and Koerner (1992) defined clogging of the fabric due to particle filtering as, “the reduction of the geotextile’s permeability to the point where flow through it results in the hydraulic system’s nonperformance.” The potential of a filter to become clogged depends on both the fabric characteristics and the parent/eroded soil characteristics. Studies by Aydilek and Edil (2003) have shown that the permittivity of the geotextile is the “main pore structure parameter” that affects its clogging. Where increases in the initial permittivity of the geotextile lead to a decrease in the potential of the fabric to become clogged with sediment. However, according to Weggel and Dortch (2012) the permittivity of the geotextile is only important initially. What controls the flow-through rate of the fabric and the ability of the fabric to become clogged is the geotextile/soil characteristics and the nature of the filter cake that forms on the fabric. In general, greater reductions in flow rate also occur in heavier and thicker geotextiles due to the increased available volume for binding and impregnation in these fabrics (Farias et al. 2006).

Geotextile/Soil Interaction

Overall, the soil characteristics relative to the geotextile's characteristics are the most important parameters affecting both the potential for fabric clogging and the ability of the fabric to filter the concentrated slurry. In general, soils that contain particles that are for the most part larger than the geotextiles opening pores will operate with high efficiency and will not clog, but will build a stable filter cake on the geotextile (Sansone and Koerner 1992). The filter cake will continue to thicken over time as additional particles adhere to the filter cake, however, the flow rate will remain relatively constant and will be dependent on the permittivity of the accumulated filter cake (Sansone and Koerner 1992, Weggel and Ward 2012).

For soils where all the particles are smaller than the pore size of the fabric, the silt fence will operate with a low filtering efficiency, but clogging is not likely to occur (Sansone and Koerner 1992). Soils consisting of primarily silts and clays fall into this category. For this reason silt fence is generally not an effective filter of silty and clayey soils (Fisher and Jarrett 1984).

The last soil type consists of particles that are both larger (i.e. sands) and smaller (i.e. silts and clays) than the pore size openings of the fabric. These types of soils can lead to excessive clogging of the geotextile depending on how well graded the soil is (Sansone and Koerner 1992). Initially the larger sand particles are filtered by the fabric, decreasing the pore sizes of the fabric. This leads to smaller particles also being filtered by the fabric. As the pore size of the fabric continues to decrease due to smaller and smaller particles being filtered, the ability of the system to transmit water also decreases. In this fashion, the fabric may become

completely clogged over time, and the flow-through rate of the fabric will be severely diminished.

Previous Silt Fence Research

This section describes previous research that has been conducted on the performance efficiency of silt fence. These studies were conducted in a number of ways, including; monitoring silt fence in the field under actual storm events, bench and field scale studies with simulated rainfall, and flume studies. A summary of previous research on silt fence that has been conducted these three types of studies is presented in this section.

Flume Studies

A flume study is a controlled test performed in the laboratory. The test is conducted by mixing a mass of parent soil with a certain volume of water to create concentrated slurry. The concentration of the slurry becomes the influent concentration to the flume. The slurry is pumped into the flume and flows down the flume, where it is exposed to a silt fence that sits at the bottom of the flume. The concentration that is discharged through the silt fence is the effluent concentration. The efficiency of the silt fence is then calculated by comparing the effluent concentration to the initial influent concentration.

Farias et al. (2006) tested four nonwoven silt fence fabrics of various opening sizes and thicknesses using flume tests. The slope of the flume was not stated. The opening sizes of the geotextiles ranged from 0.11 mm to 0.60 mm and the thickness of the geotextiles ranged from 0.8 mm to 4.5 mm. Three soil types were used with a sediment concentration of 10,000 mg/L; namely two silty soils and one sandy soil. Results showed that sediment reduction under these

conditions ranged from 93 to 96 percent for all fabrics and soil combination pairs tested. The opening size and thickness of the fabrics did not affect the reduction efficiencies; however, these parameters did affect the flow rate. The thicker and less opened geotextiles had the greatest flow rate reductions, whereas the lighter and more opened geotextile presented the smallest reductions in flow rate (Farias et al. 2006). Thus, the study concluded that the thicker and less opened the geotextile, the easier it would be for the fabric to become clogged; reducing its ability to transmit water. Results from this study also showed that silt fence, even those with large opening sizes of 0.60 mm could efficiently remove silty soils.

Risse et al. (2008) also tested silt fence fabrics using flumes. The flume was raised to a grade of 8 percent, and both a woven and a nonwoven fabric were tested. The nonwoven fabric was a polyester silt fence that was introduced by Silt-Saver Inc. and is called a Belted Silt Retention Fence (BSRF). Three soils, Tifton sand, Fannin silt, and Cecil clay loam, were used at concentrations of approximately 3000 mg/L and 6000 mg/L. Sediment removal efficiencies under all test conditions were at least 87 percent, indicating high removal for both fabrics under all soil conditions. Risse et al. (2008) concluded that the high sediment removal efficiencies were attributed to the low slope gradient and the extended holding time created under these conditions, and that much of the released sediment settled out of suspension prior to reaching the silt fence. Risse et al. (2008) also investigated the performance of silt under a large slope of 58%, and found that sediment removal still remained high (upwards of 80%). So it seems the low slope gradient did not have that large of an effect on reduction after all. Although sediment removals were high, turbidity reduction was significantly lower and ranged from 25 to 58 percent for the woven fabric and 55 to 90 percent for the nonwoven fabric.

Risse et al. (2008) also found that the flow rate through the fabrics decreased with increasing influent concentration. These results indicate that soil particles have an influence on the flow rate and suggested that the sediment trapped behind the fence was controlling the flow rate more than the fence itself (Risse et al. 2008). Note that flow rates were significantly higher with the sandy soil than the silty or clayey soils. The reason for this may be that the silty and clayey soils have better graded distribution of soil particle sizes than the sandy soil; which consisted mostly of sand sized particles. As was discussed in the section on filtering theory, the well-graded soils can progressively clog silt fence fabrics due to progressively smaller sediments clogging the pores of the filter.

Results from this study show that silt fence is capable of high sediment removals of silt, sand, and clay loams. However, it is less effective in removing turbidity from these soil types. The lower turbidity removal shows that the larger sediment particles most likely settled out of suspension, while the smaller particles did not, and were discharged through the silt fence. While the large sediment particles that settled out affect the mass of sediment discharged and to some extent the turbidity, the smaller silt and clay particles affect the turbidity to a larger extent (Bilotta and Brazier 2008). However, due to their small size, they do not contribute to the total solid mass to the extent that the larger particles do. This explains why turbidity removal was lower.

Field Testing

Barrett et al. (1995) investigated the performance of silt fences under controlled conditions in an outdoor flume as well as in the field under actual rainfall on active construction sites. The flume slope was 0.33% and a slurry was made using Austin silty clay soil at a

concentration of 3000 mg/L. Sediment removal efficiencies ranged from 68 to 90 percent. The high removal efficiencies were attributed to the geometry of the upstream ponding volume; the low slope allowed adequate detention time for the suspended solids to settle out before reaching the silt fence. Barrett et al. (1995) was able to show that silt fence was capable of removing silt and clay sized particles under low sloped conditions. The mechanism for removal however was not due to filtering through the silt fence, but through settling.

Barrett et al. (1995) also investigated silt fence performance in the field by monitoring installations on active highway construction sites. However, information regarding the intensity, duration, or quantity of each rainfall event was not obtained due to limited equipment. In total six different sites were monitored, two of which used nonwoven fabrics and four of which used woven fabrics. Over the course of seven rainfall events, the average removal efficiencies ranged from negative 61 to 54 percent with a median of 0 percent and negative 32 to 49 percent with a median of 2 percent for sediment and turbidity, respectively. According to Britton et al. (2000), due to the magnitude and random nature of the measured concentration, the instantaneous comparison of these values were not valid. An accurate estimate of the overall operation efficiency would need to be approximated by collecting samples over the entire duration of a storm event in order to determine the total load into and out of the control device over time.

Bench Scale Testing

Faucette et al. (2008) investigated the performance of silt fence using bench scale tests. The bench scale testing bed was 100 cm length by 35 cm width by 25 cm depth (39 in × 14 in × 10 in). The test beds were filled with a silt loam and raised to a 10 percent slope and exposed to rainfall intensity of 7.45 mm/h (2.93 in/h). Removal efficiencies ranged from 78 to 87 percent

and from 54 to 76 percent for sediment concentration and turbidity, respectively. This result shows further that silt fence does not reduce turbidity as well as it does sediment. The results also showed that even though silt fence removed sediment from 78 to 87 percent, effluent concentrations were still high. Effluent sediment concentrations ranged from 9,000 mg/L to 14,000 mg/L despite the large reduction efficiencies, which indicates that the erosion rate of the soil was high during the bench scale testing.

Field Scale Testing

Due to the uncontrollable nature of actual field testing on construction sites and the need to further investigate the performance of silt fences under these conditions, Gogo-Abite and Chopra (2013) studied the performance of both woven and nonwoven (BSRF) silt fence fabrics. The study was done using a tilted test bed filled with a sandy soil and rainfall simulator in order to simulate field conditions in a controlled environment. In order to simulate worst case conditions that would be found in the field, high slopes of 10 and 25 percent, and high intensities of 27, 76, 127 millimeter per hour (1, 3, and 5 inches per hour) were evaluated. The woven fabric reduced turbidity by 18 percent and reduced sediment by 28 percent. The nonwoven fabric achieved reductions of 52 and 57 percent for turbidity and sediment, respectively. The low removal percentages were caused by inadequate time for settling due to the large slopes and because a large portion of the suspended sediment was smaller than the AOS of either fabric. Gogo-Abite and Chopra (2013) concluded that due to the low removal efficiencies, silt fence as a standalone process installed at the toes of high slopes of 10% and greater would not be adequate enough to meet the reductions of turbidity and sediment as required by regulatory agencies.

Summary

Literature related to silt fence show that sediment removal is by gravity settling and by filtration of the fabric. The performance efficiency of the fabrics is dependent on the particle size characteristics as well as the geotextile properties such as opening pore size and thickness. The flow-through rate of these fabrics in the field is also a function of the ease with which the fabric can become clogged and is therefore a function of the soil characteristics, the gradation of the soil, and the geotextiles opening pore size.

It is common for silt fence to be characterized by both its permittivity and apparent opening size, however, this literature review has shown that both these properties do not correctly describe silt fence performance under field conditions. The initial permittivity in particular will not give indication to the expected hydraulic performance of the fabric in the field due to filter clogging when exposed to concentrated flows. The apparent opening size can give an indication of what particle sizes may be intercepted by the fabric in the field, however, ponding water upstream of the silt fence creates a load on the silt fence that induces a strain that can result in an increase in the opening size of the fabric. This would increase the particle sizes that could pass through the fabric and decrease the fabric efficiency.

Previous research on silt fence performance has been conducted on active construction sites under monitored storm events, in flume studies, and in both pilot and field scale test beds. Results from flume studies have shown that silt fence reduces sediment concentrations of sandy soils as well as silty and clayey loams at high efficiencies upwards of 70 percent. However, silt fence did not reduce turbidity to this extent due to the difficulty of silt fence in removing small silt and clay sized particles.

While flume studies have shown high removal efficiencies, field tests and field scale tests have shown that silt fence does not reduce turbidity or sediment as well under field conditions. In particular, field scale testing with tilted test beds and active rainfall have shown that silt fence reduces sediment and turbidity in the range of only 20 to 50 percent depending on the type of geotextile used. These studies have shown a need for additional field scale testing of silt fence geotextiles in order to further evaluate their performance in the field.

CHAPTER 3: METHODOLOGY

Introduction

This project compared and evaluated the performance of two silt fence geotextiles exposed to a simulated rain event over a silty-sand-soil. The evaluation and comparison was performed using a field scale tilted test bed and rainfall simulator located at University of Central Florida's Stormwater Management Academy Research and Testing Laboratory (SMARTL). This chapter will describe the soil type that was used in the study, the types of silt fence geotextiles used, the test preparation and set up, the field scale testing method, and the limitations encountered during the study.

Soil Characteristics

A series of bench scale tests were used in order to characterize the soil that was loaded in the test bed. Testing was done in order to determine the soils particle size distribution, maximum compaction, and permeability. Brief discussions on the results of these tests are the topic of the next few sections.

Soil Classification and Particle Size Distribution

Defining the soils classification and particle size distribution is particularly important when evaluating the performance of silt fence fabrics. The ability of the geotextile to filter the concentrated slurry and the settling velocity of the suspended particles are primarily dependent on both the soil particle sizes and on the distribution and uniformity of these particle sizes. Due to this dependence, the AASHTO Classification system was used because this system distinguishes between clay and silt particles based on grain diameter. The AASHTO

Classification system was also used because it is the common classification system for construction sites for roadway and stormwater management. The AASHTO Classification system also takes into account the plastic and liquid limits of the soil. The results of these tests showed that the soil type was non-plastic. The soil classification was therefore based solely on its grain size distribution. The grain size classification used in the AASHTO Classification system is shown in Table 2.

TABLE 2 SUMMARY OF SOIL PARTICLE CLASSIFICATION ANALYSES

Particle Type	AASHTO Classification, grain diameter (mm)	Percentage of Soil (%)
Gravel	76.2 to 2	0
Sand	2 to 0.075	84
Silt	0.075 to 0.002	4
Clay	< 0.002	12

Particle size distribution

Three tests were completed in order to determine the particle size distribution of the soil. These tests were the standard test method for materials finer than 75 μm (No. 200) sieve in mineral aggregates by washing (ASTM C117-13 2013), sieve analysis of fine and coarse aggregates (ASTM C136-06 2013), and standard test method for particle-size analysis of soils by hydrometer analysis (ASTM D422-63 2013). The method for materials finer than 75 μm was performed first in order to determine the percentage of the soil that was finer than 75 μm (No. 200 mesh). Following the method for materials finer than 75 μm , those particles with diameters that were greater than 75 μm and that were retained on the number 200 sieve were used in the sieve analysis in order to determine the distribution of those particles which were greater than 75

µm. Finally, a hydrometer analysis was conducted in order to determine the soil distribution of those particles which had diameters less than 75 µm.

The results for material finer than 75 µm by washing, sieve for fine and coarse aggregates, and particle size analysis using hydrometer are shown in Table 21, Table 22 and Table 23, respectively, of Appendix A. A summary of these results and the particle-size distribution curve for this soil are also shown in Table 2 and Figure 2, respectively.

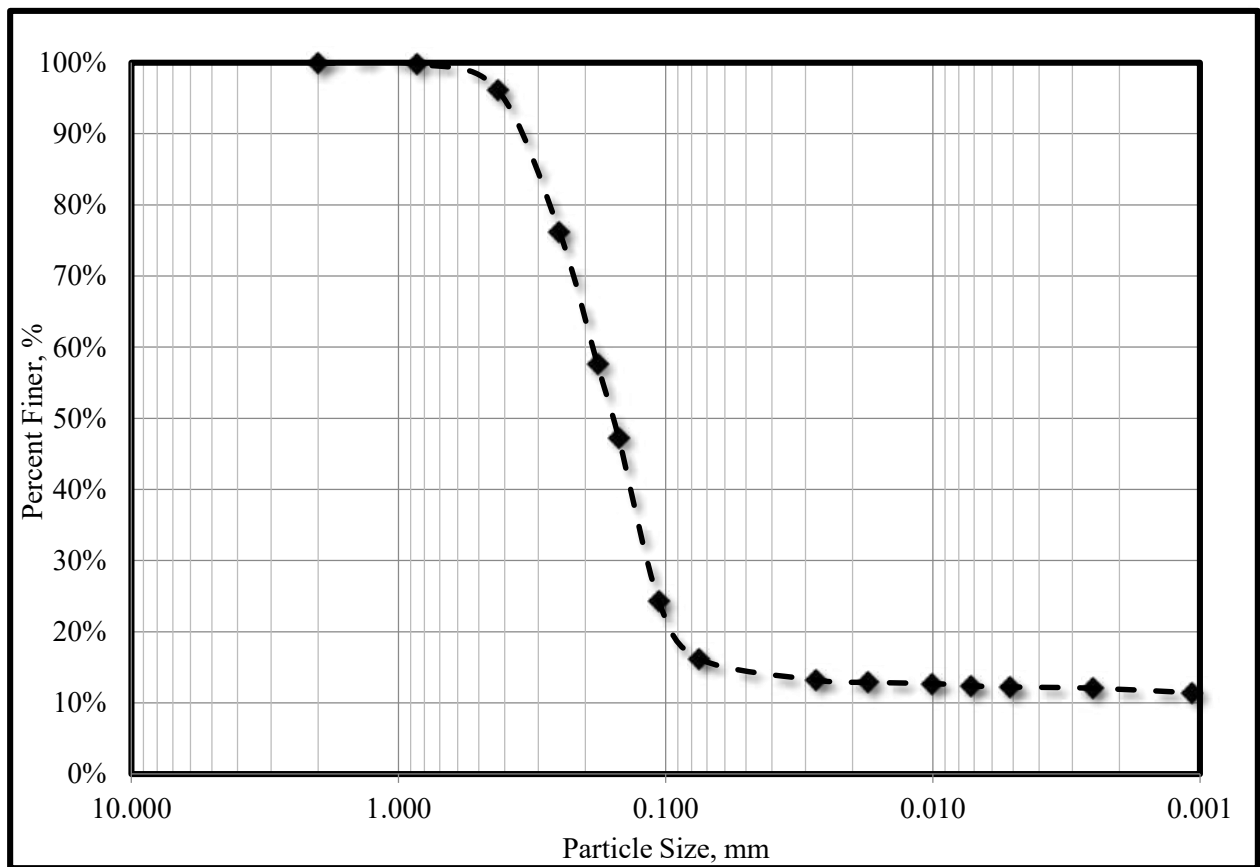


FIGURE 2 PARTICLE SIZE DISTRIBUTION CURVE

The silty-sand soil is made primarily of sand particles (84 percent sand) in the range of 0.075 mm to 4.0 mm. The remaining 16 percent of the soil distribution is made of clay particles

with diameters of less than 0.001 mm (12 percent) and silt sized particles in the range of 0.075 to 0.002 (4 percent). It will be interesting to see if silt fence is able to achieve removal efficiencies of greater than 84 percent from this soil type. Silt fence is well known for being unable to remove silt and clay sized particles due to their very small particle sizes (Fisher and Jarrett 1984). It is also well known however that the erosion rate of clay particles is lower than the erosion rate of small sands and silts (FDEP 2008). Thus, the soil composition of particles that actually erode from this parent soil may be different from the parent soil composition itself.

Proctor (Laboratory) Compaction Test

The compaction level of the soil affects both the permeability and the erodibility of the soil. The additional compaction reduces the permeability and increases the erodibility of the soil (European Commission 2012). The in situ compaction level of the soil in the test bed is therefore an important characteristic that will affect both the erodibility of the soil and the volume of sheet flow over the soil. For this reason, during testing, a constant compaction level of the soil at the beginning of each test is maintained in order to best simulate constant soil conditions from test to test. Originally, that compaction level prior to each test was 95 percent of maximum dry density of the soil, however, it was too difficult to achieve this level of compaction in the field. The difficulty in achieving this compaction level in the field is discussed in further detail in the section, Test Bed Preparation and Setup, of this chapter. Instead, the soil was compacted to 80 percent of the maximum dry density prior to each new test.

The maximum dry density and the moisture content at which this density occurs is determined using the standard proctor test Method A as described in D698-12 (2013). The results of the laboratory compaction test and compaction curve are presented in Table 24 and

Figure 20 of Appendix A. The results of the proctor test show that the maximum dry unit weight of the soil is 1.86 g/cm^3 (116 lb/ft^3) and occurs at a moisture content of 11.5%. With a compaction level of 80% in the field, an initial field density of 1.5 g/cm^3 (92 lb/ft^3) was the compaction goal prior to each field test.

Permeability Test

The permeability of the soil measures the ability of the soil to pass water through it. The permeability and hydraulic conductivity of the soil are found using the constant head method in ASTM D2434-68 (2006). The hydraulic conductivity of the soil describes the ease with which water can move through pore spaces of the soil. It is related to the permeability of the soil, the dynamic viscosity and density of the fluid, and the gravitational constant.

The results of the constant head permeability test are shown in Table 25 of Appendix A. The results of the test show that the permeability and hydraulic conductivity of the soil are $1.41\text{E-}08 \text{ cm}^2$ and 0.0014 cm/s , respectively, at a temperature of 20°C and a soil density of 1.45 g/cm^3 (91 lb/ft^3). This value of permeability is in the range for silty-sands (Geotechdata.info 2008).

Silt Fence Geotextiles

Two silt fence fabrics were evaluated in this study. The first silt fence is a woven monofilament geosynthetic which was donated by Absolute Erosion Control, Incorporated and is referred to as an ASR 1400 silt fence. This woven fabric is shown in Figure 3.



FIGURE 3 WOVEN (ASR 1400) SILT FENCE INSTALLED ON A TILTED TEST BED (GOGO-ABITE 2012)

This type of silt fence is well known for being commonly used on construction sites, however, previous studies on this type of silt fence have shown the fences inability in achieving desired performance targets (Gogo-Abite 2012). For this reason, Silt Savers, Inc. introduced a polyester nonwoven belted silt retention fence (BSRF) as shown in Figure 4. The BSRF was designed to both retain more silt and reduce turbidity and suspended sediment more than the traditional woven monofilament silt fence fabric (Risse et al. 2008).



FIGURE 4 NONWOVEN (BSRF) SILT FENCE INSTALLED ON A TILTED TEST BED

Both silt fence fabrics have been tested in a previous study by Gogo-Abite and Chopra (2013) to determine the grab strength, permittivity, and AOS of both the woven (ASR 1400) and nonwoven (BSRF) fabrics. The results from this study were compared with the ASTM D6461 (2007) recommended index test values as shown in Table 3.

TABLE 3 COMPARISON OF WOVEN AND NONWOVEN FABRICS

Property	Direction	ASTM Test Methods	Units	ASTM D6461	Woven Fabric	Nonwoven Fabric
Grab strength	Machine	D 4632	N	400	539	591
	X-Machine			400	637	726
Permittivity		D 4491	sec ⁻¹	0.05	0.11	2.5
AOS		D 451	mm	0.6	0.7	0.212

Results of the index testing show that both fabrics, for the most part, surpassed the recommended standards set by ASTM D6461 (2007). The grab strengths of both fabrics were higher than the recommended values, however, the nonwoven fabric was slightly stronger than the woven fabric. The permittivity of both fabrics were also higher than the recommended value, with the woven fabric having a permittivity over a magnitude greater than the recommended value and the nonwoven fabric having a permittivity over two magnitudes greater. The AOS of the woven fabric was the only standard that was not met. The AOS was slightly higher than the maximum value recommended. It will be interesting to see the filtering abilities of the woven and nonwoven fabrics will be affected by this difference in AOS. Recall from Figure 2 that the AOS of the nonwoven fabric (0.212 mm) is smaller than approximately 40% of the soil distribution and that the woven fabric, which AOS is 0.70 mm, is actually larger than 100 percent of the soil distribution used in this study.

Test Bed Preparation and Setup

The investigations on silt fence performance were carried out using the tilted test bed and rainfall simulator at the UCF SMARTL. The aluminum tilted test bed measures 2.4 meter (8 feet) wide by 9.1 meter (30 feet) long by 30.5 centimeter (1 foot) deep and can be set to embankment slopes ranging from 0 to 50 percent. Due to the initial test bed depth of only 30.5 centimeters, the test bed was modified by the construction of a plywood apron on its perimeter in order to increase the depth to 50.8 centimeter (20 inches) to accommodate the minimum required post embedment of 45.7 centimeter (18 inches) as shown in Figure 5a (Gogo-Abite 2012). Following the plywood apron construction a visqueen was placed over the plywood apron in order to protect it from water damage (Figure 5b). The bed was then loaded with the silty-sand

soil (84 percent sand, 12 percent clay, and 4 percent silt, AASHTO Classification Type A-2-4) in three layers of 15.2 centimeter (6 inch), and compacted to achieve 80 percent Standard Proctor compaction effort of 7 kilogram per cubic meter (92 pounds per cubic feet) maximum dry unit weight.

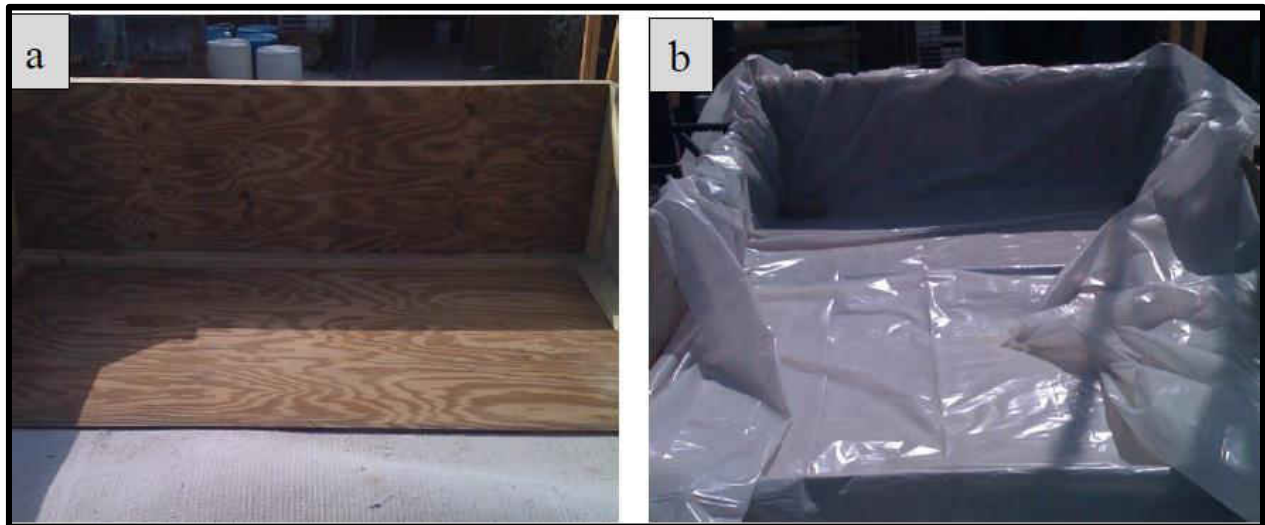


FIGURE 5 PICTURES OF TEST BED MODIFICATIONS (A) PLYWOOD FOR DEPTH, AND (B) VISQUEEN TO PROTECT PLYWOOD (GOGO-ABITE 2012)

Prior to each field scale test, a silt fence was installed along the perimeter of the test bed in an “L” shape as shown in Figure 6a. The test bed soil was then graded and compacted as shown in Figure 6b. Initially, the compaction goal prior to each test was 95% maximum dry unit weight, however, there was a difficulty in achieving this compaction goal with the silty-sand soil in the field. Instead a compaction effort of only 80 percent was able to be achieved prior to each test. A lower compaction effort would cause more percolation of water into the soil and would also reduce the erosion rate of the soil in comparison with a higher compaction effort. However, it was more important to have a compaction effort, which could be achieved on a consistent basis at the beginning of each test, so that all tests would be subjected to the same initial conditions.

For this reason, 80 percent soil compaction was chosen. After test bed soil compaction, rain gages were placed on the test bed in order to measure the rainfall intensity over the test bed, and a meter stick was installed at the face of the silt fence in order to measure the ponding depth of water behind the fence (Figure 6a). The test bed was then raised to the proper embankment slope and the rainfall simulator was placed over the tilted test bed (Figure 6c).



FIGURE 6 TEST BED SETUP (A) WOVEN FABRIC, RAIN GAGES, AND METER STICK INSTALLED, (B) TEST BED COMPACTION, (C) RAINFALL SIMULATOR AND TILTED TEST BED WITH NONWOVEN FABRIC INSTALLED

Field Scale Testing Procedure

Both the woven and nonwoven fabrics were field tested under three different embankment slopes (33, 25, and 10 percent) and three different simulated rainfall intensities – 25, 76, and 127 mm/h (1, 3, and 5 inches per hour). For each embankment slope, each rainfall intensity was simulated four times for each fabric. The testing matrix for a typical case of 10% embankment slope is shown in Figure 7.

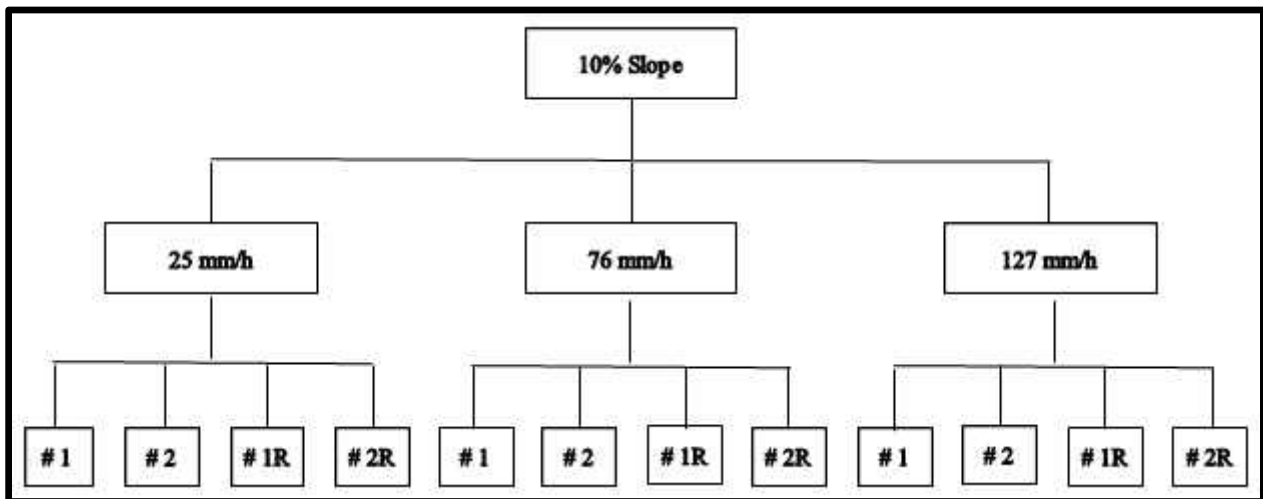


FIGURE 7 SAMPLE FIELD TEST MATRIX FOR 10 PERCENT SLOPE (REPEATED FOR 33 AND 10 PERCENT SLOPES)

Four rainfall events were simulated for each pair of embankment slope and rainfall intensity. These four rainfall events were broken up into two pairs of two rainfall events each. The first rainfall event, denoted as #1, evaluated the performance of a newly installed silt fence. After the commencement of Test #1, a minimum of three-hour interval was given before the initiation of Test #2. The second rainfall event, denoted as #2, was then simulated without performing any maintenance or retrofit to the silt fence or soil surface in order to test the silt fences performance when subjected to an additional rainfall event without having any

maintenance performed on it. When Test #2 was completed, a new silt fence was installed and the soil surface was re-graded and compacted to its initial condition of 80 percent maximum dry unit weight. Tests #1 and #2 were then repeated under the same slope and intensity as in the previous two tests. The repeated tests are referred to as # 1R and # 2R as shown in Figure 7.

For each rainfall event, simulated rainfall was allowed to fall over the tilted test bed for 30 minutes after the initiation of downstream runoff through the silt fence. During the 30-minute rainfall event, six grab samples (one grab sample every five minutes for 30 minutes) were collected both upstream (influent) of the silt fence and downstream (effluent) of the silt fence.

Figure 8 shows the downstream collection system used during testing. Runoff water flowed through the silt fence and over a white visqueen where the runoff water was channeled into two separate troughs. Water then flowed through each trough and into a white PVC pipe that connected both troughs. The water then exited the PVC pipe and flowed into a bucket as shown in Figure 8. The bucket was changed every minute and the mass of water that flowed through the fence in that one-minute interval was recorded. In addition, a grab sample was taken from the bucket as well as upstream of the silt fence every five minutes as discussed previously. The upstream sample was taken from the middle of the ponding water depth and close to the silt fence.

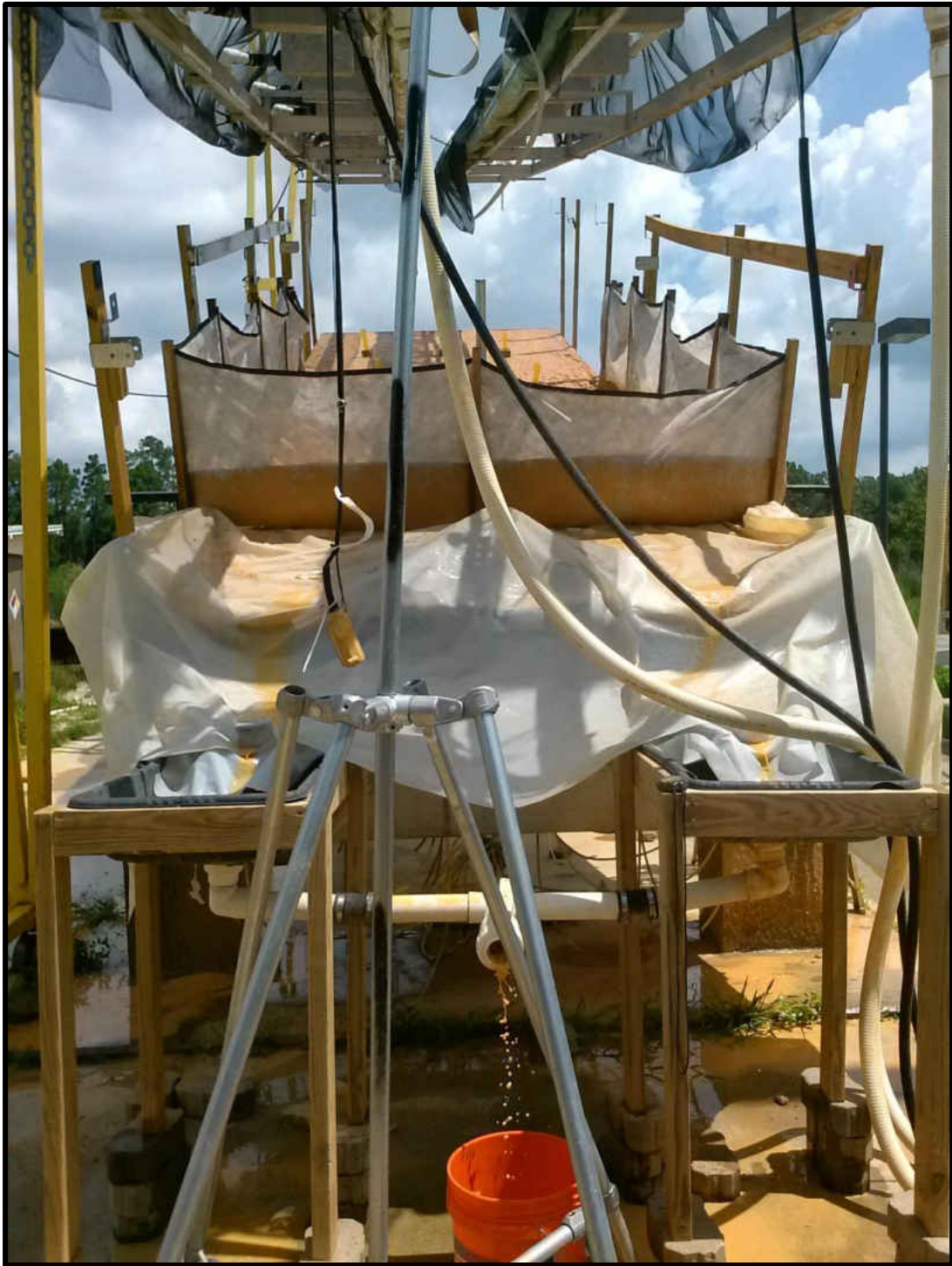


FIGURE 8 FIELD SCALE TESTING: DOWNSTREAM COLLECTION SYSTEM

At the end of the 30-minute rainfall event, the concentrated ponded water behind the silt fence was given an additional 30 minutes to flow through the silt fence in order to evaluate the performance of the fabric after the rain event had ended. During this time, six more grab samples (one grab sample every five minutes) were taken both upstream and downstream of the silt fence. All collected grab samples were then tested for both sediment concentration (total solids) and turbidity according to the Standard Methods for the Examination of Water and Wastewater (APHA et al. 2005). In addition to collected grab samples that were tested for turbidity and sediment concentration, downstream runoff was also collected at one-minute intervals from the start of when runoff first occurred to either the conclusion of the one hour test or until runoff stopped, whichever occurred first. Downstream runoff was collected in one-minute intervals in order to measure the flow rate of water with time through the silt fence fabrics.

Limitations of Field Scale Testing

There were certain limitations of the field scale testing procedure used in this study. For the most part, as will be discussed in Chapter 4, the field scale testing method was not repeatable between tests. Many factors contributed to the performance of silt fence from test to test. Changes in the initial field density and moisture content affected both the erosion rate of the soil and percolation of water through the soil. It was not possible to obtain the same exact initial conditions from test to test.

For the upstream collection, a grab sample is taken by hand from the middle of the ponding volume behind the silt fence. The sample was taken from the middle of the pond and close to the silt fence. It is assumed that the turbidity and sediment concentration of this sample represented the average concentration of suspended sediment of the entire ponding volume. However, due to human error in taking sample by hand and the unknown vertical concentration gradient of suspended solids within the pond, this sample may not have adequately represented the concentration within the ponding volume.

The samples that were taken both upstream and downstream of the silt fence also had relatively high turbidity values. Turbidity values were high enough that in order to calculate the turbidity multiple dilutions were needed. The accuracy of the turbidity measurement decreases as the dilution factor is increased.

CHAPTER 4: RESULTS AND DISCUSSION

Introduction

Results of the field scale performance of woven and nonwoven fabrics installed on a silty-sand soil are presented in this section. Both fabrics were tested on three embankment slopes (33, 25, and 10 percent) and under three rainfall intensities – 25, 76, and 125 millimeters per hour (1, 3, 5 inches per hour). In total, 78 rainfall events were simulated over the course of 15 months on both fabrics, starting from June 4, 2012 to September 20, 2013. Although 78 rainfall events were simulated, only 62 of those rainfall events were used in analysis, with the results of the other 16 tests being discarded. These 16 tests were discarded due to a series of testing errors, which led to the results from these tests being unusable. These testing errors involved errors in the upstream collection behind the fence, which yielded average efficiency values of negative 30 to negative 50 percent for both turbidity and suspended sediment concentration. These results were deemed erroneous and the tests were thrown out. The results of these tests are not presented or analyzed in this thesis. All 16 tests that were discarded occurred during testing with the woven fabric; so in total, only 27 rainfall events were used for the woven fabric and 35 rainfall events for the nonwoven fabric.

The tests that were thrown out are four tests from 10 percent slope and 127 mm/h rainfall intensity, four tests from 25 percent slope and 25 mm/h rainfall intensity, four tests from 25 percent slope and 76 mm/h rainfall intensity, and four tests from 25 percent slope and 127 mm/h rainfall intensity. If time had permitted, all 16 tests that were thrown out would have been repeated, however, due to time constraints there was only enough time to complete two additional tests instead of the usual four tests for each of the slope and intensity pairs discussed

above. More tests on the nonwoven fabric than on the woven fabric were analyzed because of the observed errors in the tests on the woven fabric.

The performance evaluation on these silt fence fabrics involve the analysis of fabric efficiency in both turbidity and suspended sediment removal as well as fabric flow-through rate of each geotextile, both during rain events and after rainfall stops. For the woven fabric, 294 grab samples were taken during the rain event and 254 grab samples after the rain event. In the case of the nonwoven fabric, 418 grab samples were taken during the rain event and 380 grab samples after the rain event. There are two discrepancies with these numbers. The first is that over 200 more grab samples were taken overall for the nonwoven fabric than for the woven fabric. The second being that more grab samples were taken during the rain event than after the rain event for both fabrics.

The reason that more samples were taken for the nonwoven fabric was discussed previously and was due to the 8 tests that were not able to be completed due to time constraints. For the second discrepancy there were more grab samples taken during the rain event than after the rain event due to overtopping of the silt fence or fence failure occurring during some of the rainfall events. The overtopping events or fence failures, such as stake breaking and fabric pullout of the fence from the staples, caused the test to be cancelled during the rain event, and no post rainfall samples were collected. In particular, no post rainfall samples were taken for the woven fabric for test on a 33 percent slope and a 127 millimeter per hour (5 inches per hour) rainfall event due to overtopping of the silt fence during all testing. For the nonwoven fabric, a stake breaking in half on a 33 percent slope and a 76 millimeter per hour (3 inches per hour)

rainfall also caused no after rain event samples taken. Fence failures that occurred during testing are discussed in more detailed in this chapter in the section: Silt Fence Failure.

For each embankment slope and intensity pair, four tests were completed for each fabric, except for the tests on the woven fabric on 10 percent and 127 mm/h rainfall and each pair on 25 percent embankment slope, as discussed previously. Of these four tests, two were repeated tests using a new fabric on the same slope and intensity as was previously tested. The tests were repeated in order to obtain additional data for each slope and intensity pair and to determine if the field-scale testing procedure was repeatable. In order to show if there was a significant difference in the upstream and downstream turbidity and suspended sediment concentrations between both sets of tests, a Wilcoxon rank sum test was performed on the samples taken during the rain event between both sets of tests. Results of these tests are shown in Table 26 and Table 27 in Appendix B for the woven and nonwoven fabrics, respectively. The tests show that initial conditions and silt fence performance between the initial test and the repeat tests were statistically different with 95 percent confidence in 20 of the 52 tests. These results show that it was difficult to obtain the constant initial conditions sought after for each test and that the erosion rate and the downstream discharge concentrations varied from test to test; and were thus, not very repeatable

Additional statistical analysis is performed throughout this chapter in order to significantly quantify the data. Three types of statistical tests were used; single factor ANOVA, Wilcoxon rank sum test, and Wilcoxon rank sum test on difference. All statistical tests were completed with a confidence level of 95 percent ($\alpha = 0.05$) and are located in the appropriate appendixes.

Tables of results of all time dependent efficiency and flow-through rates from field scale testing are presented in Table 46 through Table 48 for the woven fabric and Table 49 through Table 51 for the nonwoven fabric in Appendix D. The remainder of this chapter discusses all results pertaining to this research with field scale testing of silt fence fabrics used in conjunction with a silty-sand soil. The chapter is broken into four main sections; fabric performance during the rain event, fabric performance after the rain event, overall silt fence performance based on measured samples, and overall silt fence performance based on projection. The first section is further broken down into discussions on fabric efficiency, fabric flow-through rate, and silt fence failure; and the second section is broken into discussions on fabric efficiency and flow-through rate.

Fabric Performance during Rain Events

Fabric Reduction Efficiency during Rain Events

This section presents results of fabric performance efficiency in both turbidity and suspended sediment concentrations (SSC), which occurred during the rainfall event. On every test, both the turbidity and SCC values were obtained from all collected grab samples both downstream and upstream of the silt fence. Downstream turbidity and SCC values were weighted by the volume of runoff water which transmitted through the silt fence for that sample. Upstream values were weighted by the volume of ponding water upstream of the silt fence when the sample was taken. The volume-weighted downstream and upstream values were then compared to each other to determine a mean efficiency value. These computations are expressed in Equations 4 through 9

$$WMIT = \frac{\sum_{i=0}^n [T_{INF} * V_{upstream}]}{\sum_{i=0}^n V_{upstream}} \quad (4)$$

$$WMIC = \frac{\sum_{i=0}^n [TS_{INF} * V_{upstream}]}{\sum_{i=0}^n V_{upstream}} \quad (5)$$

$$(WMET)_{DR} = \frac{\sum_{i=0}^n [T_{EFF} * V_{downstream}]}{\sum_{i=0}^n V_{downstream}} \quad (6)$$

$$(WMEC)_{DR} = \frac{\sum_{i=0}^n [TS_{EFF} * V_{downstream}]}{\sum_{i=0}^n V_{downstream}} \quad (7)$$

$$E_T(\%)_{DR} = 100 * \left[1 - \frac{(WMET)_{DR}}{WMIT} \right] \quad (8)$$

$$E_{SSC}(\%)_{DR} = 100 * \left[1 - \frac{(WMEC)_{DR}}{WMIC} \right] \quad (9)$$

where, $WMIT$ is the volume-weighted mean influent turbidity (NTU); $(WMET)_{DR}$ is the volume-weighted mean effluent turbidity during the rain event (NTU); T_{inf} is the influent turbidity value collected for sample i (NTU); $V_{upstream}$ is the upstream ponding volume when sample i was taken (L); $WMIC$ is the volume-weighted mean influent concentration (mg/L); $(WMEC)_{DR}$ is the volume-weighted mean effluent concentration during the rain event (mg/L); SSC is the suspended sediment concentration in runoff collected for sample i (mg/L); $V_{downstream}$ is the volume of collected runoff which discharged through the silt fence in interval between sample i and sample $i - 1$ (L); n is the number of samples collected during the rain event; $E_T(\%)_{DR}$ is the mean turbidity performance efficiency during the rain event; and $E_{SSC}(\%)_{DR}$ is the mean suspended sediment concentration performance efficiency during the rain event. Table 4 and TABLE 5 present the volume-weighted turbidity and suspended sediment concentration and the respective performance efficiency that occurred during the rain event for both the ASR-1400 and BSRF silt fence fabrics. Note that from this point forward, woven fabric will be used to refer to the ASR-1400 silt fence and nonwoven fabric will be used to refer to the BSRF silt fence.

TABLE 4 WOVEN FABRIC TEST VOLUME-WEIGHTED MEAN TURBIDITY AND SSC RESULTS DURING THE RAIN EVENT

Slope % (Ratio)	Rainfall Intensity (mm/h)	Rainfall Events	Volume-Weighted Mean Turbidity			Volume-Weighted Mean SSC		
			Up-stream (NTU)	Down-stream (NTU)	Performance Efficiency (%)	Up-stream (mg/L)	Down-stream (mg/L)	Performance Efficiency (%)
33% (3:1) Slope	25	#1	50171	25054	50	32616	14186	57
		#2	33573	16998	49	23412	15867	32
		#1R	28738	19743	31	21001	13728	35
		#2R	30096	17200	43	25614	13299	48
	76	#1	43339	19359	55	40099	13496	66
		#2	--	--	--	--	--	--
		#1R	41442	20644	50	21641	12620	42
		#2R	27811	15466	44	17641	11928	32
	127	#1	48311	18760	61	31212	12121	61
		#2	--	--	--	--	--	--
		#1R	57945	27442	53	46322	21086	54
		#2R	40266	28031	30	35427	21355	40
25% (4:1) Slope	25	#1	29396	22130	25	19585	14185	28
		#2	21551	15465	28	13875	11893	14
	76	#1	19080	14532	24	13462	11312	16
		#2	25891	20995	19	11361	9797	14
	127	#1	47590	22583	53	15744	12260	22
		#2	30530	18983	38	12755	8541	33
10% (10:1) Slope	25	#1	12357	7782	37	10959	6558	40
		#2	10839	3293	70	10743	2409	78
		#1R	13365	5176	61	10468	3544	66
		#2R	9453	5113	46	5920	3621	39
	76	#1	5358	4132	23	4215	3089	27
		#2	3707	2802	24	3426	2196	36
		#1R	6036	4472	26	4610	3491	24
		#2R	2619	2092	20	2117	1681	21
	127	#1	4886	3129	36	3982	2363	41
		#2	4321	2644	39	3763	2171	42

Table entries that appear with "--" indicate that no samples were collected during those tests due to previous test failures

TABLE 5 NONWOVEN FABRIC TEST VOLUME-WEIGHTED MEAN TURBIDITY AND SSC RESULTS DURING THE RAIN EVENT

Slope % (Ratio)	Rainfall Intensity (mm/h)	Rainfall Events	Volume-Weighted Mean Turbidity			Volume-Weighted Mean SSC		
			Up-stream (NTU)	Down-stream (NTU)	Performance Efficiency (%)	Up-stream (mg/L)	Down-stream (mg/L)	Performance Efficiency (%)
33% (3:1) Slope	25	#1	29690	13544	54	27767	9356	66
		#2	39009	2467	94	25079	3001	88
		#1R	46765	24193	48	33356	16805	50
		#2R	18628	9623	48	22205	8753	61
	76	#1	40355	18276	55	31706	14155	55
		#2	32081	11134	65	24753	9700	61
		#1R	26588	20144	24	19271	12361	36
		#2R	24696	12370	50	19142	9423	51
	127	#1	37989	21601	43	31958	17041	47
		#2	--	--	--	--	--	--
		#1R	37008	16518	55	26679	13855	48
		#2R	18925	12308	35	13685	6012	56
25% (4:1) Slope	25	#1	24380	12494	49	21495	9037	58
		#2	20556	7308	64	17723	5361	70
		#1R	22906	16882	26	18459	11691	37
		#2R	22996	9191	60	17807	7024	61
	76	#1	8780	7861	10	6547	6682	-2
		#2	6976	5567	20	5256	4204	20
		#1R	8244	6002	27	5608	4274	24
		#2R	3915	2431	38	2720	1107	59
	127	#1	7772	6282	19	5544	4465	19
		#2	19213	10394	46	14032	8048	43
		#1R	14489	8965	38	13018	6301	52
		#2R	8384	4284	49	7123	3221	55
10% (10:1) Slope	25	#1	13512	1848	86	14449	1327	91
		#2	13824	2101	85	14555	2136	85
		#1R	6631	2512	62	5962	1891	68
		#2R	9973	3539	65	7318	2660	64
	76	#1	9472	4769	50	10330	3303	68
		#2	10282	2686	74	11088	2222	80
		#1R	7217	5072	30	5932	3611	39
		#2R	4736	1545	67	3441	1178	66

Slope % (Ratio)	Rainfall Intensity (mm/h)	Rainfall Events	Volume-Weighted Mean Turbidity			Volume-Weighted Mean SSC		
			Up- stream (NTU)	Down- stream (NTU)	Performance Efficiency (%)	Up- stream (mg/L)	Down- stream (mg/L)	Performance Efficiency (%)
		#1	12466	7966	36	7147	4606	36
	127	#2	14303	5764	60	10503	2715	74
		#1R	8629	5817	33	6416	4544	29
		#2R	6044	3298	45	4779	2457	49

Table entries that appear with "--" indicate that no samples were collected during those tests due to previous test failures

Table 4 and TABLE 5 show the volume-weighted mean influent and effluent, and efficiency values for both the turbidity and SSC for both fabrics for every test during the rain event. These results show that overall for the woven fabric, turbidity performance efficiency during the rain event for all slopes and intensities tested ranged from 19 to 70 percent with a mean and median of 40 and 38 percent, respectively. The SCC performance efficiency ranged from 14 to 78 percent with a mean and median of 39 and 37 percent, respectively. For the nonwoven fabric, performance efficiency during the rain event ranged from 10 to 94 percent with a mean and median of 49 percent, and from negative 2 to 91 percent with a mean of 53 percent and a median of 55 percent for the turbidity and SCC, respectively. From these results, a Wilcoxon rank sum test was performed to determine if the nonwoven fabric performance efficiencies were significantly higher than those occurring with the woven fabric. The test was completed using the volume-weighted mean efficiencies that were shown in Table 4 and TABLE 5 for each embankment slope. The results of these tests are shown in Table 28 of Appendix B. The statistical analysis showed that the nonwoven fabric significantly reduced both turbidity and SSC to a greater extent than the woven fabric over the combination of all embankment slopes.

The greater reduction by the nonwoven fabric can be attributed to the smaller pore size of this fabric when compared to the woven fabric.

Fabric Reduction Efficiency based on Embankment Slope

For each fabric, testing was completed on three embankment slopes; 10, 25, and 33 percent slopes. Comparison between the efficiency values occurring between slopes can give insight into a possible relation of silt fence effectiveness with change in slope. The comparison was done using a single factor ANOVA analysis in order to test if the efficiency values occurring on each slope stem from the same underlying distribution. If the ANOVA test were to be significant, it would indicate that the efficiency values occurring on at least one of the slopes differed significantly from the others. The analyses were done on the volume-weighted mean efficiency values for all embankment slopes (that is, 10, 25 and 33 percent) during the rainfall event. The results and discussion of these tests are presented in the following two sections for the woven and nonwoven fabrics.

Woven Fabric Performance Efficiency based on Embankment Slope

Results showed that during rainfall, the woven fabric had 40 and 39 percent turbidity and SSC performance efficiencies, respectively, for all embankment slopes and rainfall intensities. Statistical analysis shows however that the efficiency values of both turbidity and SSC were significantly different when compared on different embankment slopes as shown in Table 32 of Appendix B. The changes in the turbidity and SSC performance efficiency with changes in slope are shown graphically in Figure 9 and FIGURE 10, respectively.

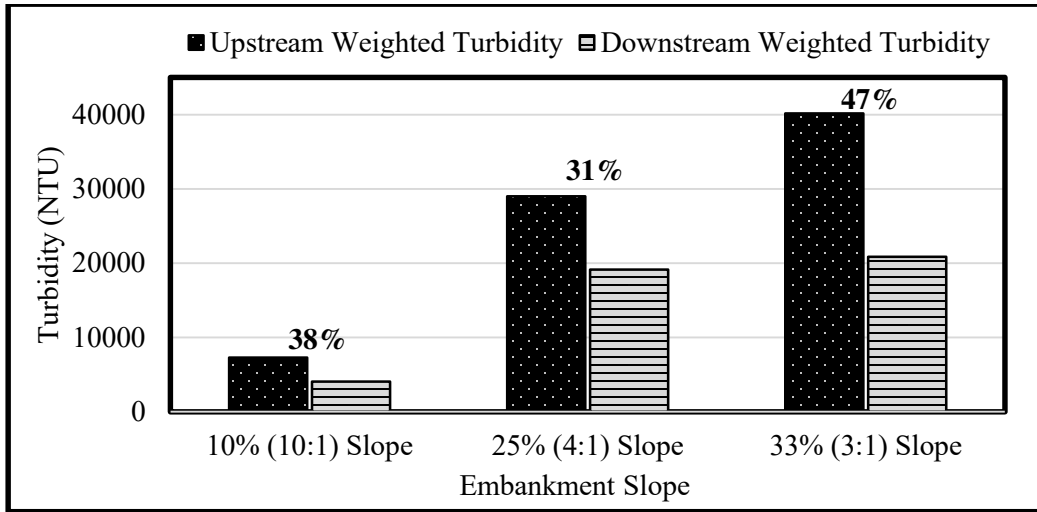


FIGURE 9 WOVEN FABRIC VOLUME-WEIGHTED MEAN TURBIDITY PERFORMANCE EFFICIENCY WITH EMBANKMENT SLOPE

Shown directly above both bars on each embankment slope is the average performance efficiency on the respective embankment slope. The highest mean performance efficiency occurred on the 33 percent embankment slope and the lowest efficiency occurred on the 25 percent slope.

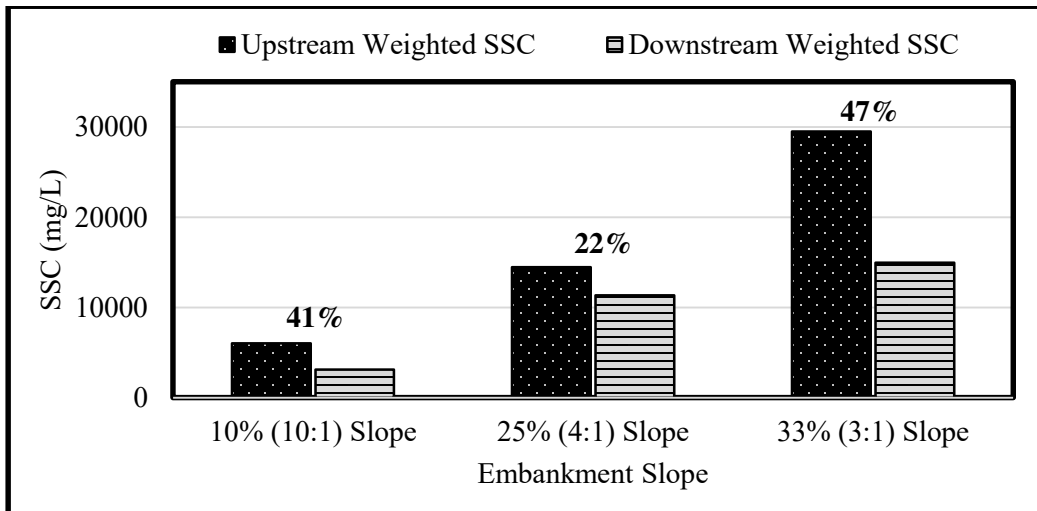


FIGURE 10 WOVEN FABRIC VOLUME-WEIGHTED MEAN SSC PERFORMANCE EFFICIENCY WITH EMBANKMENT SLOPE

Results for the SCC performance efficiency show a similar trend to those of the turbidity, with efficiencies of 41 and 47 percent on 10 and 33 percent slopes, respectively, but with mean performance efficiency of only 21 percent on the 25 percent slope. Once again, the lowest mean efficiencies occurred on the 25 percent slope. It is not completely understood why the performance efficiency decreased on the 25 percent slope, however, a possible theory is given in the following section.

Although there was not much of a trend in performance efficiency with degree of slope, Figure 9 and FIGURE 10 show the significant increase in both upstream and downstream turbidity and sediment concentrations with increases in slope percent, respectively. The reason for the increasing trend was due to the increase in the rate of erosion caused by increasing degree of slope; as the degree of slope increased, erosion rate increased, and more particles were available to runoff through the silt fence. The trend shows that although performance efficiency was similar on 10 and 33 percent embankment slopes, the effluent turbidity and sediment concentrations were significantly higher on the 33 percent slope. It is also interesting that even though the lowest volume-weighted mean reduction efficiencies occurred on 25 percent embankment slopes, the volume-weighted mean effluent turbidity and concentration were still lower on the 25 percent slope when compared to the 33 percent slope due to the higher erosion rate occurring on the 33 percent slope.

Nonwoven Fabric Reduction Efficiency Based on Embankment Slope

For the nonwoven fabric, performance results during rainfall event showed that turbidity and SSC were reduced by a mean value of 49 and 53 percent, respectively, for all embankment slopes and rainfall intensities. Similar to the woven fabric, statistical analysis on

the nonwoven fabric as shown in Table 33 of Appendix B showed that the efficiency values of both turbidity and SSC were significantly different when compared on different embankment slopes. The changes in the turbidity and SSC performance efficiency with changes in slope are shown in Figure 11 and FIGURE 12, respectively.

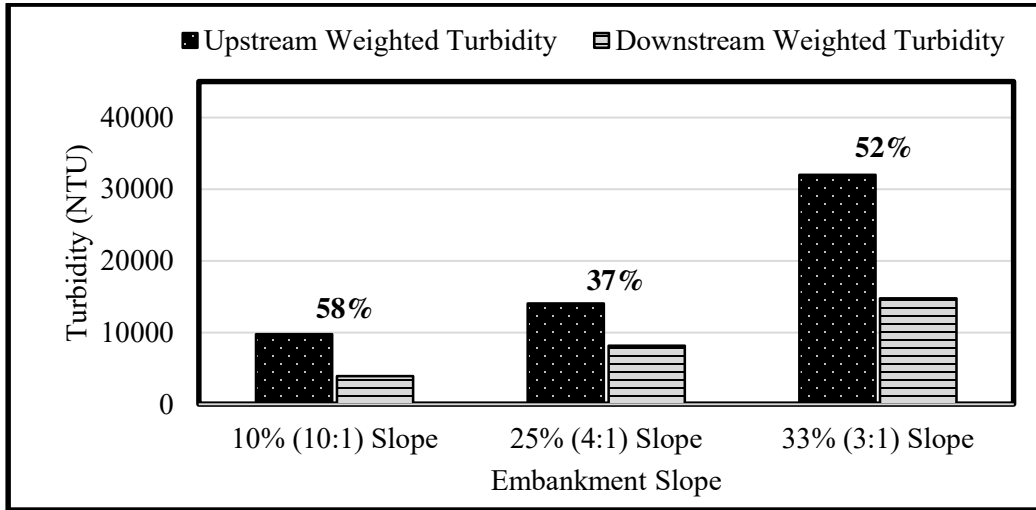


FIGURE 11 NONWOVEN FABRIC VOLUME-WEIGHTED MEAN TURBIDITY PERFORMANCE EFFICIENCY WITH EMBANKMENT SLOPE

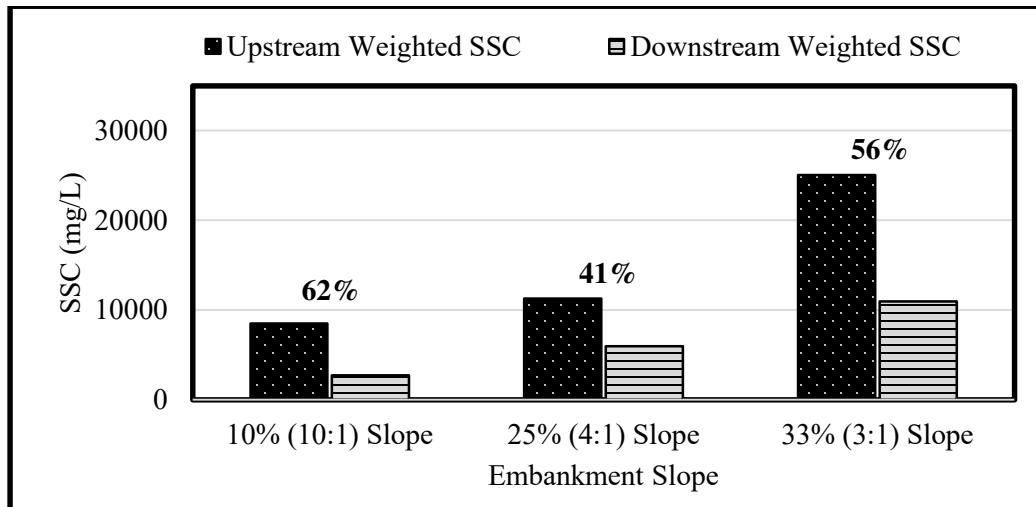


FIGURE 12 NONWOVEN FABRIC VOLUME-WEIGHTED MEAN SSC PERFORMANCE EFFICIENCY WITH EMBANKMENT SLOPE

For the nonwoven fabric the average volume-weighted performance efficiencies were 58 and 62 percent for the turbidity and SSC on the 10 percent slope, 37 and 41 percent for the turbidity and SSC on the 25 percent slope, and 52 and 56 percent for the turbidity and SSC on the 33 percent slope. These results show that the average performance efficiencies of both turbidity and SSC were higher on the nonwoven fabric than on the woven fabric for the three embankment slopes tested.

As was the case with the woven fabric, the 25 percent slope had the lowest performance efficiencies of both turbidity and SSC, and the efficiency on this slope was significantly different from the reduction on 10 and 33 percent slopes. A possible explanation for this trend, which occurred on testing with both silt fence fabrics, could be due to the effect of settling and filtering on these slopes. On the high slope of 33 percent, the erosion rate was very high, leading to a large amount of suspended sediment in the upstream ponding volume. Due to the large portion of suspended sediment, the filtering of the fabric was increased due to increased opportunity for particles to clog the pore spaces of the fabric; leading to a relatively high efficiency on the 33 percent slope. On the lower slope of 10 percent, the amount of suspended particles in the pond was much lower due to the decreased erosion rate. However, due to the low slope, the ponding volume height is also much lower; possibly allowing a large portion of the suspended solids within the ponding volume to settle before discharging through the silt fence and leading once again to a relatively high efficiency. On the 25 percent slope, based on geometry of the slope and assuming a constant flow-through rate, the ponding height would be 2.5 times that of the 10 percent slope, which would lead to a much smaller portion of the suspended mass settling out than was the case with the 10 percent slope. The ponding depth on the 25 percent slope would

be much closer to the case of the 33 percent slope, with the ponding depth on the 33 percent slope only being 1.3 times higher than on the 25 percent slope. Although the ponding depths would be similar, the added erosion caused from increasing the slope from 25 to 33 percent led to the upstream suspended solids concentration doubling as shown in Figure 10 and FIGURE 12. The settling taking place on the 25 and 33 percent slopes would therefore be similar but the filtering on the 33 percent slope would be much larger due to the much higher influent SSC. This is a possible explanation for why the performance efficiency is seen to decrease on the 25 percent slope when compared to the 10 and 33 percent slopes. This result also shows that it is likely that if a constant influent concentration were to be used for all three embankment slopes, there would most likely be a trend of decreasing efficiency with increasing embankment slope.

Fabric Reduction Efficiency from Test 1 to Test 2

For each rainfall intensity and embankment slope, four tests were completed on each fabric. Test 1 was performed on a new silt fence material and Test 2 was performed on the silt fence used in Test 1 without any maintenance being performed on the silt fence. These two tests were then repeated on a new silt fence under the same intensity and slope. Comparison between Test 1 and Test 2 can help show how silt fence fabric performance is affected by being used previously without having any maintenance performed. The comparison was done using a Wilcoxon signed rank test and was completed in order to determine if a change in performance efficiency was significant between Test 1 and Test 2 for both fabrics. The signed rank test was completed on the time dependent efficiency values between each test that occurred during the rain event. The results and discussion of these tests are shown in the following two sections for the woven fabric and the nonwoven fabric, respectively.

Woven Fabric Reduction Efficiency from Test 1 to Test 2

A summary of the volume-weighted mean turbidity and SCC performance efficiencies that occurred on the woven fabric from Test 1 to Test 2 are shown in Table 6.

TABLE 6 WOVEN FABRIC TURBIDITY AND SCC PERFORMANCE EFFICIENCY FROM TEST 1 TO TEST 2

Slope % (Ratio)	Rainfall Intensity (mm/h)	Rainfall Events	Volume-Weighted Mean Turbidity Efficiency (%)		Volume-Weighted Mean SSC Efficiency (%)	
			Test 1 (New Fabric)	Test 2 (Used Fabric)	Test 1 (New Fabric)	Test 2 (Used Fabric)
33% (3:1) Slope	25	#1, #2	51	50	58	34
		#1R, #2R	35	43	37	48
	76	#1, #2	55	--	67	--
		#1R, #2R	51	45	43	34
	127	#1, #2	64	--	67	--
		#1R, #2R	53	30	54	40
25% (4:1) Slope	25	#1, #2	24	28	26	13
	76	#1, #2	25	23	18	17
	127	#1, #2	53	41	22	35
10% (10:1) Slope	25	#1, #2	36	69	40	78
		#1R, #2R	61	49	66	42
	76	#1, #2	30	26	33	37
		#1R, #2R	33	24	31	25
	127	#1, #2	36	42	41	44

Table entries that appear with "--" indicate that no samples were collected during those tests due to previous test failures.

Overall, the volume-weighted mean turbidity efficiency for all tests from Test 1 to Test 2 showed a slight decrease; having mean performance efficiency of 44 percent on Test 1 and mean efficiency of 39 percent on Test 2. The volume-weighted mean SSC for all tests was similar as well; having mean performance efficiency of 43 percent on Test 1 and mean efficiency of 37 percent on Test 2.

The statistical analysis however, showed that a change in fabric efficiency was not significant with 95 percent confidence from Test 1 to Test 2. The statistical analysis is shown in Table 34 and Table 35 of Appendix B for the turbidity and SSC, respectively.

The overall decrease in efficiency from Test 1 to Test 2 may indicate that the woven fabric pore spaces were stretched and enlarged from Test 1 to Test 2. The pore spaces could have been enlarged due to the stress brought on by the ponding volume on the silt fence from the previous test. The increase in pore size would have decreased the filtration ability of the fabric, decreasing the filtration mechanism of the woven fabric from Test 1 to Test 2. Previous studies by (Gogo-Abite 2012) have indicated a similar result of the pore sizes of the woven fabric increasing due to increased ponding depth on the upstream side of the silt fence. However, results from this study show that a change in efficiency between Test 1 to Test 2 was not significant with the woven fabric.

Nonwoven Fabric Reduction Efficiency from Test 1 to Test 2

Statistical analysis on the change in turbidity and SSC performance efficiency from Test 1 to Test 2 of nonwoven fabrics is shown in Table 36 and Table 37 of Appendix B. Table 7 shows a summary of the performance efficiencies that occurred from Test 1 to Test 2 for the nonwoven fabric.

TABLE 7 NONWOVEN FABRIC TURBIDITY AND SSC PERFORMANCE EFFICIENCY FROM TEST 1 TO TEST 2

Slope % (Ratio)	Rainfall Intensity (mm/h)	Rainfall Events	Volume-Weighted Mean Turbidity Efficiency (%)		Volume-Weighted Mean SSC Efficiency (%)	
			Test 1 (New Fabric)	Test 2 (Used Fabric)	Test 1 (New Fabric)	Test 2 (Used Fabric)
33% (3:1) Slope	25	#1, #2	56	94	67	88
		#1R, #2R	49	49	50	61
	76	#1, #2	56	66	58	62
		#1R, #2R	27	50	38	50
	127	#1, #2	47	--	48	--
		#1R, #2R	58	38	51	58
25% (4:1) Slope	25	#1, #2	49	64	59	70
		#1R, #2R	27	58	37	59
	76	#1, #2	13	20	1	20
		#1R, #2R	32	39	30	59
	127	#1, #2	35	48	23	45
		#1R, #2R	40	51	55	57
10% (10:1) Slope	25	#1, #2	86	85	91	85
		#1R, #2R	64	65	71	64
	76	#1, #2	50	74	68	80
		#1R, #2R	32	67	42	66
	127	#1, #2	39	60	39	74
		#1R, #2R	34	46	30	49

Table entries that appear with "--" indicate that no samples were collected during those tests due to previous test failures.

The overall volume-weighted mean efficiency values that occurred for the nonwoven fabric from Test 1 to Test 2 were 44 to 57 percent and 48 to 62 percent for the turbidity and SSC efficiencies, respectively. The statistical analysis showed that there was a significant increase in the turbidity and sediment performance efficiencies from Test 1 to Test 2 on 10, 25, and 33 percent slopes for the nonwoven fabric. These results indicate that clogged particles within and on the fabric from previous tests influenced the performance of the nonwoven fabric and led to

the increase in efficiency from Test 1 to Test 2. The clogged particles would have increased the efficiency from Test 1 to Test 2 because they would decrease the pore size of the fabric and allowed additional filtration to occur.

In general, both impingement of particles on the fabric and pore space enlargement due to ponding water will affect the performance of silt fence from Test 1 to Test 2, as well as over the lifespan of the silt fence in the field over many rainfall events. Although both mechanisms will contribute to the future performance of the silt fence, from the results of the field scale testing of these two fabrics indicate that the dominate mechanism for the nonwoven fabric was the impingement of particles on the fabric which increased the efficiency of the silt fence. The dominating mechanism for the woven fabric however could not be determined with a significant degree of confidence.

Flow-through rate during the Rain Event

The water flux through the silt fence fabrics, herein referred to as flow-through rate, is a measure of the volume of water that flows through the silt fence per unit area of silt fence. In this study the flow-through rate is calculated as the volume of water which flowed through the fabric in time interval t , divided by the average area of submerged silt fence during the same time period as expressed in Equation 10. For each test, the calculated flow-through rate for each time interval during the rain event was then averaged to obtain a representative mean flow-through rate for each test as expressed in Equation 11. Table 8 presents summary results for the average flow-through rate encountered on each embankment slope during the rain event for each fabric.

$$q_i = \frac{V_{downstream}}{\left[\frac{1}{2}*(PD_{i-1}+PD_i)\right]*b_{TB}*\Delta t} \quad (10)$$

$$q_{DR} = \frac{\sum_{i=2}^n q_i}{n-1} \quad (11)$$

where, i refers to the time dependent order with which the ponding depth upstream of the silt fence is measured; n refers to the number of measurements taken; q_i is the flow-through rate of the silt fence fabric during the rain event occurring during measurement i ($L/m^2/h$); q_{DR} is the average flow-through rate occurring during the rain event; $V_{\text{downstream}}$ is the volume of collected runoff which discharged through the silt fence in interval between measurement $i - 1$ and measurement i (L); PD_i is the ponding depth occurring at measurement i ; b_{TB} is the width of the test bed; and Δt is the time interval between measurement $i - 1$ and measurement i .

TABLE 8 SUMMARY RESULTS FOR FLOW-THROUGH RATE OF WOVEN AND NONWOVEN FABRICS DURING THE RAIN EVENT

Embankment Slope (%)	Rainfall Intensity (mm/h)	Flow-through rate ($L/m^2/h$)					
		Woven Fabric			Nonwoven Fabric		
		Mean	Median	Standard Deviation	Mean	Median	Standard Deviation
33	25	60	57	42	310	293	176
	76	132	103	74	416	442	231
	127	72	64	27	460	419	289
25	25	125	128	26	880	973	460
	76	214	178	96	1512	1566	234
	127	397	377	177	1155	1136	624
10	25	830	902	408	1267	766	1018
	76	1494	1448	570	2377	2248	837
	127	1360	1376	209	2564	2686	1266

Results from Table 8 show that nonwoven fabric achieved a higher mean flow-through rate during the rain event on every slope and intensity pair tested. Higher flow-through rates would decrease the chances of developing high ponding depths which could lead to silt fence

failure or overtopping of the silt fence. Lower flow through rates, however, would decrease the volume of water that is discharged during the rain event. This would lead to a higher overall efficiency of the silt fence as will be discussed in this chapter in the section: Overall Performance Efficiency (Projected).

The results also suggest a trend of increasing flow-through rate with decreasing embankment slope. The mean flow-through rate is shown to increase by approximately a magnitude when comparing results on the 33 percent slope to those on the 10 percent slope. For the woven fabric, the flow-through rate is shown to range from 57 L/m²/h on a 33 percent slope to 1494 L/m²/h on a 10 percent slope, and in the case of the nonwoven fabric, from 310 L/m²/h on a 33 percent slope to 2564 L/m²/h on a 10 percent slope.

A statistical analysis was performed in order to determine if the trend of increasing flow-through rate with decreasing embankment slope was significant during the tests. The statistical analysis was completed by performing a Wilcoxon rank sum test between the time dependent flow-through rate values on 10 and 25 percent slopes and then again between the flow-through rate values on 25 and 33 percent slopes for both fabrics. The results of these statistical analyses are shown in Table 40 and Table 41 of Appendix C for the woven and nonwoven fabrics, respectively. Results revealed that the flow-through rate of both silt fence fabrics was significantly higher on the 10 percent slope when compared to the 25 percent slope and that the flow-through rates were also significantly higher on the 25 percent slope when compared to the 33 percent slope.

The results of this statistical analysis; decreases in flow-through rate with increases in embankment slope, goes against what would be commonly expected. In theory, given clean

water, an increase in embankment slope should cause an increase in the flow-through rate, not a decrease. The reason for this is that the ponding depth behind the silt fence will be higher on the higher slope if the influent water volume remains constant. Higher ponding depths would cause a larger force on the silt fence and would cause the pores of the fabric to be enlarged, increasing the flow-through rate of the fabric. The result from this study however shows the opposite; that increases in embankment slope caused a decrease in the flow-through rate.

The observed contradiction is because the flow-through rate is directly related to the concentration of suspended sediment in contact with each fabric. Recall from Figure 10 and Figure 12 that the erosion rate and the concentration of upstream suspended solids increased with increasing embankment slope. The increase in upstream SSC led to a decrease in the flow-through rate because the mass of particles that had the potential to be filtered by the fabric increased. Filtering of the soil particles by the fabric clogged the fabrics pores and decreased the ability of the fabric to transmit water. Risse et al. (2008) and Britton et al. (2000) also observed that increasing sediment concentration led to a decrease in flow-through rate of silt fence. Figure 13 shows the trend of decreasing flow-through rate with increasing upstream suspended sediment concentration encountered for both the woven and nonwoven fabrics for this soil type.

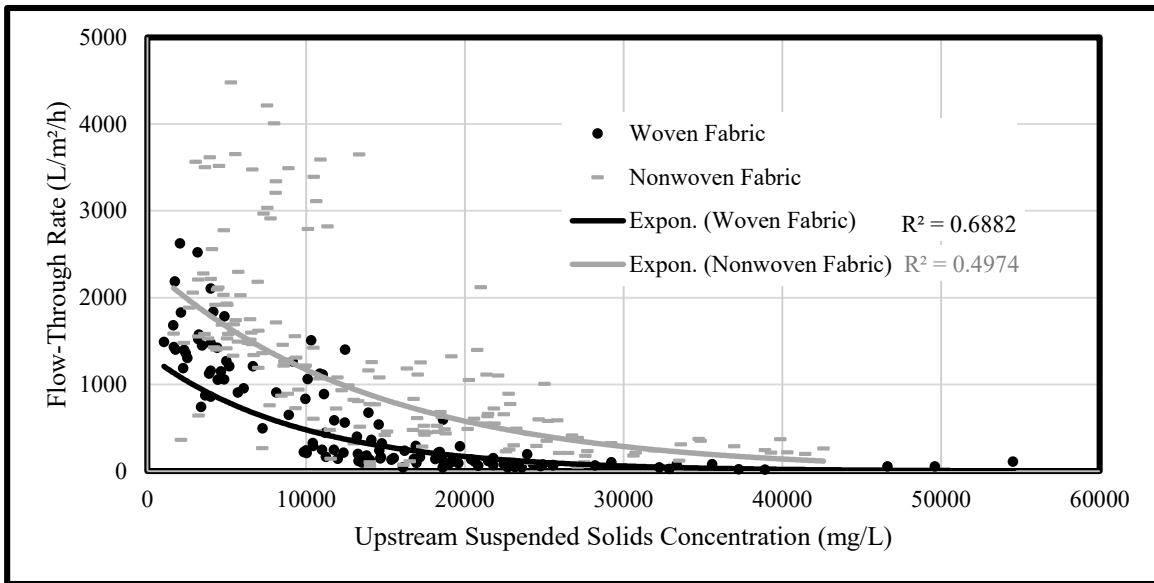


FIGURE 13 TREND OF DECREASING FLOW-THROUGH RATE WITH INCREASING UPSTREAM SSC FOR BOTH WOVEN AND NONWOVEN FABRICS

Figure 13 is a plot of the SSC in the ponding water volume upstream of the silt fence (x-axis) verse the average flow-through rate of the silt fence (y-axis). Note that the plot is only of samples taken during the rain event. In total, 112 samples for the woven fabric and 163 samples for the nonwoven fabric. According to Figure 13, the flow-through rate tended to decrease exponentially with increases in the upstream solids concentration ($R^2 = 0.69$ for the woven fabric and $R^2 = 0.52$ for the nonwoven fabric). This trend was due to the increased filtering and impingement of soil particles on the fabric with increases in the SSC in contact with the silt fence. This increase in filtering caused reduction of the fabric pore size and limited the ability of water to flow through the silt fence. The plot shows how strongly influenced the flow-through rate of silt fence fabrics can be on the concentration of suspended solids in contact with them. The plot also shows that the flow-through rates encountered in the field are more a function of the upstream suspended solids concentration than the initial permittivity or AOS of the fabric.

It would have been interesting to test the effect of changing upstream SSC on the flow-through rate of used fabrics. For instance, testing the fabric under a high slope (high concentration) condition during Test 1. Then, during Test 2, testing the same silt fence under a lower slope (lower concentration) condition to see if the high influent concentration from Test 1 would have affected the flow-through rate encountered in Test 2. In this study, these tests were not conducted, however, changing rainfall intensity under the same embankment slope was, and is the topic of the next section.

Comparing flow-through rate from Test 1 to Test 2

Comparing the flow-through rate of the silt fence from Test 1 to Test 2 can give insight into how the fabric is affected by multiple rain events occurring without maintenance being performed. A Wilcoxon signed rank test on the difference between Test 1 and Test 2 was completed on the time dependent flow-through rate values to determine if a significant change in the flow-through rate occurred from Test 1 to Test 2 for each embankment slope. The test was conducted on the difference between Test 1 and Test 2 because the flow-through rate data show a trend of increasing with time during the rain event due to the increasing ponding depth. For this reason, the statistical analysis is performed by pairing the flow-through rates on a time dependent basis between Test 1 and Test 2. The statistical analysis is shown in Table 42 of Appendix C for both woven and nonwoven fabrics.

The mean flow-through rates for both fabrics occurring on Test 1 and Test 2 during the rain event are presented in Table 9 for each embankment slope and intensity pair tested.

TABLE 9 AVERAGE FLOW-THROUGH RATE OCCURRING DURING THE RAIN EVENT BETWEEN TEST 1 AND TEST 2 FOR BOTH WOVEN AND NONWOVEN FABRICS

Slope % (Ratio)	Rainfall Intensity (mm/h)	Rainfall Events	Average Flow-through rate During the Rain Event (L/m ² /h)			
			Woven Fabric		Nonwoven Fabric	
			Test 1 (New Fabric)	Test 2 (Used Fabric)	Test 1 (New Fabric)	Test 2 (Used Fabric)
33% (3:1) Slope	25	#1, #2	27	68	198	228
		#1R, #2R	44	102	340	476
	76	#1, #2	131	--	254	324
		#1R, #2R	97	167	583	504
	127	#1, #2	154	--	344	--
		#1R, #2R	51	--	389	648
25% (4:1) Slope	25	#1, #2	117	132	636	411
		#1R, #2R	--	--	1386	1085
	76	#1, #2	167	260	1620	1629
		#1R, #2R	--	--	1433	1368
	127	#1, #2	370	424	1985	652
		#1R, #2R	--	--	1091	892
10% (10:1) Slope	25	#1, #2	805	1279	464	604
		#1R, #2R	244	992	1142	2859
	76	#1, #2	2057	1516	3384	1293
		#1R, #2R	1129	1272	2690	2141
	127	#1, #2	1458	1262	1513	1265
		#1R, #2R	--	--	3774	3702

Table entries that appear with "--" indicate that the flow-through rate could not be calculated during these tests due to test failures

The statistical analysis showed that, for the woven fabric, there was a trend of increasing flow-through rate from Test 1 to Test 2 on the combination of all embankment slope tested. This trend was also significant on the 25 and 33 percent slopes, however, it was not significant on the 10 percent slope. The increase in flow-through rate suggest that the pore spaces

of the fabric increased from Test 1 to Test 2, allowing an increase in the rate at which water was allowed to flow through the silt fence.

The statistical analysis also showed that, for the nonwoven fabric, there was a trend of decreasing flow through rate from Test 1 to Test 2 on 10 and 25 percent slopes, however the trend was only significant with 95 percent confidence on the 25 percent slope. The decrease in flow-through rate conforms with the results from the section: Nonwoven Fabric Reduction Efficiency from Test 1 to Test 2, in which the reduction efficiency was found to increase from Test 1 to Test 2. These tests suggest that it is likely that the impingement of particles within the fabric decreased the pore size of the fabric and caused both an increase in the reduction efficiency and a decrease in the flow-through rate from Test 1 to Test 2.

However, for the nonwoven fabric on the 33 percent slope, the statistical analysis showed that there was a trend of increasing flow-through rate from Test 1 to Test 2, but the result was not significant for 95 percent confidence interval. Although the trend suggest an increase in flow-through rate from Test 1 to Test 2, review of the time dependent flow-through rate results shown in Table 51 of Appendix C suggest that the impingement of particles within the fabric from Test 1 did decreased the flow-through rate of this fabric in Test 2. The decrease in flow-through rate however only occurred for the first couple of samples taken. The reason for this is shown graphically in Figure 14 below for testing done on a 33 percent slope and 76 mm/h rainfall event on the nonwoven fabric.

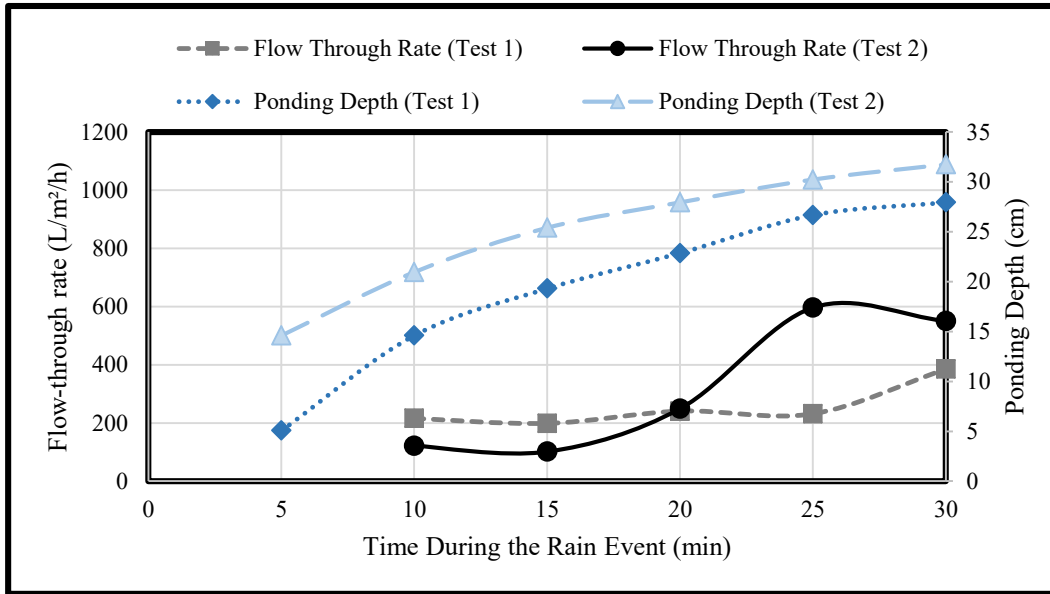


FIGURE 14 NONWOVEN FABRIC CHANGE IN FLOW RATE WITH CHANGE IN PONDING DEPTH BETWEEN TEST 1 AND TEST 2 ON A 33 PERCENT SLOPE

Figure 14 shows the flow-through rate and ponding depth during Test 1 and Test 2 on a 33 percent slope and a 76 mm/h rainfall event for the nonwoven fabric. Results for other tests on the 33 percent slope show similar trends. Note the point where the ponding depth during Test 2 surpasses the maximum ponding depth that occurred during all of Test 1. This point occurs at minute 20 at a ponding depth of 30 cm. During Test 2, when the ponding depth is less than the maximum ponding depth that occurred during Test 1, the flow-through rate is less than the flow-through rate during Test 1. This indicates that impingement of particles within the fabric from Test 1 decreased the flow-through rate that occurred during Test 2. However, at minute 20 of Test 2, the ponding depth became higher than the maximum depth that occurred during Test 1 and the flow-through rate increased substantially. The increase in flow-through rate was because the ponding water was no longer influenced by the impinged particles from Test 1.

This trend and the overlying results with the nonwoven fabric show its susceptibility to forming a filter cake within and on its fabric. Although the woven fabric also filters the concentrated water, the impingement of particles within this fabric did not seem to affect its performance in future tests. It is possible that once the woven fabric is given time to dry, the impinged particles fall off the surface of the fabric. However, for the nonwoven fabric, the particles remained impinged within the fabric itself and affected its future performance.

Figure 15 shows the filter cake formation on the nonwoven fabric over the span of Test 1 and Test 2. When the concentrated water was in contact with the nonwoven fabric, a filter cake formed on its surface as shown in Figure 15b. During Test 2, when the ponding depth was in contact with the fabric with filter cake on it, the flow-through rate of the fabric was decreased and the efficiency of the fabric was increased. When the ponding depth during Test 2 became higher than the filter cake from Test 1, a new filter cake started to form on this new fabric. Figure 15c shows the increase in filter cake height from Test 1 to Test 2.

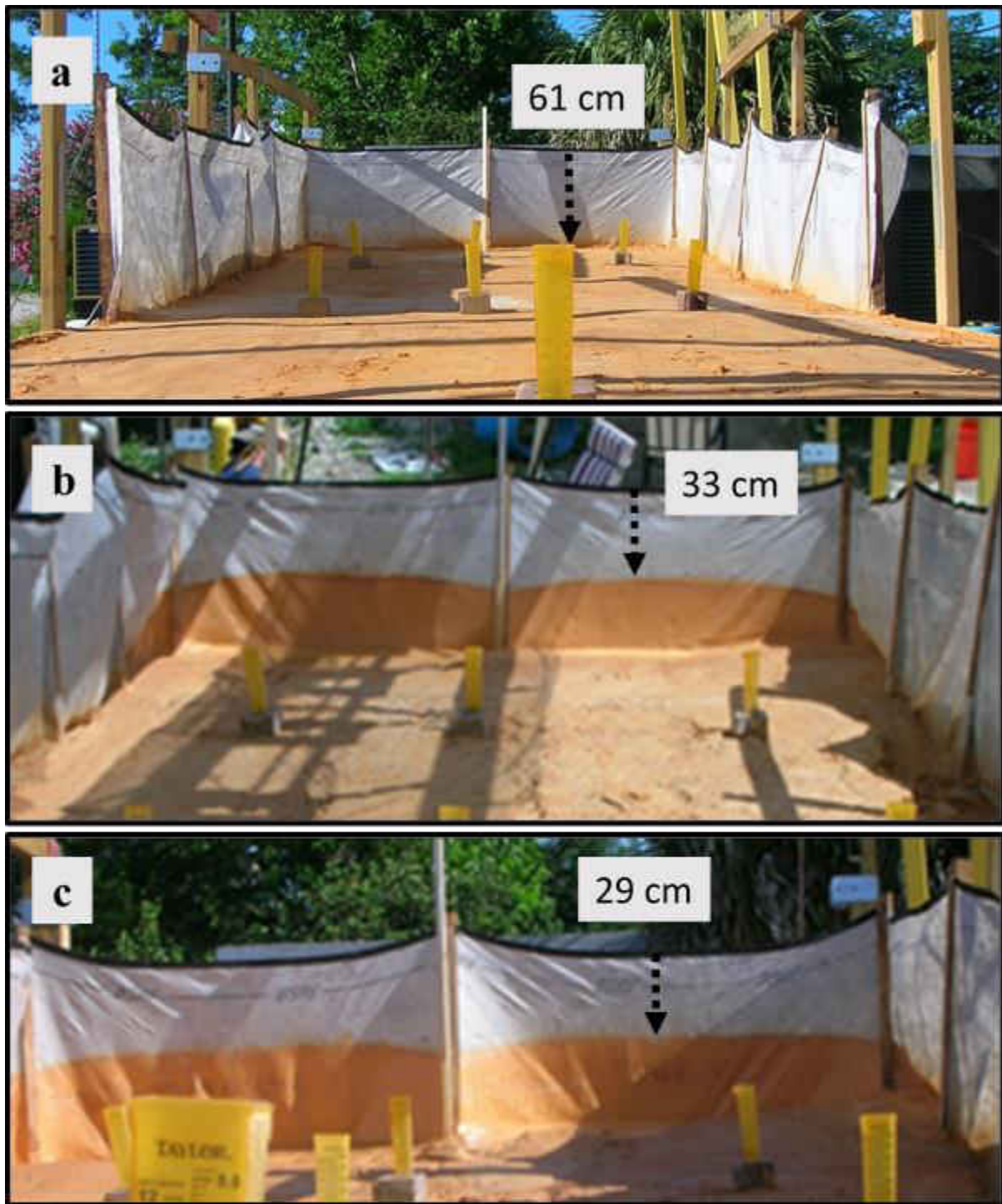


FIGURE 15 FILTER CAKE FORMATION ON NONWOVEN (A) UNTESTED FABRIC (B) CAKE FORMATION AFTER COMPLETION OF TEST 1 (C) CAKE FORMATION AFTER COMPLETION OF TEST 2

Overall, the results of the analyses show that the flow-through rate for both fabrics changed from Test 1 to Test 2. For the woven fabric, testing on the fabric caused an increase in the flow-through rate that is most likely caused by an increase in the pore size of the fabric. For the nonwoven fabric, previous testing on the fabric caused decreases in the flow-through rate due to impingement of particles within and on the fabric. It is interesting that even though the flow-through rate increased for the woven fabric and decreased for the nonwoven fabric from Test 1 to Test 2, the flow-through rates on the nonwoven fabric remained higher than the woven fabric during Test 2. It would have been interesting to test if this trend of increasing flow-through rate of the woven fabric and decreasing flow-through rate of the nonwoven fabric would have continued over additional testing on both fabrics.

Comparing flow-through rates due to changing rainfall intensity

A single factor ANOVA was performed on the flow-through rates to determine if changes in the rainfall intensity affected the flow-through rate of the fabrics on each embankment slope. Results of these tests are shown in Table 43 and Table 44 of Appendix C for the woven and nonwoven fabrics, respectively. Similar with results presented by Gogo-Abite and Chopra (2013), the rainfall intensity significantly affected the flow-through rate of the woven fabric with probabilities of 0.000, 0.000, and 0.002 for falsely rejecting the null hypotheses on 10, 25 and 33 percent slopes, respectively. The rainfall intensity also significantly affected the flow-through rate through the nonwoven fabric as well on 10 and 25 percent slopes, with probabilities of 0.001 and 0.000, respectively. The rainfall intensity however did not significantly affect the flow-through rate on the 33 percent slope for the nonwoven fabric, with probability of 0.176.

Results show that the lowest mean flow-through rates occurred on the lowest rainfall intensity of 25 mm/h for both fabrics on all embankment slopes tested. The reason for the higher flow-through rates occurring on the higher intensity rainfall events may be attributed to the fabrics stretching and elongation under stress caused by these higher intensity rainfall events. The higher rainfall intensity increases the upstream ponding volume, which causes a larger pressure on the silt fence. The increased water pressure may have caused a greater force to develop which pushed water through the fabric at a greater rate.

Silt Fence Failure

Due to the trend of decreasing flow-through rate with increasing embankment slope and the decreased storage volume on the higher slopes, the ponding depth behind the silt fence reached high levels during testing with both fabrics on the 33 percent slope. The high ponding depths increased the chance of silt fence failure by means of both tearing and ripping of the silt fence or by failure of the wooden stakes due to the increased hydrostatic pressure brought on by the high ponding depth. In addition, low flow-through rate of the silt fence caused it to fail by means of overtopping. Throughout the field scale testing with both fabrics, five silt fence failures and two overtopping events occurred over the span of all tests. The types of silt fence failures that occurred during testing are shown in Figure 16.



FIGURE 16 SILT FENCE FAILURES: (A) PULLOUT OF FABRIC FROM MIDDLE STAKE ON 33% SLOPE (B) OVERTOPPING ON 33% SLOPE (C) CORNER STAKE FAILURE ON 33% SLOPE (D) CORNER STAKE TEAR ON 25% SLOPE

For the woven fabric, it was observed that high slopes (33%) and high intensity (127 mm/h) caused the ponding water to overtop the silt fence during each rainfall event in less than 30 minutes. This failure is depicted in Figure 16b. Failures of this nature were not observed while testing the nonwoven fabric due to the ability of this fabric to transmit water at a large enough rate to avoid overtopping failures under the conditions evaluated in this study. Other failures that occurred during testing with the woven fabric include pullout of the fabric from the

stake and fabric tears occurring at corner stakes as shown in Figure 16a and Figure 16d. Pullout of the fabric from the stake occurred during only one test, on a 33 percent slope and 76 mm/h rainfall event, while the failures involving fabric tears at corner stakes occurred multiple times on 25 and 33 percent slopes. Once again, no such failures of this nature were observed for the nonwoven fabric. However, during testing on a 33 percent slope and a 127 mm/h rainfall event, a corner stake broke in half as shown on Figure 16c and caused failure to occur with the nonwoven fabric. It should be noted however, that during the repeat test on this same slope and intensity the nonwoven silt fence did not fail or overtop.

One of the reason that failures such as pullout of the fabric from the stake and fabric tearing at the corners occurred on the woven fabric and not on the nonwoven fabric was because the common woven silt fence used in this study did not come furnished with nailing strips attached to the stakes. These nailing strips are thin pieces of wood that sandwich the silt fence between the stake and the nailing strip itself. This construction helped to distribute the load caused by ponding water over the entire length of the post rather than at discrete points as would be the case if the material was just stapled without the nailing strips attached (Risse et al. 2008). The difference in strength between the fabrics may also have contributed, but it seems that the nailing strips were very helpful in preventing the nonwoven fabric from failing by pullout or tear.

Fabric Performance following Rain Events

Fabric Reduction Efficiency following Rain Events

Grab samples were collected both upstream and downstream of the silt fence for 30 minutes after rainfall ended. Samples were collected in order to determine the performance of silt fence after rainfall stopped. Under high intensity rainfall as was simulated in these tests, the flow rate of water that was transmitted through the silt fence was less than the flow rate of runoff water. For this reason a ponding volume of runoff water accumulated on the upstream side of the silt fence. When rainfall stopped, grab samples were taken both upstream and downstream of the silt fence as the ponding volume continued to flow through the fabric, in order to evaluate the performance of the silt fence after rainfall had stopped. It should be noted that samples were taken for only 30 minutes after rainfall stopped, however, the estimated hydraulic detention time of the ponding volume ranged from 1 hour to over 15 hours depending on the rainfall intensity, embankment slope, and fabric type tested. Due to the large hydraulic detention times it was not possible to collect samples over the entire time period. However, results show that performance efficiency increased with time after rainfall ended and that downstream concentration values decreased with time after rainfall ended. For this reason, the results discussed in this section, which take into account only the first 30 minutes after rainfall ended, can be thought of as conservative estimates of the true performance of silt fence after rainfall ends.

The efficiency values for after rainfall were calculated in a similar way as the during rainfall calculations. Downstream samples were weighted by the volume of water which discharged through the fabric in the time interval with which the sample was taken. The after rainfall efficiency was then calculated by comparing the after rainfall volume-weighted mean

effluent concentration to the during rainfall volume-weighted mean influent concentration. The expressions for the after rainfall efficiencies are shown in Equations 12 through 15.

$$(WMET)_{AR} = \frac{\sum_{i=0}^m [T_{eff} * V_{downstream}]}{\sum_{i=0}^m V_{downstream}} \quad (12)$$

$$(WMEC)_{AR} = \frac{\sum_{i=0}^m [TS_{eff} * V_{downstream}]}{\sum_{i=0}^m V_{downstream}} \quad (13)$$

$$E_T(\%)_{AR} = 100 * \left[1 - \frac{(WMET)_{AR}}{WMIT} \right] \quad (14)$$

$$E_{SSC}(\%)_{AR} = 100 * \left[1 - \frac{(WMEC)_{AR}}{WMIC} \right] \quad (15)$$

where, $(WMET)_{AR}$ is the volume-weighted mean effluent turbidity after rainfall (NTU);

$(WMEC)_{AR}$ is the volume-weighted mean effluent concentration after rainfall (mg/L);

$V_{downstream}$ is the volume of collected runoff which discharged through the silt fence in interval between sample i and sample $i - 1$ (L); m is the number of samples collected after rainfall;

$E_T(\%)_{AR}$ is the mean turbidity performance efficiency after rainfall; and $E_{SSC}(\%)_{AR}$ is the mean suspended sediment concentration performance efficiency after rainfall. $WMIT$ and $WMIC$

where defined previously in Equations 4 and 5, respectively. The volume-weighted mean

turbidity and suspended sediment concentrations as well as the performance efficiencies that

occurred after the rain event for both fabrics are shown in Table 10 and TABLE 11, respectively.

TABLE 10 WOVEN FABRIC TEST VOLUME-WEIGHTED MEAN TURBIDITY AND SSC RESULTS
AFTER THE RAIN EVENT

Slope % (Ratio)	Rainfall Intensity (mm/h)	Rainfall Events	Volume-Weighted Mean Turbidity			Volume-Weighted Mean SSC		
			Up- stream (NTU)	Down- stream (NTU)	Performance Efficiency (%)	Up- stream (mg/L)	Down- stream (mg/L)	Performance Efficiency (%)
33% (3:1) Slope	25	#1	50171	15791	69	32616	9010	72
		#2	33573	6159	82	23412	4973	79
		#1R	28738	5817	80	21001	4187	80
		#2R	30096	3800	87	25614	3034	88
	76	#1	43339	--	--	40099	--	--
		#2	--	--	--	--	--	--
		#1R	41442	11000	73	21641	6096	72
		#2R	27811	4579	84	17641	3677	79
	127	#1	48311	--	--	31212	--	--
		#2	--	--	--	--	--	--
		#1R	57945	--	--	46322	--	--
		#2R	40266	--	--	35427	--	--
25% (4:1) Slope	25	#1	29396	9426	68	19585	6422	67
		#2	21551	6689	69	13875	4558	67
	76	#1	19080	5993	69	13462	4380	67
		#2	25891	6760	74	11361	3558	69
	127	#1	47590	7676	84	15744	4123	74
		#2	30530	2942	90	12755	2042	84
10% (10:1) Slope	25	#1	12357	2104	83	10959	1722	84
		#2	10839	1093	90	10743	915	91
		#1R	13365	904	93	10468	787	92
		#2R	9453	1614	83	5920	1165	80
	76	#1	5358	1116	79	4215	1026	76
		#2	3707	1170	68	3426	920	73
		#1R	6036	932	85	4610	886	81
		#2R	2619	916	65	2117	789	63
	127	#1	4886	761	84	3982	781	80
		#2	4321	907	79	3763	1000	73

Table entries that appear with "--" indicate that no samples were collected during those tests due to previous test failures

TABLE 11 NONWOVEN FABRIC TEST VOLUME-WEIGHTED MEAN TURBIDITY AND SSC RESULTS AFTER THE RAIN EVENT

Slope % (Ratio)	Rainfall Intensity (mm/h)	Rainfall Events	Volume-Weighted Mean Turbidity			Volume-Weighted Mean SSC		
			Up-stream (NTU)	Down-stream (NTU)	Performance Efficiency (%)	Up-stream (mg/L)	Down-stream (mg/L)	Performance Efficiency (%)
33% (3:1) Slope	25	#1	29690	2775	91	27767	1479	95
		#2	39009	1538	96	25079	1227	95
		#1R	46765	3552	92	33356	2952	91
		#2R	18628	2103	89	22205	1914	91
	76	#1	40355	1681	96	31706	1835	94
		#2	32081	969	97	24753	851	97
		#1R	26588	802	97	19271	405	98
		#2R	24696	954	96	19142	1027	95
	127	#1	37989	--	--	31958	--	--
		#2	--	--	--	--	--	--
		#1R	37008	1312	96	26679	1075	96
		#2R	18925	460	98	13685	1235	91
25% (4:1) Slope	25	#1	24380	4230	83	21495	3298	85
		#2	20556	2981	85	17723	2053	88
		#1R	22906	1692	93	18459	1290	93
		#2R	22996	3509	85	17807	2752	85
	76	#1	8780	946	89	6547	768	88
		#2	6976	3210	54	5256	2729	48
		#1R	8244	729	91	5608	599	89
		#2R	3915	269	93	2720	237	91
	127	#1	7772	1016	87	5544	834	85
		#2	19213	4184	78	14032	319	98
		#1R	14489	1523	89	13018	1212	91
		#2R	8384	2326	72	7123	1732	76
10% (10:1) Slope	25	#1	13512	770	94	14449	647	96
		#2	13824	525	96	14555	660	95
		#1R	6631	1681	75	5962	1280	79
		#2R	9973	1812	82	7318	1476	80
	76	#1	9472	3765	60	10330	2224	78
		#2	10282	2031	80	11088	1497	87
		#1R	7217	823	89	5932	697	88
		#2R	4736	803	83	3441	696	80

Slope % (Ratio)	Rainfall Intensity (mm/h)	Rainfall Events	Volume-Weighted Mean Turbidity			Volume-Weighted Mean SSC		
			Up- stream (NTU)	Down- stream (NTU)	Performance Efficiency (%)	Up- stream (mg/L)	Down- stream (mg/L)	Performance Efficiency (%)
		#1	12466	3408	73	7147	1999	72
		#2	14303	1725	88	10503	1371	87
	127	#1R	8629	2104	76	6416	1642	74
		#2R	6044	1919	68	4779	1524	68

Table entries that appear with "--" indicate that no samples were collected during those tests due to previous test failures

The turbidity performance efficiency that occurred after the rain event in the first 30 minutes, for all slopes and intensities tested, for the woven and nonwoven fabrics had a mean of 79 and 86 percent; median of 81 and 89 percent, and ranged from 65 to 93 percent and from 54 to 98 percent, respectively. The SSC performance efficiency was similar, with mean of 77 and 87 percent; median of 77 and 89 percent; and ranged from 63 to 92 percent and from 48 to 98 percent for the woven and nonwoven fabrics, respectively.

Using the volume-weighted mean turbidity and SSC efficiencies shown in Table 10 and TABLE 11 a Wilcoxon rank sum test was completed in order to determine if the performance efficiencies on the nonwoven fabric were significantly greater than the efficiencies on the woven fabric. The results of the analysis are shown in Table 29 of Appendix B. As was the case of the results during rainfall, the after rainfall results also show that the nonwoven fabric significantly reduced both turbidity and SSC to a greater extent than did the woven fabric when analyzed on all embankment slopes combined. The greater removal by the nonwoven fabric can be attributed to the smaller pore size of the nonwoven fabric in comparison to the woven fabric.

The above performance efficiencies were normalized based on the volume-weighted mean influent turbidity and SCC occurring during the rain event. The efficiency after rainfall can also be calculated on a time dependent basis by comparing the downstream concentration that discharged through the fence at time t to the upstream concentration of the ponding volume at the same time t . In this calculation, the effect of particle settling has been largely ignored and the efficiency values are based on the filtering of the fabric at time t .

The results of these time dependent calculations are shown in Table 46 through Table 48 of Appendix D for the woven fabric and Table 49 through Table 51 of Appendix D for the nonwoven fabric. A Wilcoxon rank sum test on the difference between the during and after rainfall efficiencies was also conducted and is presented in Table 38 and Table 39 of Appendix B for the woven and nonwoven fabrics, respectively. The statistical test was conducted on both the during rainfall average performance efficiencies and the after rainfall average efficiencies in order to determine if there was a statistically significant change in performance efficiency from during rainfall to after rainfall on each embankment slope for each fabric. The results of the analysis show that the performance efficiency for both the turbidity and SSC increased significantly from during the rain event to after the rain event on all embankment slopes for both fabrics. The efficiency increase was dependent on time, as the time since rainfall ended increased, the efficiency of the fabric in removing turbidity and SSC increased. Figure 17 depicts the typical trend encountered for the increased mean turbidity performance efficiency and the decrease in effluent turbidity with time after rainfall stopped. The plot shows the average efficiencies and concentrations occurring on a 25 percent slope for both fabrics. This trend was similar on all embankment slopes and also was similar for the SSC efficiency and

concentrations. Plots associated with the other embankment slopes as well as the SSC reductions are shown in Figure 21 through Figure 25 in Appendix D.

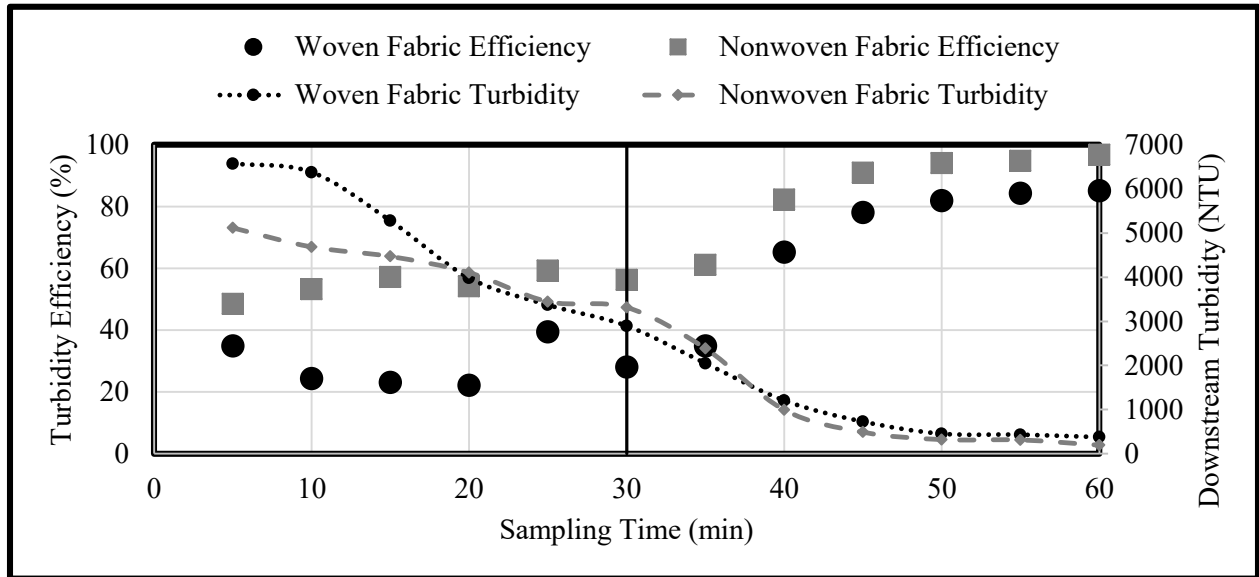


FIGURE 17 TIME DEPENDENT AVERAGE TURBIDITY REDUCTION EFFICIENCY AND DOWNSTREAM VALUE ON 10 PERCENT SLOPE

The black vertical line indicates the point at which rainfall stops. Points to the left are efficiency and turbidity values during the rain event and points to the right are efficiency and turbidity values after the rain event. After rainfall stopped the efficiency of the silt fence increased substantially with time before leveling off. The opposite is true for the downstream effluent turbidity, which decreased with time after rainfall stopped.

The increase in efficiency after rainfall ended was perhaps due to a combination of the filtration ability of the fabric and the settling of the suspended sediments. A possible theory as to why the observed filtration efficiency increased after rainfall ended is the topic of the next couple of sections. Filtration is discussed first and a discussion on sedimentation follows.

Filtration Mechanism

The ability of the silt fence fabric to filter the concentrated water volume is dependent on the opening of the pore sizes of the fabric and on the relative size distribution of soil particles in the ponding volume. At first, only those particle sizes that are in close or larger than the opening size of the fabric will be filtered, while smaller particles will pass through. However, over time, the opening size of the fabric will decrease due to impregnation of soil particles on the fabric. The filtration efficiency of the fabric will therefore increase with time as it is exposed to the concentrated water volume. This process is taking place both during and after the rain event. The efficiency values remain somewhat low and do not increase during the rain event because the ponding water volume behind the fence is constantly increasing and exposing new fabric to the concentrated water volume with time. When the concentrated water volume reaches the new fabric, the process repeats (i.e. a large portion of the soil distribution will pass through this portion of the fabric until particles become impinged it). Figure 18 shows the typical relationship between the height of ponding water behind the fence and the time dependent efficiency values.

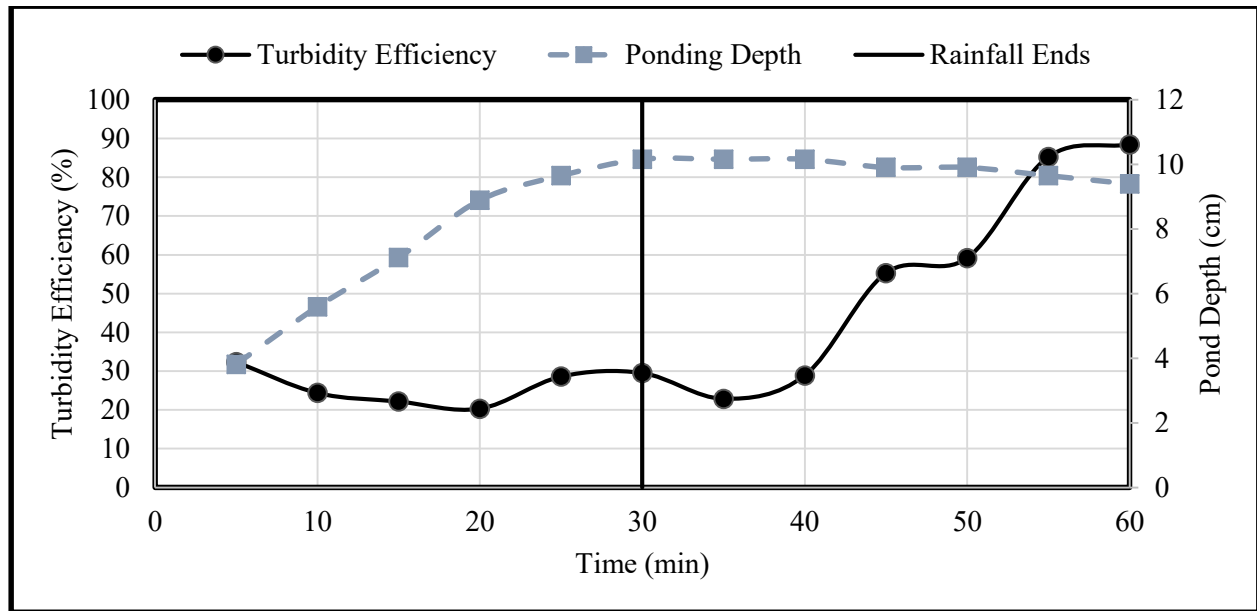


FIGURE 18 WOVEN FABRIC TIME DEPENDENT EFFICIENCY VALUES AND PONDING DEPTH ON 25 PERCENT SLOPE AND 25 MM/H RAINFALL INTENSITY

The plot shows that during the rain event, as the ponding depth is constantly increasing, exposing new fabric to the ponding water volume, the efficiency values remain relatively low and constant. When rainfall stopped, the efficiency of the silt fence system started to increase with time. This increase with time was due in part to the clogging mechanism described above, however, the main mechanism by which the efficiency increased was likely due to the concentration gradient which forms within the pond after rainfall ends. Settling and concentration gradient is discussed below.

Settling Mechanism

In the ponding volume upstream of the silt fence a vertical concentration gradient exists due to settling. The lowest concentration exists at the top of the pond and the concentration

increases as the depth increases. The increasing concentration gradient that forms after the rain event ends is most likely main reason for the observed increasing efficiency.

During the rain event, the concentration gradient was not as noticeable as it was after the rain event. Falling rainfall impacting the ponding volume as well as sheet flow colliding with the ponding volume decreased the potential for the suspended sediments to settle. Although, these collisions may disrupt sedimentation, the suspended particles will still settle during the rain event. However, new sediment is constantly being introduced into the ponding volume replacing particles which have settled. Therefore, during the rain event, a noticeable concentration gradient did not form and the concentration throughout the vertical height of ponding water remained relatively constant.

When rainfall stops, no new sediment is introduced into the ponding water volume and a concentration gradient starts to form as suspended particles settle. Figure 19 shows a possible trend of the concentration gradient which may form over time after rainfall ends.

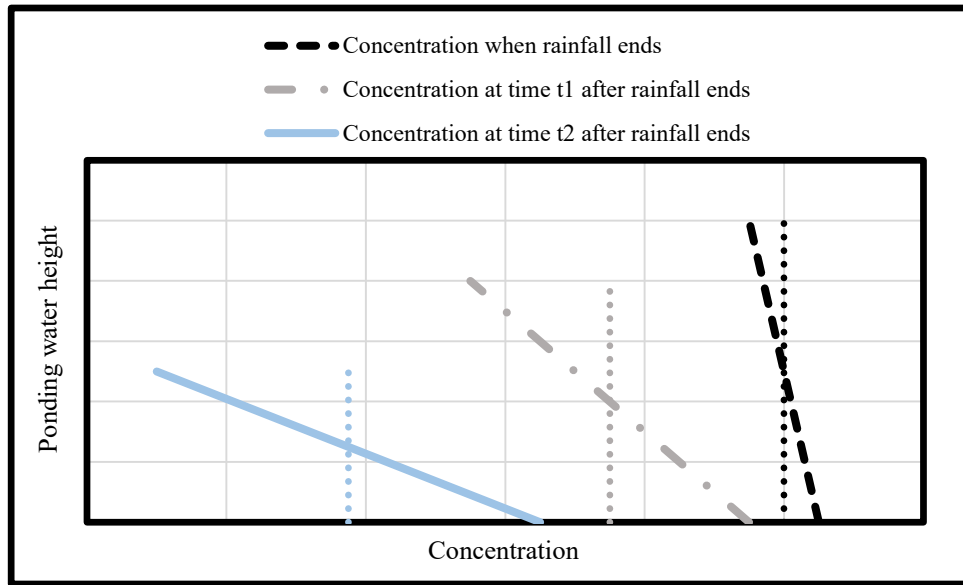


FIGURE 19 CONCEPTUAL EXAMPLE OF HOW CONCENTRATION GRADIENT IN PONDING VOLUME MAY CHANGE OVER TIME AFTER RAINFALL ENDS

The slanting lines represent the concentration in the ponding volume with depth. The vertical dotted lines indicate the average concentration in the pond at that time. Figure 19 shows that over time, due to settling, the average concentration in the ponding volume decreases. As settling occurs, a concentration gradient may start to become more spread out over time.

Recall from the previous section: Filtration Mechanism, that over time, particles clog the silt fence fabric, reducing its pore size. The reduction in pore size not only increase the reduction efficiency of the fabric, but also limit the ability of the fabric to transmit water. For this reason, parts of the fabric at the bottom will be transmit flow at a lesser rate than parts near the top of the ponding volume. The increase in efficiency is due to both this difference in flow-through rate and the increasing spread of the concentration gradient.

For example, referring to Figure 19 and the far right lines, the concentration at the top of pond is relatively close to the average concentration in the pond, leading to low efficiency.

When rainfall stops, the suspended particles settle and no new sediment is introduced into the system. The concentration gradient becomes more spread out, with the ratio between the concentrations at the top of the pond to the average concentration in the pond increasing. This leads to an observed increase in efficiency because a greater flow-through rate occurs near the top of the ponding volume when compared to lower portions due to filter clogging. Essentially, the increase in efficiency is because the rate of sedimentation at the top of the pond where the flow-through rate is highest is greater than the overall settling velocity of the ponding volume as a whole.

Flow-through rate after the Rainfall Event

The flow-through rate after the rain event decreased due to fabric clogging as was observed with the downstream turbidity and SSC. A Wilcoxon rank sum test on the difference between flow-through rates occurring during and after the rain event is shown in Table 45 in Appendix C for the woven and nonwoven fabrics. The statistical analysis showed that there was a significant decrease in the flow-through rate from during the rain event to after the rain event for both fabrics on all embankment slopes tested, except for the woven fabric on a 10 percent slope. The lower flow-through rate after rainfall ended is another indication that filter cake formation on both fabrics affects the performance. Table 12 shows the average flow-through rates that occurred during and after the rain event on all embankment slopes and rainfall intensities tested.

TABLE 12 AVERAGE FLOW-THROUGH RATES DURING AND AFTER RAIN EVENTS

Embankment Slope (%)	Rainfall Intensity (mm/h)	Mean Flow through rate (L/m ² /h)			
		Woven Fabric		Nonwoven Fabric	
		During Rainfall	After Rainfall	During Rainfall	After Rainfall
33	25	60	32	310	130
	76	132	104	416	109
	127	72	--	460	132
25	25	125	75	880	295
	76	214	132	1512	386
	127	397	227	1155	262
10	25	830	771	1267	716
	76	1494	1467	2377	520
	127	1360	1084	2564	926

Table entries that appear with "--" indicate that no after rainfall samples were taken due to overtopping events

Due to the low flow-through rate encountered on the higher slopes and the decreasing flow-through rate after rainfall ended, the hydraulic detention time of the ponding volume increased for some of the tests. More hydraulic detention time of the ponding volume gives additional time for settling to occur. Thus, a high hydraulic detention time post rainfall would therefore lead to higher efficiency removal. In this section, the efficiency values are based on only the first 30 minutes after rainfall ended. However, the estimated hydraulic detention times of the pond show that water would have discharged through the silt fence anywhere from 1 hour to 15 hours depending on the embankment slope and fabric tested. The estimated hydraulic detention time of the pond was calculated using the equation expressed in Equation 16. A summary of the estimated average hydraulic detention times on each embankment slope for each fabric are shown in Table 13.

$$\tau_{HD} = \frac{(V_{pond})_{end\ test} * (PD)_{end\ test} * b_{TB}}{(q)_{end\ test}} + (t)_{end\ test} \quad (16)$$

where, τ_{HD} is the hydraulic detention time of the ponding volume when rainfall stops (h); V_{pond} is the ponding volume for the 30 minutes after rainfall test sampling was completed; PD is the ponding depth for the 30 minutes after rainfall test sampling was completed; b_{TB} is the width of silt fence perpendicular to flow; q is the measured flow-through rate for the 30 minutes after rainfall test sampling was completed; and t is the 30 minutes after rainfall test event (h).

TABLE 13 ESTIMATED AVERAGE HYDRAULIC DETENTION TIME OF THE PONDING VOLUME

Embankment slope (%)	Rainfall intensity (mm/h)	Average Hydraulic Detention Time (h)	
		Woven Fabric	Nonwoven Fabric
33	25	15.2	4
	76	11.7	9.5
	127	--	10
25	25	4.2	2.2
	76	6.6	3.5
	127	7	6.3
10	25	1.1	1.8
	76	0.9	4.5
	127	1.3	4.7

Table entries that appear with "--" indicate that test failures occurred during the rain event and the hydraulic detention time could not be calculated

In general the woven fabric had higher hydraulic detention times due to its low flow-through rate. The exception occurs on the 10 percent slope where the nonwoven fabric had very low measured flow-through rates at the end of the 30 minutes after rainfall test, leading to relatively high estimated detention times on this slope in comparison with the woven fabric. The reason for this is unknown. It can also be seen that the detention times, for the most part,

increased with increasing embankment slope. This was due to the trend of decreasing flow-through rate with increasing upstream suspended solids concentration caused by the increasing embankment slope.

Overall Performance Efficiency (Collected): Both During and After Rain events

In order to quantify the overall efficiency of silt fence, an overall weighted mean effluent value was calculated based on discharge volume. The overall weighted mean effluent value was then compared to the volume-weighted influent occurring during the rain event to obtain an overall performance efficiency of the silt fence. The expression for the overall efficiency is shown in Equations 17 through 20.

$$(WMET)_{Overall} = \frac{\sum_{i=0}^n [T_{eff_{DR}} * V_{down_{DR}}] + \sum_{i=0}^m [T_{eff_{AR}} * V_{down_{AR}}]}{\sum_{i=0}^n V_{down_{DR}} + \sum_{i=0}^m V_{down_{AR}}} \quad (17)$$

$$(WMEC)_{Overall} = \frac{\sum_{i=0}^n [SSC_{eff_{DR}} * V_{down_{DR}}] + \sum_{i=0}^m [SSC_{eff_{AR}} * V_{down_{AR}}]}{\sum_{i=0}^n V_{down_{DR}} + \sum_{i=0}^m V_{down_{AR}}} \quad (18)$$

$$E_T(\%)_{Overall} = 100 * \left[1 - \frac{(WMET)_{Overall}}{WMIT} \right] \quad (19)$$

$$E_{SSC}(\%)_{Overall} = 100 * \left[1 - \frac{(WMEC)_{Overall}}{WMIC} \right] \quad (20)$$

where, $(WMET)_{Overall}$ is the overall volume-weighted mean effluent turbidity (NTU); $(WMEC)_{Overall}$ is the overall volume-weighted mean effluent concentration (mg/L); V_{down} is the volume of collected runoff which discharged through the silt fence in interval between sample i and sample $i - 1$ (L); n is the number of samples collected during rainfall; m is the number of samples collected after rainfall; EFF stands for effluent; DR stands for during rainfall; AR stands for after rainfall; $E_T(\%)_{Overall}$ is the overall mean turbidity performance efficiency; and $E_{SSC}(\%)_{Overall}$ is the mean suspended sediment concentration performance efficiency. WMIT and WMIC were defined previously in Equations 4 and 5, respectively.

Note that the calculation takes into account only those samples that were collected during the 1-hour test. Flow would have continued to discharged through the silt fence for upwards of 14 additional hours depending on the test type, and would have led to an increased overall efficiency value. Therefore, the results shown in this section can be thought of as conservative estimates of the performance efficiency of silt fence. The mean overall efficiency values under all embankment slope and intensity pairs for both the woven and nonwoven fabrics are shown in Table 14 and Table 15, respectively. Discussion of a projected overall efficiency calculation, which would take into account the entire hydraulic detention time of the test, is the topic of the next section.

TABLE 14 OVERALL PERFORMANCE EFFICIENCY OF WOVEN SILT FENCE (COLLECTED SAMPLES)

Slope % (Ratio)	Rainfall Intensity (mm/h)	Rainfall Events	Volume-Weighted Mean Turbidity			Volume-Weighted Mean SSC		
			Up- stream (NTU)	Down- stream (NTU)	Performance Efficiency (%)	Up- stream (mg/L)	Down- stream (mg/L)	Performance Efficiency (%)
33% (3:1) Slope	25	#1	50171	20002	60	32616	11363	65
		#2	33573	12059	64	23412	10902	53
		#1R	28738	13334	54	21001	9337	56
		#2R	30096	12518	58	25614	9712	62
	76	#1	43339	--	--	40099	--	--
		#2	--	--	--	--	--	--
		#1R	41442	16522	60	21641	9831	55
		#2R	27811	9668	65	17641	7534	57
	127	#1	48311	--	--	31212	--	--
		#2	--	--	--	--	--	--
		#1R	57945	--	--	46322	--	--
		#2R	40266	--	--	35427	--	--
25% (4:1) Slope	25	#1	29396	16928	42	19585	11006	44
		#2	21551	11151	48	13875	8287	40
	76	#1	19080	11187	41	13462	8597	36
		#2	25891	14189	45	11361	6815	40
	127	#1	47590	16708	65	15744	9053	42
		#2	30530	12383	59	12755	5867	54
10% (10:1) Slope	25	#1	12357	4719	62	10959	3950	64
		#2	10839	2164	80	10743	1642	85
		#1R	13365	2830	79	10468	2030	81
		#2R	9453	3478	63	5920	2473	58
	76	#1	5358	2678	50	4215	2095	50
		#2	3707	2160	42	3426	1694	51
		#1R	6036	2375	61	4610	1947	58
		#2R	2619	1668	36	2117	1359	36
	127	#1	4886	2227	54	3982	1761	56
		#2	4321	2024	53	3763	1753	53

Table entries that appear with "--" indicate that no samples were collected during those tests due to previous test failures

Table 15 OVERALL PERFORMANCE EFFICIENCY OF NONWOVEN SILT FENCE (COLLECTED SAMPLES)

Slope % (Ratio)	Rainfall Intensity (mm/h)	Rainfall Events	Volume-Weighted Mean Turbidity			Volume-Weighted Mean SSC		
			Up-stream (NTU)	Down-stream (NTU)	Performance Efficiency (%)	Up-stream (mg/L)	Down-stream (mg/L)	Performance Efficiency (%)
33% (3:1) Slope	25	#1	29690	9039	70	27767	6061	78
		#2	39009	2049	95	25079	2203	91
		#1R	46765	17232	63	33356	12133	64
		#2R	18628	6490	65	22205	5904	73
	76	#1	40355	11954	70	31706	9462	70
		#2	32081	7750	76	24753	6754	73
		#1R	26588	15692	41	19271	9609	50
		#2R	24696	9682	61	19142	7446	61
	127	#1	37989	--	--	31958	--	--
		#2	--	--	--	--	--	--
		#1R	37008	12601	66	26679	10563	60
		#2R	18925	9646	49	13685	4939	64
25% (4:1) Slope	25	#1	24380	9056	63	21495	6650	69
		#2	20556	5820	72	17723	4224	76
		#1R	22906	13817	40	18459	9592	48
		#2R	22996	7336	68	17807	5629	68
	76	#1	8780	6759	23	6547	5740	12
		#2	6976	5043	28	5256	3876	26
		#1R	8244	4979	40	5608	3561	37
		#2R	3915	2050	48	2720	954	65
	127	#1	7772	5546	29	5544	3958	29
		#2	19213	8063	58	14032	5147	63
		#1R	14489	6957	52	13018	4928	62
		#2R	8384	3513	58	7123	2635	63
10% (10:1) Slope	25	#1	13512	1615	88	14449	1180	92
		#2	13824	1248	91	14555	1338	91
		#1R	6631	2144	68	5962	1620	73
		#2R	9973	3136	69	7318	2384	67
	76	#1	9472	4518	52	10330	3033	71
		#2	10282	2526	75	11088	2045	82
		#1R	7217	4480	38	5932	3205	46
		#2R	4736	1415	70	3441	1093	68

Slope % (Ratio)	Rainfall Intensity (mm/h)	Rainfall Events	Volume-Weighted Mean Turbidity			Volume-Weighted Mean SSC		
			Up- stream (NTU)	Down- stream (NTU)	Performance Efficiency (%)	Up- stream (mg/L)	Down- stream (mg/L)	Performance Efficiency (%)
		#1	12466	6737	46	7147	3903	45
	127	#2	14303	4585	68	10503	2322	78
		#1R	8629	4872	44	6416	3805	41
		#2R	6044	2935	51	4779	2211	54

Table entries that appear with "--" indicate that no samples were collected during those tests due to previous test failures

The overall performance efficiency of the woven fabric ranged from 36 to 80 percent and from 36 to 85 percent with a mean of 57 and 54 percent for the turbidity and suspended sediment concentrations, respectively. For the nonwoven fabric, the overall performance efficiency ranged from 23 to 95 percent and 12 to 92 percent with a mean of 59 and 62 percent for the turbidity and sediment concentrations, respectively. These performance results show that the nonwoven fabric performed slightly better than the woven fabric in the overall removal of turbidity and suspended sediment concentrations.

Table 16 shows a summary of the above overall efficiency results as well as a summary of efficiency results from during and after the rain event.

TABLE 16 SUMMARY OF VOLUME-WEIGHTED MEAN TURBIDITY AND SSC PERFORMANCE EFFICIENCY

Performance criteria	Slope (%)	Statistical parameter	Woven			Nonwoven			
			During rainfall	After rainfall	Overall	During rainfall	After rainfall	Overall	
Turbidity Performance Efficiency (%)	All slopes	Mean	40	79	57	49	86	59	
		Median	38	81	59	49	89	62	
	33	Mean	47	79	60	52	95	66	
		Median	50	81	60	50	96	66	
	25	Mean	31	76	50	37	83	48	
		Median	26	71	47	38	86	50	
	10	Mean	38	81	58	58	80	63	
		Median	36	83	58	61	81	68	
	SSC Performance Efficiency (%)	All slopes	Mean	39	77	54	53	87	62
			Median	37	77	54	55	89	64
33		Mean	47	78	58	56	94	68	
		Median	45	79	56	55	95	68	
25		Mean	21	71	43	41	85	52	
		Median	19	68	41	47	88	63	
10		Mean	41	79	59	62	82	67	
		Median	40	80	57	67	80	69	

The overall efficiency values show that the nonwoven achieved slightly higher fabric efficiency values for both the turbidity and SSC on every slope and intensity pair except on the 25 percent slope for turbidity. A statistical analysis in the form of a Wilcoxon rank sum test was performed on the overall volume-weighted mean performance efficiencies in order to determine if the nonwoven fabric significantly reduced turbidity and SSC to a greater extent than the woven fabric. Presented in Table 30 of Appendix B are the results of this analysis. Results show that there was not a significant difference in the overall turbidity performance efficiency of the woven and nonwoven fabric on any embankment slope. However, there was a significant difference in the overall SSC performance efficiency of the woven and nonwoven fabrics on 25

and 33 percent slopes. All other embankment slopes showed no significant difference between the performance efficiencies of either fabric.

The result of the woven and nonwoven not having statistically different performance efficiencies is interesting since the nonwoven fabric significantly removed both turbidity and SCC to a greater extent than the woven fabric on combination of all embankment slopes both during and after the rain event. The reason for the similar performance efficiencies was due to the flow-through rates of both fabrics. How the flow-through rate affects the overall efficiency is discussed in the following section: Overall Performance Efficiency (Projected).

Overall Performance Efficiency (Projected)

The field-scale testing procedure allowed for only 1-hour sampling time. However, as shown in Chapter 4, section: Flow-through rate after the rainfall event, the projected hydraulic detention time of the ponding volume was as high as 15 hours. Much of the turbidity and SCC removal will occur during the long hydraulic detention time after rainfall has ended due to settling and increased filtration. The focus of this section is to calculate an overall projected performance efficiency of silt fence which takes into the removal which occurs during the entire hydraulic detention time of the system.

Two assumptions are needed in order to calculate the projected performance efficiency.

1) The entire ponding volume upstream of the silt fence would have discharge through the silt fence. This assumption negates water losses through infiltration of the soil and evaporation. 2) The concentration of the last downstream measurement taken during sampling would have continued to discharge through the silt fence. This assumption can be considered conservative. Due to settling and increased filtration, the downstream discharge concentration was shown to decrease with time after rainfall ended as shown in Chapter 4, section: Fabric reduction efficiency following rain events. Noting these assumption, the overall projected efficiency is calculated as expressed in Equations 21 through 24.

$$(WMET)_{Projected} = \frac{\sum_{i=0}^n [T_{eff_{DR}} * V_{down_{DR}}] + \sum_{i=0}^m [T_{eff_{AR}} * V_{down_{AR}}] + [(T_{EFF_{AR}})_m * (V_{up})_m]}{\sum_{i=0}^n V_{down_{DR}} + \sum_{i=0}^m V_{down_{AR}} + (V_{up})_m} \quad (21)$$

$$(WMEC)_{Projected} = \frac{\sum_{i=0}^n [SSC_{eff_{DR}} * V_{down_{DR}}] + \sum_{i=0}^m [SSC_{eff_{AR}} * V_{down_{AR}}] + [(SSC_{EFF_{AR}})_m * (V_{up})_m]}{\sum_{i=0}^n V_{down_{DR}} + \sum_{i=0}^m V_{down_{AR}} + (V_{up})_m} \quad (22)$$

$$E_T(\%)_{Projected} = 100 * \left[1 - \frac{(WMET)_{Projected}}{WMIT} \right] \quad (23)$$

$$E_{SSC}(\%)_{Projected} = 100 * \left[1 - \frac{(WMEC)_{Projected}}{WMIT} \right] \quad (24)$$

where $(WMET)_{Projected}$ is the projected weighted mean effluent turbidity (NTU); $(T_{EFFAR})_m$ is the effluent turbidity of the last sample taken during the 1-hour test (NTU); $(V_{up})_m$ is the volume of ponding water upstream of the silt fence when the last sample during the test was taken (L); $(WMEC)_{Projected}$ is the projected weighted mean effluent SCC (mg/L); $(SSC_{EFFAR})_m$ is the effluent SSC of the last sample taken during the 1-hour test (mg/L); $E_T(\%)_{Projected}$ is the projected turbidity performance efficiency; $E_{SSC}(\%)_{Projected}$ is the projected SSC performance efficiency. All other terms have been describe previously. The mean overall projected volume-weighted turbidity and SCC efficiencies are shown in Table 17 and Table 18 and for the woven and nonwoven fabrics, respectively.

TABLE 17 PROJECTED OVERALL WOVEN FABRIC PERFORMANCE EFFICIENCY

Slope % (Ratio)	Rainfall Intensity (mm/h)	Rainfall Events	Volume-Weighted Mean Turbidity			Volume-Weighted Mean SSC		
			Up- stream (NTU)	Down- stream (NTU)	Performance Efficiency (%)	Up- stream (mg/L)	Down- stream (mg/L)	Performance Efficiency (%)
33% (3:1) Slope	25	#1	50171	1534	97	32616	1091	97
		#2	33573	1554	95	23412	1507	94
		#1R	28738	756	97	21001	709	97
		#2R	30096	1916	94	25614	1705	93
	76	#1	43339	--	--	40099	--	--
		#2	--	--	--	--	--	--
		#1R	41442	1755	96	21641	994	95
		#2R	27811	1331	95	17641	1282	93
	127	#1	48311	--	--	31212	--	--
		#2	--	--	--	--	--	--
		#1R	57945	--	--	46322	--	--
		#2R	40266	--	--	35427	--	--
25% (4:1) Slope	25	#1	29396	2803	90	19585	2007	90
		#2	21551	3199	85	13875	2487	82
	76	#1	19080	2168	89	13462	1776	87
		#2	25891	2926	89	11361	1640	86
	127	#1	47590	3950	92	15744	1700	89
		#2	30530	2509	92	12755	1420	89
10% (10:1) Slope	25	#1	12357	4399	64	10959	3693	66
		#2	10839	2005	82	10743	1531	86
		#1R	13365	1383	90	10468	1093	90
		#2R	9453	3167	66	5920	2273	62
	76	#1	5358	2605	51	4215	2044	52
		#2	3707	1889	49	3426	1513	56
		#1R	6036	1856	69	4610	1558	66
		#2R	2619	1297	50	2117	1091	48
	127	#1	4886	1873	62	3982	1523	62
		#2	4321	1713	60	3763	1516	60

Table entries that appear with "--" indicate that no samples were collected during those tests due to previous test failures

TABLE 18 PROJECTED OVERALL NONWOVEN FABRIC PERFORMANCE EFFICIENCY

Slope % (Ratio)	Rainfall Intensity (mm/h)	Rainfall Events	Volume-Weighted Mean Turbidity			Volume-Weighted Mean SSC		
			Up- stream (NTU)	Down- stream (NTU)	Performance Efficiency (%)	Up- stream (mg/L)	Down- stream (mg/L)	Performance Efficiency (%)
33% (3:1) Slope	25	#1	29690	1609	95	27767	1153	96
		#2	39009	758	98	25079	875	97
		#1R	46765	4222	91	33356	3135	91
		#2R	18628	2771	85	22205	2665	88
	76	#1	40355	1121	97	31706	1073	97
		#2	32081	1080	97	24753	1127	95
		#1R	26588	2750	90	19271	1886	90
		#2R	24696	1834	93	19142	1624	92
	127	#1	37989	--	--	31958	--	--
		#2	--	--	--	--	--	--
		#1R	37008	1364	96	26679	1296	95
		#2R	18925	2265	88	13685	1279	91
25% (4:1) Slope	25	#1	24380	3549	85	21495	2701	87
		#2	20556	2016	90	17723	1626	91
		#1R	22906	11037	52	18459	7684	58
		#2R	22996	5581	76	17807	4324	76
	76	#1	8780	3867	56	6547	3397	48
		#2	6976	2819	60	5256	2251	57
		#1R	8244	2648	68	5608	2032	64
		#2R	3915	1195	69	2720	614	77
	127	#1	7772	3061	61	5544	2269	59
		#2	19213	1955	90	14032	1410	90
		#1R	14489	2729	81	13018	2042	84
		#2R	8384	1354	84	7123	1115	84
10% (10:1) Slope	25	#1	13512	878	94	14449	714	95
		#2	13824	855	94	14555	971	93
		#1R	6631	1985	70	5962	1515	75
		#2R	9973	2889	71	7318	2215	70
	76	#1	9472	3831	60	10330	2599	75
		#2	10282	1751	83	11088	1480	87
		#1R	7217	3556	51	5932	2578	57
		#2R	4736	1152	76	3441	926	73
	127	#1	12466	4105	67	7147	2410	66

Slope % (Ratio)	Rainfall Intensity (mm/h)	Rainfall Events	Volume-Weighted Mean Turbidity			Volume-Weighted Mean SSC		
			Up- stream (NTU)	Down- stream (NTU)	Performance Efficiency (%)	Up- stream (mg/L)	Down- stream (mg/L)	Performance Efficiency (%)
		#2	14303	2638	82	10503	1450	86
		#1R	8629	4342	50	6416	3413	47
		#2R	6044	2466	59	4779	1890	60

Table entries that appear with "--" indicate that no samples were collected during those tests due to previous test failures

The overall projected turbidity performance efficiency for the woven fabric under all slopes and intensities tested ranged from 50 to 98 percent with a mean and median of 78 and 82 percent, respectively. The SCC performance efficiency ranged from 48 to 97 percent with a mean and median of 79 and 86 percent, respectively. For the nonwoven fabric, performance efficiency during the rain event ranged from 50 to 98 percent with a mean and median of 78 and 82 percent, respectively, and from 47 to 97 percent with a mean of 79 percent and a median of 85 percent for the turbidity and SCC, respectively.

Using the volume-weighted mean turbidity and SSC removals shown in Table 17 and Table 18, a Wilcoxon rank sum test was completed in order to determine if the performance efficiencies on the woven and nonwoven fabric were significantly different from each other. The results of the analysis are shown in Table 31 of Appendix B. The results show that there was only a significant difference between the performance efficiencies of either fabric on a 25 percent embankment slope; with the woven fabric significantly reducing turbidity to a greater extent than the nonwoven fabric. Table 19 shows summary results of the overall projected efficiencies for both fabrics.

TABLE 19 SUMMARY OF OVERALL PROJECTED PERFORMANCE EFFICIENCY

Performance criteria	Slope (%)	Statistical parameter	Projected Overall Performance		
			Woven Fabric	Nonwoven Fabric	
Turbidity Performance Efficiency (%)	All slopes	Mean	80	78	
		Median	89	82	
	33	Mean	96	93	
		Median	96	94	
	25	Mean	89	73	
		Median	90	73	
	10	Mean	64	71	
		Median	63	71	
	SSC Performance Efficiency (%)	All slopes	Mean	79	79
			Median	86	85
33		Mean	95	93	
		Median	94	93	
25		Mean	87	73	
		Median	88	77	
10		Mean	65	74	
		Median	62	74	

Table 19 shows that the projected performance of the woven fabric is actually better than the nonwoven fabric on every slope except for 10 percent. This is interesting because during the rain event as well as after the rain event, the nonwoven significantly reduced both turbidity and SCC to a greater extent than the woven fabric.

The reason for the greater performance efficiency occurring on the woven fabric is due to the lower flow-through rate of this fabric. Lower flow through-rates lead to greater performance efficiencies because water discharges at a slower rate during the rain event where the performance efficiencies are low. The lower flow-through rate allows a greater portion of the influent water to discharge after the rain event where the performance efficiency is significantly

higher due to increased filtration and sedimentation. Comparing the woven and nonwoven fabrics, the woven fabric achieved overall greater performance efficiency because less flow discharged during rainfall in comparison with the nonwoven fabric. This explains why even though the nonwoven fabric achieved higher removals both during and after the rainfall event, the woven fabric still achieved an overall comparable performance efficiency.

The effect of how flow-through rate on performance efficiency can affect the overall performance can be seen in Table 19 by noting the trend of increasing efficiency with increasing embankment slope for both fabrics. Recall from Chapter 4, section: Flow-through rates during the rain event, that the flow-through rate of both fabrics decreased with increasing embankment slope. The decrease in flow-through rate with embankment slope is what led to the trend of increasing efficiency with increasing embankment slope.

The reason for the woven fabric having a higher performance efficiency in comparison with the nonwoven fabric and the trend of increasing performance efficiency with increasing embankment slope can be better explained by comparing the volumes of water which discharged through both fabrics both during and after the rain event, as presented in Table 20.

TABLE 20 DISCHARGE WATER VOLUME BOTH DURING AND AFTER RAINFALL

Embankment Slope (%)	Rainfall Intensity (mm/h)	Volume Discharged (L)					
		Woven Fabric			Nonwoven Fabric		
		During Rainfall	After Rainfall	Ratio, During/After	During Rainfall	After Rainfall	Ratio, During/After
33	25	9	155	0.06	24	63	0.38
	76	37	434	0.09	86	330	0.26
	127	16	--	--	128	468	0.27
25	25	10	50	0.2	48	34	1.41
	76	44	281	0.16	206	109	1.89
	127	124	616	0.2	230	269	0.86
10	25	47	53	0.89	69	72	0.96
	76	162	173	0.94	220	131	1.68
	127	111	264	0.42	240	193	1.24

Table 20 shows the volume of water discharged through both fabrics during and after the rain event. Additionally, presented is the ratio of during rainfall to after rainfall volume for both fabrics. Comparing the ratios between both fabrics, the nonwoven fabric had a greater ratio on each embankment slope and rainfall intensity tested because the nonwoven fabric allowed a greater volume of water to discharge through the silt fence during the rain event. The greater ratio of the nonwoven fabric is what helped lead to the lower overall projected efficiency. There is also a trend of decreasing ratio with increasing embankment slope, which helps to further explain the trend of increasing performance efficiency with increasing embankment slope.

Overall, projections show that both silt fences would have removed both turbidity and SSC with comparable efficiencies. The woven fabric removed more sediment through ponding of water and sedimentation than the nonwoven fabric did, while the nonwoven fabric removed more sediment through filtration than did the woven fabric. Although both fabrics removed

turbidity and SSC at similar rates, the nonwoven fabric did so with a higher flow-through rate, thus decreasing the chances of this fabric attaining high ponding depths, which could lead to failure or overtopping.

CHAPTER 5: CONCLUSION

This study presented an investigation on active field-scale performance of two silt fence fabrics, woven (ASR 1400) and nonwoven (BSRF). Both fabric types were evaluated in both turbidity and suspended sediment concentration performance efficiencies as well as flow-through rate for different simulated rainfall events and embankments slopes using a tilted test-bed and rainfall simulator.

Overall measured results showed that woven and nonwoven fabrics achieved performance efficiencies of 57 and 59 percent in turbidity, and 59 and 62 percent in suspended sediment concentrations, respectively. Projected results also showed that the woven and nonwoven fabrics would have achieved performance efficiencies of 80 and 78 percent in turbidity, and 78 and 79 percent in suspended sediment concentrations, respectively.

The overall efficiency was dependent on the filtration efficiency occurring during the rain event, the filtration and settling efficiencies occurring after the rain event, and the flow-through rate of the fabrics. The flow-through rate was found to affect the overall efficiency due to the performance efficiency after rainfall being significantly higher ($\alpha = 0.05$) than the performance efficiency during rainfall. Lower flow-through rates limited the volume of water discharged during the rain event where the performance efficiencies were relatively low. Thus, allowing additional hydraulic detention time for the settling mechanism to occur and for discharge to occur after the rainfall event where performance efficiencies were higher. There was therefore a tradeoff between the flow-through rate of the fabric and the overall efficiency of the silt fence.

The AOS of both fabrics affected their performance efficiencies. Due in part to the nonwoven fabrics smaller AOS, the nonwoven fabric achieved significantly ($\alpha = 0.05$) greater performance efficiencies both during and after the rain event when compared to the woven fabric. The woven fabric achieved average performance efficiencies of 40 and 78 percent, and the nonwoven fabric achieved average efficiencies of 50 and 85 percent during and after the rain event, respectively. Although AOS was found to influence the filtration and performance efficiency of the silt fence fabrics, AOS could not be used to predict particle size capture. The woven fabrics AOS was larger than 100% of the particle sizes used in the study, however, the filtration efficiency of this fabric during the rain event was 40 percent. It is therefore likely that the particle sizes captured by silt fence in the field can be smaller than the AOS of the silt fence.

Results of the field-scale study showed that silt fence was not adequate as a stand-alone treatment installed on a silty-sand soil at the toes of embankment slopes of 10 percent and greater. Due to the large erosion rate of the silty-sand soil, the effluent discharge turbidities of both fabrics were on average, at least 2 magnitudes greater than the regulated maximum discharge turbidity of 29 NTU above background. Additional treatment processes would need to be installed in conjunction with silt fence in order to form a treatment train if effluent discharge limits were to be met.

Both the woven and nonwoven fabrics performed similarly, however, there were differences in how they operated as silt fence. Both fabrics reduced the discharge of the silty-sand soil through filtration, with the nonwoven fabric achieving higher efficiency due to its smaller AOS. Both fabrics also reduced sediment through ponding of water and sedimentation; however, the woven fabric removed sediment to a greater extent using this mechanism due to its

lower flow-through rate. Overall, both fabrics reduce turbidity and suspended sediment concentrations by approximately 60 percent. The nonwoven fabric however, achieved this performance efficiency while maintaining a higher flow-through rate. Thus, decreasing the chance of this fabric failing or overtopping due to high ponding ponds depths.

APPENDIX A: ANALYSES OF SOIL TESTING

Soil Particle Distribution

TABLE 21 MATERIALS FINER THAN 75- μm BY WASHING ANALYSIS

Parameter	Unit	Value
Total dry soil mass	g	715.2
Dry mass retained on number 200 sieve	g	601.7
Dry mass finer than number 200 sieve	g	113.5
Percent finer than number 200 sieve	%	16

TABLE 22 SIEVE ANALYSIS

Sieve Number	Sieve Opening (mm)	Mass of Sieve (g)	Mass of Soil and Sieve (g)	Mass Retained (g)	Retained (%)	Cumulative Percent Retained (%)	Percent Finer (%)
10	2	486.1	486.6	0.5	0	0	100
20	0.85	570.7	571.7	1	0	0	100
40	0.425	390.7	417	26.3	4	4	96
60	0.25	407.6	549.5	141.9	20	24	76
80	0.18	526	659.6	133.6	19	42	58
100	0.15	351.3	424.9	73.6	10	53	47
140	0.106	337	501.5	164.5	23	76	24
200	0.075	337.6	395.5	57.9	8	84	16

TABLE 23 HYDROMETER ANALYSIS

Time (min)	Reading	Rcp	Percent Finer (%)	Rcl	L (cm)	Particle Diameter (mm)
2	44.5	40.62	13.2	45.5	8.8	0.027
5	43.5	39.62	12.9	44.5	9	0.017
15	43	39.12	12.7	44	9.1	0.01
30	42	38.12	12.4	43	9.2	0.007
60	41.5	37.62	12.2	42.5	9.3	0.005
250	41	37.12	12.1	42	9.4	0.003
1440	39	35.12	11.4	40	9.7	0.001

Compaction Testing

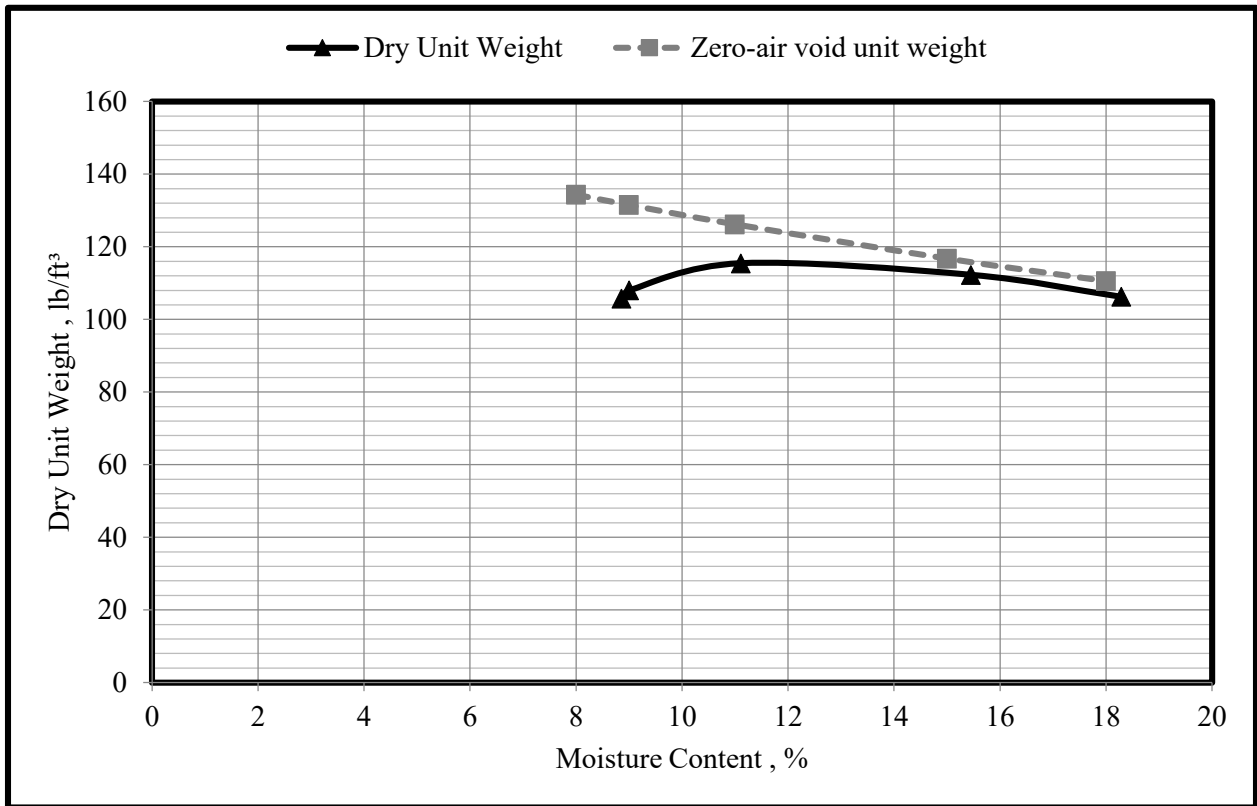


FIGURE 20 MAXIMUM DRY UNIT WEIGHT OF SILTY-SAND SOIL

TABLE 24 MAXIMUM DRY UNIT WEIGHT FOR SILTY-SAND

Moisture Content Determination										
Trial No.	Mass of Moist Specimen + Mold (kg)	Mass of Moist Specimen (kg)	Moist Density of Compacted Specimen (Mg/m ³)	Theoretical Moisture Content (%)	Mass of Wet Soil + Can (g)	Mass of Dry Soil + Can (g)	Mass of Water (g)	Mass of Can (g)	Mass of Dry Soil (g)	Moisture Content (%)
1	6.02	1.74	1.84	8	162.9	153.74	9.16	50.37	103.37	8.86
2	6.06	1.78	1.89	9	126.25	119.92	6.33	49.65	70.27	9
3	6.22	1.94	2.06	11	187.8	174.01	13.79	49.92	124.09	11.11
4	6.24	1.96	2.08	15	133.11	122.02	11.09	50.24	71.78	15.46
5	6.18	1.9	2.01	18	151.19	135.58	15.61	50.21	85.37	18.29

Unit Weight Determination					
Trial No.	Dry Density of Compacted Specimen (Mg/m ³)	Dry Unit Weight, (lb/ft ³)	Moist Density of Compacted Specimen, (Mg/m ³)	Moist Unit Weight, (lb/ft ³)	zero-air-void Unit Weight, (lb/ft ³)
1	1.69	105.73	1.84	115.1	134.37
2	1.73	108.02	1.89	117.74	131.54
3	1.85	115.49	2.06	128.33	126.22
4	1.8	112.29	2.08	129.65	116.78
5	1.7	106.25	2.01	125.68	110.57

Volume of Mold = 0.000944 m³

Specific Gravity = 2.60

Unit Weight of Water = 62.4 lb/ft³

Mass of Mold = 4.28 kg

Constant Head Permeability Testing

TABLE 25 SILTY-SAND SOIL PERMEABILITY

Test #	1			2		
	1A	1B	1C	2A	2B	2C
Volume Collected, cm ³	19.61	17.61	14.53	42.26	36.6	30.67
Time of Collection, sec	60			60		
Temperature of Water, °C	24.2	24.2	24.2	24.1	24.9	24.7
Head difference "h" (cm)	98.63	87.63	87.63	98.63	87.63	74.63
Diameter of Specimen, mm	75.62			75.62		
Length of Specimen, mm	130.69	130.07	130.04	137.2	138.48	139.8
Area of Specimen, cm ²	44.91			44.91		
Hydraulic Conductivity, cm/s	0.00096	0.00097	0.0008	0.00218	0.00215	0.00213
$\eta_{T^{\circ}\text{C}}/\eta_{20^{\circ}\text{C}}$	0.9058	0.9058	0.9058	0.9079	0.8911	0.8953
Corrected Hydraulic Conductivity, cm/s	0.000873	0.000879	0.000725	0.001981	0.001913	0.001909
Hydraulic Conductivity @ 20°C, cm/s	0.0014					
Permeability @ 20°C, cm ²	1.41E-08					

Dry Density Calculations

Mass of empty container, g	2096.1
mass of soil + container, g	3005.4
mass of soil, g	909.3
Volume of specimen, cm ³	625.4008
Dry Density, g/cm ³	1.453948
Dry Density, lb/ft ³	90.76699

Temperature, T (°C)	$\eta_{T^{\circ}\text{C}}/\eta_{20^{\circ}\text{C}}$	Temperature, T (°C)	$\eta_{T^{\circ}\text{C}}/\eta_{20^{\circ}\text{C}}$
15	1.135	23	0.931
16	1.106	24	0.910
17	1.077	25	0.889
18	1.051	26	0.869
19	1.025	27	0.850
20	1.000	28	0.832
21	0.976	29	0.814
22	0.953	30	0.797

**APPENDIX B: STATISTICAL ANALYSES OF PERFORMANCE
EFFICIENCY**

Statistical Difference between Initial and Repeat Tests

TABLE 26 WILCOXON RANK SUM TEST: WOVEN FABRIC SIGNIFICANT P-VALUES BETWEEN INITIAL AND REPEAT TESTS

Embankment Slope (%)	Rainfall Intensity (mm/h)	p-Value			
		Upstream Turbidity	Downstream Turbidity	Upstream SSC	Downstream SSC
33	25	0.045	0.810	0.013	0.575
	127	1.000	0.530	0.676	0.403
10	25	0.522	0.020	0.575	0.013
	76	0.810	0.940	1.000	0.936

TABLE 27 WILCOXON RANK SUM TEST: NONWOVEN FABRIC SIGNIFICANT P-VALUES BETWEEN INITIAL AND REPEAT TESTS

Embankment Slope (%)	Rainfall Intensity (mm/h)	p-Value			
		Upstream Turbidity	Downstream Turbidity	Upstream SSC	Downstream SSC
33	25	0.013	0.013	0.298	0.008
	76	0.689	0.689	0.008	0.575
	127	0.523	0.523	0.410	0.411
25	25	0.005	0.005	0.020	0.013
	76	0.470	0.471	0.379	0.128
	127	0.066	0.093	0.005	0.128
10	25	0.031	0.031	0.013	0.031
	76	0.571	0.571	0.093	1.000
	127	0.045	0.045	0.047	0.575

Statistical Analysis of woven fabric performance efficiency verse nonwoven fabric performance efficiency

TABLE 28 WILCOXON RANK SUM TEST: SIGNIFICANT P-VALUES FOR NONWOVEN FABRIC HAVING GREATER PERFORMANCE EFFICIENCY THAN WOVEN FABRIC DURING THE RAIN EVENT

Embankment Slope (%)	p-Value	
	Volume-weighted Turbidity Efficiency	Volume-weighted SSC Efficiency
33, 25 and 10	0.041	0.001
33	0.252	0.049
25	0.303	0.010
10	0.016	0.009

TABLE 29 WILCOXON RANK SUM TEST: SIGNIFICANT P-VALUES FOR NONWOVEN FABRIC HAVING GREATER PERFORMANCE EFFICIENCY THAN WOVEN FABRIC AFTER THE RAIN EVENT

Embankment Slope (%)	p-Value	
	Volume-weighted Turbidity Efficiency	Volume-weighted SSC Efficiency
33, 25 and 10	0.003	0.000
33	0.000	0.000
25	0.050	0.004
10	0.435	0.383

TABLE 30 WILCOXON RANK SUM TEST: SIGNIFICANT P-VALUES FOR NONWOVEN FABRIC HAVING AN OVERALL GREATER PERFORMANCE EFFICIENCY THAN WOVEN FABRIC

Embankment Slope (%)	p-Value	
	Volume-weighted Turbidity Efficiency	Volume-weighted SSC Efficiency
33, 25 and 10	0.238	0.012
33	0.087	0.029
25	0.750	0.014
10	0.244	0.153

TABLE 31 WILCOXON RANK SUM TEST: SIGNIFICANT P-VALUES FOR WOVEN AND NONWOVEN FABRIC HAVING SIGNIFICANTLY DIFFERENT PROJECTED OVERALL PERFORMANCE EFFICIENCY

Embankment Slope (%)	p-Value	
	Volume-weighted Turbidity Efficiency	Volume-weighted SSC Efficiency
33, 25 and 10	0.597	0.980
33	0.303	0.255
25	0.008	0.083
10	0.249	0.121

Performance Efficiency Based on Embankment Slope

TABLE 32 SINGLE FACTOR ANOVA: WOVEN FABRIC STATISTICAL DIFFERENCE OF VOLUME-WEIGHTED MEAN EFFICIENCY BETWEEN DIFFERENT SLOPES

Parameter	Embankment Slope (%)	No. Sample	Average (%)	Variance	p-Value	Significance ($\alpha = 0.05$)
Turbidity Efficiency	33	10	48	97	0.026	Significant
	25	6	32	149		
	10	10	37	121		
SSC Efficiency	33	10	48	162	0.003	Significant
	25	6	22	63		
	10	10	44	262		

TABLE 33 SINGLE FACTOR ANOVA: NONWOVEN FABRIC STATISTICAL DIFFERENCE OF VOLUME-WEIGHTED MEAN EFFICIENCY BETWEEN DIFFERENT SLOPES

Parameter	Embankment Slope (%)	No. Sample	Average (%)	Variance	p-Value	Significance ($\alpha = 0.05$)
Turbidity Efficiency	33	11	54	285	0.030	Significant
	25	12	40	235		
	10	12	58	342		
SSC Efficiency	33	11	58	166	0.026	Significant
	25	12	43	430		
	10	12	63	368		

Performance Efficiency Change of Test 1 to Test 2

TABLE 34 WILCOXON RANK SUM TEST: WOVEN FABRIC STATISTICAL DIFFERENCE OF TURBIDITY PERFORMANCE EFFICIENCY BETWEEN TEST 1 AND TEST 2

Embankment Slope (%)	Test	No. Samples	Median	p-Value	Significance ($\alpha = 0.05$)
33, 25, and 10	# 1	68	35.5	0.886	Not Significant
	# 2	68	35.5		
33	# 1	21	51	0.753	Not Significant
	# 2	21	54		
25	# 1	17	30	0.270	Not Significant
	# 2	17	29		
10	# 1	30	27	0.616	Not Significant
	# 2	30	30		

TABLE 35 WILCOXON RANK SUM TEST: WOVEN FABRIC STATISTICAL DIFFERENCE OF SEDIMENT PERFORMANCE EFFICIENCY BETWEEN TEST 1 AND TEST 2

Embankment Slope (%)	Test	No. Samples	Median	p-Value	Significance ($\alpha = 0.05$)
33, 25, and 10	# 1	68	32	0.407	Not Significant
	# 2	68	28		
33	# 1	21	49	0.178	Not Significant
	# 2	21	41		
25	# 1	17	22	0.318	Not Significant
	# 2	17	19		
10	# 1	30	32	0.842	Not Significant
	# 2	30	32		

TABLE 36 WILCOXON RANK SUM TEST: NONWOVEN FABRIC STATISTICAL DIFFERENCE OF TURBIDITY PERFORMANCE EFFICIENCY BETWEEN TEST 1 AND TEST 2

Embankment Slope (%)	Test	No. Samples	Median	p-Value	Significance ($\alpha = 0.05$)
33, 25, and 10	# 1	102	39	0.000	Significant
	# 2	102	63		
33	# 1	30	44.5	0.000	Significant
	# 2	30	65		
25	# 1	36	28.5	0.001	Significant
	# 2	36	54.5		
10	# 1	36	45.5	0.006	Significant
	# 2	36	66		

TABLE 37 WILCOXON RANK SUM TEST: NONWOVEN FABRIC STATISTICAL DIFFERENCE OF SEDIMENT PERFORMANCE EFFICIENCY BETWEEN TEST 1 AND TEST 2

Embankment Slope (%)	Test	No. Samples	Median	p-Value	Significance ($\alpha = 0.05$)
33, 25, and 10	# 1	102	46	0.000	Significant
	# 2	102	64		
33	# 1	30	57	0.006	Significant
	# 2	30	67.5		
25	# 1	36	32.5	0.006	Significant
	# 2	36	54.5		
10	# 1	36	52.5	0.032	Significant
	# 2	36	70		

Change in Efficiency from During Rainfall to After Rainfall

TABLE 38 WILCOXON RANK SUM TEST: WOVEN FABRIC STATISTICAL DIFFERENCE OF PERORMANCE EFFICIENCY DURING AND AFTER RAINFALL

Parameter	Embankment Slope (%)	No. Sample	Estimated Efficiency Difference, During - After (%)	p-Value	Significance ($\alpha = 0.05$)
Turbidity Efficiency	33, 25, and 10	22	-30	0.000	Significant
	33	6	-28	0.036	Significant
	25	6	-29	0.036	Significant
	10	10	-31	0.006	Significant
SSC Efficiency	33, 25, and 10	22	-28	0.000	Significant
	33	6	-28	0.036	Significant
	25	6	-36	0.036	Significant
	10	10	-23	0.006	Significant

TABLE 39 WILCOXON RANK SUM TEST: NONWOVEN FABRIC STATISTICAL DIFFERENCE OF PERFORMANCE EFFICIENCY FROM DURING RAINFALL TO AFTER RAINFALL

Parameter	Embankment Slope (%)	No. Sample	Estimated Efficiency Difference, During - After (%)	p-Value	Significance ($\alpha = 0.05$)
Turbidity Efficiency	33, 25, and 10	34	-40	0.000	Significant
	33	10	-43	0.006	Significant
	25	12	-48	0.003	Significant
	10	12	-27	0.003	Significant
SSC Efficiency	33, 25, and 10	34	-32	0.000	Significant
	33	10	-36	0.006	Significant
	25	12	-39	0.003	Significant
	10	12	-17	0.003	Significant

APPENDIX C: STATISTICAL ANALYSES OF FLOW-THROUGH RATE

Change in Flow Through Rate with Change in Embankment Slope

TABLE 40 WILCOXON RANK SUM TEST: WOVEN FABRIC STATISTICAL DIFFERENCE FOR FLOW THROUGH RATE BETWEEN SLOPES

Testing	Embankment Slope (%)	No. of Samples	Median	p-Value	Significance ($\alpha = 0.05$)
10% vs. 25%	10	50	1193	0.000	Significant
	25	30	169		
25% vs. 33%	25	30	169	0.000	Significant
	33	36	68		

TABLE 41 WILCOXON RANK SUM TEST: NONWOVEN FABRIC STATISTICAL DIFFERENCE FOR FLOW THROUGH RATE BETWEEN SLOPES

Testing	Embankment Slope (%)	No. of Samples	Median	p-Value	Significance ($\alpha = 0.05$)
10% vs. 25%	10	60	1975	0.000	Significant
	25	60	1234		
25% vs. 33%	25	60	1234	0.000	Significant
	33	53	324		

Change in Flow Through Rate from Test 1 to Test 2

TABLE 42 WILCOXON RANK SUM TEST: STATISTICAL DIFFERENCE OF FLOW-THROUGH RATE BETWEEN TEST 1 AND TEST 2

Fabric Type	Embankment Slope (%)	No. Samples	Estimated Flow rate Difference, Test 1 - Test 2 (L/m ² /h)	p-Value	Significance ($\alpha = 0.05$)
Woven Fabric	33, 25, and 10	55	-48.5	0.010	Significant
	33	15	-40	0.001	Significant
	25	15	-43.5	0.003	Significant
	10	25	-128	0.226	Not Significant
Nonwoven Fabric	33, 25, and 10	85	64	0.227	Not Significant
	33	25	-93	0.060	Not Significant
	25	30	299	0.020	Significant
	10	30	138	0.399	Not Significant

Change in Flow-Through Rate due to Change in Rainfall Intensity

TABLE 43 SINGLE FACTOR ANOVA: WOVEN FABRIC STATISTICAL DIFFERENCE OF FLOW-THROUGH RATE BASED ON DIFFERENT RAINFALL INTENSITIES

Embankment Slope (%)	Rainfall Intensity (mm/h)	No. of Sample	Average Flow rate (L/m ² /h)	p-Value	Significance ($\alpha = 0.05$)
33	25	19	63	0.002	Significant
	76	9	139		
	127	--	--		
25	25	9	123	0.000	Significant
	76	9	220		
	127	9	427		
10	25	20	830	0.000	Significant
	76	20	1494		
	127	10	1360		

TABLE 44 SINGLE FACTOR ANOVA: NONWOVEN FABRIC STATISTICAL DIFFERENCE OF FLOW-THROUGH RATE BASED ON DIFFERENT RAINFALL INTENSITIES

Embankment Slope (%)	Rainfall Intensity (mm/h)	No. of Sample	Average Flow rate (L/m ² /h)	p-Value	Significance ($\alpha = 0.05$)
33	25	20	310	0.176	Significant
	76	20	416		
	127	13	458		
25	25	20	860	0.000	Significant
	76	20	1512		
	127	20	1155		
10	25	19	1310	0.001	Significant
	76	19	2355		
	127	19	2652		

Change in Flow Through Rate from During Rainfall to After Rainfall

TABLE 45 WILCOXON RANK SUM TEST: STATISTICAL DIFFERENCE OF FLOW THROUGH RATE BETWEEN DURING AND AFTER THE RAIN EVENT

Fabric Type	Embankment Slope (%)	No. Samples	Estimated Flow rate Difference, During - After (L/m ² /h)	p-Value	Significance ($\alpha = 0.05$)
Woven Fabric	33, 25, and 10	22	61	0.002	Significant
	33	6	24	0.036	Significant
	25	6	89	0.036	Significant
	10	10	74	0.103	Not Significant
Nonwoven Fabric	33, 25, and 10	34	752	0.000	Significant
	33	10	272	0.006	Significant
	25	12	896	0.003	Significant
	10	12	1278	0.003	Significant

APPENDIX D: MISCELLANEOUS

Time Dependent Efficiency and Flow Rate Results

TABLE 46 WOVEN FABRIC TIME DEPENDENT EFFICIENCY AND FLOW-THROUGH RATE RESULTS ON 10% SLOPE

Intensity (mm/h)	Test	During Rainfall			After Rainfall				
		time (min)	Turbidity Efficiency (%)	SSC Efficiency (%)	Flow Rate (L/m ² /h)	time (min)	Turbidity Efficiency (%)	SSC Efficiency (%)	Flow Rate (L/m ² /h)
25	# 1	5	37	47	--	35	39	59	1114
		10	46	11	584	40	71	83	1014
		15	29	52	670	45	92	94	873
		20	4	32	829	50	91	93	793
		25	27	39	884	55	94	95	673
		30	57	49	1058	60	96	96	709
	# 2	5	66	65	--	35	77	84	1570
		10	29	63	1111	40	84	89	1457
		15	69	77	1119	45	89	92	1311
		20	67	74	1262	50	94	95	1151
		25	80	84	1398	55	95	95	938
		30	72	80	1503	60	94	95	749
	# 1R	5	75	79	--	35	87	87	233
		10	50	56	236	40	84	85	277
		15	50	57	241	45	96	94	292
		20	67	67	241	50	95	93	238
		25	57	63	217	55	96	95	230
		30	79	83	286	60	96	95	190
	# 2R	5	34	6	--	35	57	57	1121
		10	33	26	903	40	72	75	902
		15	31	21	953	45	90	85	844
		20	44	45	902	50	93	87	756
		25	55	46	1055	55	87	87	606
		30	57	53	1147	60	90	86	477
76	# 1	5	17	15	--	35	9	13	2414
		10	1	-1	1206	40	60	53	2268
		15	-5	-5	1834	45	80	71	2122
		20	16	28	2103	50	80	76	1704
		25	21	27	2518	55	86	77	1638
		30	-3	13	2623	60	82	75	--
	# 2	5	0	-12	--	35	-14	17	1964
		10	0	-14	737	40	46	58	1296
		15	28	49	1265	45	69	73	999
		20	9	44	1571	50	74	70	768
		25	12	15	1825	55	76	70	626
		30	-19	5	2182	60	--	--	--
# 1R	5	49	51	--	35	9	9	1937	
	10	8	-20	489	40	59	39	1740	
	15	-50	-55	855	45	73	56	1558	

Intensity (mm/h)	Test	During Rainfall			After Rainfall				
		time (min)	Turbidity Efficiency (%)	SSC Efficiency (%)	Flow Rate (L/m ² /h)	time (min)	Turbidity Efficiency (%)	SSC Efficiency (%)	Flow Rate (L/m ² /h)
127		20	-1	7	1155	50	81	72	1333
		25	26	32	1470	55	83	72	1032
		30	-15	-11	1677	60	84	74	856
	# 2R	5	9	12	--	35	9	5	1444
		10	29	34	870	40	37	34	1176
		15	16	17	1182	45	54	44	1002
		20	-41	6	1425	50	--	--	--
		25	38	22	1398	55	--	--	--
		30	-15	-26	1487	60	--	--	--
		# 1	5	8	10	--	35	27	47
	10		5	5	1122	40	72	60	1227
	15		27	39	1421	45	78	66	1017
	20		33	32	1518	50	49	28	895
	25		50	45	1446	55	56	66	690
	30		55	66	1782	60	48	24	552
	# 2	5	53	51	--	35	42	49	1570
		10	43	40	1051	40	67	54	1457
		15	35	56	1204	45	74	71	1311
20		23	13	1302	50	79	72	1151	
25		28	31	1357	55	86	81	938	
30		13	22	1395	60	89	82	749	

TABLE 47 WOVEN FABRIC TIME DEPENDENT EFFICIENCY AND FLOW-THROUGH RATE RESULTS ON 25% SLOPE

Intensity (mm/h)	Test	During Rainfall				After Rainfall			
		time (min)	Turbidity Efficiency (%)	SSC Efficiency (%)	Flow Rate (L/m ² /h)	time (min)	Turbidity Efficiency (%)	SSC Efficiency (%)	Flow Rate (L/m ² /h)
25	# 1	5	34	32	--	35	4	23	109
		10	15	24	135	40	11	29	62
		15	30	22	127	45	32	55	50
		20	11	20	87	50	65	59	41
		25	29	29	105	55	87	85	35
		30	22	29	133	60	89	88	42
	# 2	5	22	3	--	35	11	7	168
		10	17	10	129	40	33	33	113
		15	3	8	115	45	86	84	90
		20	92	14	96	50	91	87	78
		25	29	19	143	55	90	84	63
		30	1	14	176	60	87	81	47
76	# 1R	5	50	57	--	35	3	13	129
		10	41	44	156	40	-3	29	80
		15	28	28	148	45	38	35	74
		20	32	15	157	50	63	56	64
		25	4	-4	162	55	68	69	58
		30	18	3	212	60	72	68	62
	# 2R	5	41	28	--	35	14	10	379
		10	31	19	194	40	33	42	238
		15	31	14	139	45	77	73	184
		20	10	3	207	50	88	81	139
		25	8	2	322	55	92	86	103
		30	11	21	440	60	92	88	79
127	# 1	5	52	33	--	35	32	-3	402
		10	65	16	130	40	58	37	280
		15	60	5	237	45	65	44	208
		20	28	-3	358	50	63	53	160
		25	39	16	535	55	66	83	120
		30	59	43	590	60	--	--	--
	# 2	5	--	--	--	35	43	32	443
		10	41	25	232	40	82	79	318
		15	33	28	288	45	90	88	230
		20	21	23	395	50	94	61	159
		25	29	31	558	55	97	91	111
		30	40	31	644	60	95	84	72

TABLE 48 WOVEN FABRIC TIME DEPENDENT EFFICIENCY AND FLOW-THROUGH RATE RESULTS ON 33% SLOPE

Intensity (mm/h)	Test	During Rainfall			After Rainfall				
		time (min)	Turbidity Efficiency (%)	SSC Efficiency (%)	Flow Rate (L/m ² /h)	time (min)	Turbidity Efficiency (%)	SSC Efficiency (%)	Flow Rate (L/m ² /h)
25	# 1	5	67	75	--	35	12	41	58
		10	78	81	15	40	53	53	26
		15	71	76	18	45	88	87	17
		20	56	56	23	50	92	91	14
		25	42	43	41	55	93	93	13
		30	21	43	39	60	96	95	10
	# 2	5	84	73	--	35	4	24	73
		10	65	48	63	40	48	13	49
		15	52	21	65	45	80	65	36
		20	57	30	75	50	68	66	33
		25	35	16	76	55	73	66	35
		30	29	30	59	60	86	83	34
	# 1R	5	69	63	--	35	16	25	41
		10	32	30	42	40	62	64	26
		15	33	35	55	45	86	83	22
		20	39	47	44	50	90	87	24
		25	9	17	40	55	96	94	26
		30	24	32	39	60	96	93	20
	# 2R	5	-11	15	--	35	65	68	55
		10	67	55	217	40	73	75	34
		15	61	67	98	45	80	78	32
		20	70	72	67	50	85	84	31
		25	54	65	67	55	87	84	29
		30	72	72	64	60	91	89	22
76	# 1	5	84	90	--	35	--	--	--
		10	55	58	69	40	--	--	--
		15	10	24	192	45	--	--	--
		20	--	--	--	50	--	--	--
		25	--	--	--	55	--	--	--
		30	--	--	--	60	--	--	--
	# 2	5	--	--	--	35	--	--	--
		10	--	--	--	40	--	--	--
		15	--	--	--	45	--	--	--
		20	--	--	--	50	--	--	--
		25	--	--	--	55	--	--	--
		30	--	--	--	60	--	--	--
	# 1R	5	79	83	--	35	48	-27	150
		10	69	65	73	40	80	51	69
		15	51	49	77	45	90	77	45
		20	38	26	88	50	97	68	34
		25	45	33	114	55	94	84	24
		30	43	25	135	60	95	79	25

Intensity (mm/h)	Test	During Rainfall			After Rainfall				
		time (min)	Turbidity Efficiency (%)	SSC Efficiency (%)	Flow Rate (L/m ² /h)	time (min)	Turbidity Efficiency (%)	SSC Efficiency (%)	Flow Rate (L/m ² /h)
127	# 2R	5	75	75	--	35	28	22	282
		10	65	57	87	40	78	63	187
		15	53	41	91	45	21	89	152
		20	42	27	131	50	94	93	119
		25	42	27	211	55	90	88	88
		30	29	17	316	60	97	95	69
	# 1	5	93	95	--	35	--	--	--
		10	98	98	108	40	--	--	--
		15	73	77	76	45	--	--	--
		20	33	24	147	50	--	--	--
		25	31	9	284	55	--	--	--
		30	--	--	--	60	--	--	--
	# 2	5	--	--	--	35	--	--	--
		10	--	--	--	40	--	--	--
		15	--	--	--	45	--	--	--
		20	--	--	--	50	--	--	--
		25	--	--	--	55	--	--	--
		30	--	--	--	60	--	--	--
# 1R	5	82	85	--	35	--	--	--	
	10	82	84	51	40	--	--	--	
	15	81	82	51	45	--	--	--	
	20	40	51	143	50	--	--	--	
	25	31	40	2429	55	--	--	--	
	30	--	--	--	60	--	--	--	
# 2R	5	63	70	--	35	--	--	--	
	10	35	37	220	40	--	--	--	
	15	29	38	5325	45	--	--	--	
	20	--	--	--	50	--	--	--	
	25	--	--	--	55	--	--	--	
	30	--	--	--	60	--	--	--	

TABLE 49 NONWOVEN FABRIC TIME DEPENDENT EFFICIENCY AND FLOW-THROUGH RATE RESULTS ON 10% SLOPE

Intensity (mm/h)	Test	During Rainfall			After Rainfall				
		time (min)	Turbidity Efficiency (%)	SSC Efficiency (%)	Flow Rate (L/m ² /h)	time (min)	Turbidity Efficiency (%)	SSC Efficiency (%)	Flow Rate (L/m ² /h)
25	# 1	5	82	87	--	35	90	93	387
		10	88	93	453	40	94	95	234
		15	87	90	459	45	96	96	147
		20	90	93	475	50	--	--	--
		25	82	88	475	55	--	--	--
		30	86	91	457	60	--	--	--
	# 2	5	39	52	--	35	88	87	575
		10	78	71	321	40	93	94	623
		15	88	88	606	45	98	97	698
		20	84	86	772	50	98	96	768
		25	87	87	809	55	98	97	755
		30	86	89	511	60	99	97	632
	# 1R	5	49	56	--	35	42	48	1890
		10	70	88	774	40	77	79	1246
		15	70	71	725	45	91	88	557
		20	61	65	761	50	94	91	364
		25	56	57	1529	55	95	91	305
		30	54	59	1919	60	--	--	--
# 2R	5	42	47	--	35	51	50	2526	
	10	38	41	2560	40	83	80	933	
	15	72	72	3033	45	85	77	431	
	20	72	68	2912	50	95	88	295	
	25	64	61	2969	55	95	90	236	
	30	71	71	2820	60	--	--	--	
76	# 1	5	29	-5	--	35	24	47	3239
		10	52	69	2792	40	78	81	993
		15	49	73	3651	45	91	89	327
		20	40	73	3593	50	94	93	192
		25	46	60	3491	55	96	94	144
		30	62	70	3394	60	97	94	119
	# 2	5	70	81	--	35	30	59	1103
		10	81	86	1216	40	81	86	368
		15	40	62	1331	45	91	92	152
		20	82	85	1396	50	93	91	123
		25	68	72	1307	55	95	93	103
		30	80	80	1217	60	96	94	87
# 1R	5	18	31	--	35	75	70	1251	
	10	30	41	3209	40	89	83	333	
	15	47	62	3112	45	93	86	186	
	20	21	27	2775	50	95	89	144	
	25	45	49	2296	55	96	90	113	
	30	25	22	2058	60	--	--	--	

Intensity (mm/h)	Test	During Rainfall				After Rainfall			
		time (min)	Turbidity Efficiency (%)	SSC Efficiency (%)	Flow Rate (L/m ² /h)	time (min)	Turbidity Efficiency (%)	SSC Efficiency (%)	Flow Rate (L/m ² /h)
127	# 2R	5	44	39	--	35	71	69	1551
		10	52	55	1885	40	83	78	449
		15	62	67	2278	45	90	82	239
		20	74	73	2117	50	93	87	125
		25	73	72	2218	55	95	88	92
		30	76	66	2208	60	--	--	--
	# 1	5	49	43	--	35	45	44	1764
		10	23	30	892	40	88	87	448
		15	31	30	1259	45	96	94	198
		20	28	20	1463	50	94	74	123
		25	35	22	1918	55	87	88	94
		30	26	37	2032	60	97	96	75
	# 2	5	75	73	--	35	67	74	1294
		10	59	42	605	40	92	92	501
		15	46	49	1287	45	96	95	276
		20	38	81	1422	50	98	96	201
		25	70	83	1556	55	98	96	157
		30	52	79	1458	60	98	96	126
	# 1R	5	34	18	--	35	48	45	2932
		10	39	22	4215	40	71	68	1284
		15	32	37	4008	45	88	85	937
		20	25	22	3653	50	95	91	819
		25	40	42	3477	55	96	92	557
		30	25	23	3518	60	96	92	380
# 2R	5	51	53	--	35	34	29	--	
	10	28	40	4480	40	81	77	3774	
	15	64	69	3340	45	88	84	1151	
	20	37	38	3618	50	91	84	2344	
	25	46	41	3505	55	94	88	--	
	30	33	26	3567	60	94	88	--	

TABLE 50 NONWOVEN FABRIC TIME DEPENDENT EFFICIENCY AND FLOW-THROUGH RATE RESULTS ON 25% SLOPE

Intensity (mm/h)	Test	During Rainfall			After Rainfall				
		time (min)	Turbidity Efficiency (%)	SSC Efficiency (%)	Flow Rate (L/m ² /h)	time (min)	Turbidity Efficiency (%)	SSC Efficiency (%)	Flow Rate (L/m ² /h)
25	# 1	5	84	85	--	35	59	61	522
		10	49	64	1007	40	93	93	306
		15	50	64	776	45	97	96	156
		20	52	59	579	50	98	97	108
		25	43	44	458	55	99	97	94
		30	54	64	361	60	98	98	89
	# 2	5	78	83	--	35	64	74	504
		10	65	74	104	40	96	95	235
		15	63	63	418	45	98	98	116
		20	69	77	490	50	99	98	81
		25	66	70	522	55	99	98	62
		30	66	68	524	60	--	--	--
	# 1R	5	-15	-5	--	35	85	87	716
		10	35	39	2122	40	98	97	299
		15	26	37	1322	45	99	99	181
		20	33	32	1255	50	99	99	170
		25	32	34	1182	55	--	--	--
		30	27	54	1051	60	--	--	--
	# 2R	5	57	64	--	35	44	45	1086
		10	-4	4	939	40	96	94	562
		15	52	46	1161	45	99	97	271
		20	63	59	1114	50	99	97	188
		25	69	69	1112	55	99	97	156
		30	68	73	1101	60	--	--	--
76	# 1	5	14	-17	--	35	72	75	882
		10	61	1	1715	40	95	87	236
		15	-19	-8	1751	45	96	85	136
		20	13	9	1620	50	90	57	105
		25	16	11	1597	55	90	43	88
		30	-16	-4	1416	60	--	--	--
	# 2	5	16	16	--	35	11	6	1403
		10	6	6	1693	40	82	73	398
		15	21	19	1601	45	93	82	138
		20	26	28	1739	50	95	82	89
		25	26	28	1581	55	--	--	--
		30	28	21	1531	60	--	--	--
# 1R	5	23	16	--	35	70	69	877	
	10	13	7	1359	40	95	84	233	
	15	30	30	1480	45	96	82	143	
	20	27	32	1494	50	98	88	113	
	25	39	25	1428	55	99	89	98	
	30	33	36	1403	60	99	83	83	

Intensity (mm/h)	Test	During Rainfall			After Rainfall				
		time (min)	Turbidity Efficiency (%)	SSC Efficiency (%)	Flow Rate (L/m ² /h)	time (min)	Turbidity Efficiency (%)	SSC Efficiency (%)	Flow Rate (L/m ² /h)
127	# 2R	5	77	71	--	35	61	74	780
		10	71	70	642	40	88	81	227
		15	33	65	1581	45	92	81	145
		20	3	47	1479	50	95	80	106
		25	43	72	1552	55	97	80	92
		30	34	32	1586	60	97	85	85
	# 1	5	9	8	--	35	21	20	874
		10	13	17	2181	40	81	64	224
		15	16	20	2027	45	87	70	151
		20	6	8	2093	50	87	71	110
		25	27	28	1934	55	93	63	89
		30	36	31	1688	60	91	72	47
	# 2	5	96	95	--	35	47	96	987
		10	85	85	113	40	97	97	271
		15	56	42	613	45	99	97	145
		20	21	25	723	50	99	96	102
		25	39	35	821	55	99	95	80
		30	47	46	988	60	99	95	66
# 1R	5	25	46	--	35	77	81	835	
	10	11	56	833	40	96	93	355	
	15	26	46	1080	45	98	98	194	
	20	51	60	1256	50	98	95	152	
	25	33	44	1071	55	99	97	118	
	30	52	54	1214	60	98	96	100	
# 2R	5	65	80	--	35	39	35	1414	
	10	92	93	144	40	95	94	422	
	15	54	61	267	45	97	95	207	
	20	55	62	1192	50	97	93	141	
	25	32	45	1515	55	96	91	116	
	30	49	50	1340	60	98	96	105	

TABLE 51 NONWOVEN FABRIC TIME DEPENDENT EFFICIENCY AND FLOW-THROUGH RATE RESULTS ON 33% SLOPE

Intensity (mm/h)	Test	During Rainfall			After Rainfall				
		time (min)	Turbidity Efficiency (%)	SSC Efficiency (%)	Flow Rate (L/m ² /h)	time (min)	Turbidity Efficiency (%)	SSC Efficiency (%)	Flow Rate (L/m ² /h)
25	# 1	5	57	60	--	35	72	88	170
		10	74	72	181	40	91	93	153
		15	58	63	214	45	98	98	89
		20	33	57	177	50	99	99	70
		25	64	70	208	55	99	99	48
		30	46	70	209	60	99	99	40
	# 2	5	81	94	--	35	91	92	370
		10	85	84	51	40	99	98	163
		15	86	81	96	45	99	98	107
		20	89	85	230	50	99	90	81
		25	92	93	349	55	99	99	56
		30	98	86	413	60	99	97	53
	# 1R	5	14	-24	--	35	84	81	298
		10	30	41	369	40	96	94	122
		15	41	47	287	45	98	97	71
		20	44	47	371	50	99	98	45
		25	60	57	349	55	99	98	35
		30	58	57	324	60	99	98	34
	# 2R	5	31	38	--	35	79	84	550
		10	57	71	586	40	94	94	223
		15	65	82	137	45	95	96	133
		20	71	80	300	50	99	98	91
		25	37	55	635	55	99	99	65
		30	47	55	722	60	100	98	56
76	# 1	5	17	62	--	35	88	70	267
		10	29	32	216	40	99	97	125
		15	49	59	198	45	99	97	71
		20	49	59	240	50	100	98	56
		25	57	58	231	55	100	98	44
		30	64	55	385	60	100	97	31
	# 2	5	82	82	--	35	90	91	332
		10	65	64	122	40	99	98	132
		15	69	61	101	45	99	98	88
		20	61	62	249	50	99	98	69
		25	65	57	596	55	100	98	57
		30	67	59	550	60	99	95	50
	# 1R	5	3	8	--	35	92	97	248
		10	12	12	891	40	98	96	121
		15	29	33	656	45	97	94	77
		20	38	31	484	50	98	95	60
		25	38	47	437	55	99	95	52
		30	40	92	447	60	98	93	52

Intensity (mm/h)	Test	During Rainfall			After Rainfall				
		time (min)	Turbidity Efficiency (%)	SSC Efficiency (%)	Flow Rate (L/m ² /h)	time (min)	Turbidity Efficiency (%)	SSC Efficiency (%)	Flow Rate (L/m ² /h)
127	# 2R	5	98	97	--	35	92	90	347
		10	89	75	61	40	99	97	110
		15	52	56	488	45	99	97	86
		20	49	48	683	50	99	96	63
		25	46	47	628	55	98	96	49
		30	51	55	660	60	99	93	39
	# 1	5	50	16	--	35	--	--	--
		10	55	63	261	40	--	--	--
		15	47	54	214	45	--	--	--
		20	28	31	291	50	--	--	--
		25	41	45	472	55	--	--	--
		30	--	--	480	60	--	--	--
	# 2	5	--	--	--	35	--	--	--
		10	--	--	--	40	--	--	--
		15	--	--	--	45	--	--	--
		20	--	--	--	50	--	--	--
		25	--	--	--	55	--	--	--
		30	--	--	--	60	--	--	--
# 1R	5	62	59	--	35	87	86	280	
	10	41	48	243	40	99	97	119	
	15	47	52	310	45	99	97	81	
	20	93	39	426	50	99	97	59	
	25	33	33	419	55	99	97	47	
	30	45	50	548	60	100	97	39	
# 2R	5	100	99	--	35	91	66	320	
	10	97	98	73	40	99	95	232	
	15	60	96	283	45	98	96	145	
	20	26	46	933	50	98	93	110	
	25	16	43	1082	55	99	95	86	
	30	2	24	868	60	99	95	69	

Change in Performance Efficiency and Discharge Concentration with Time

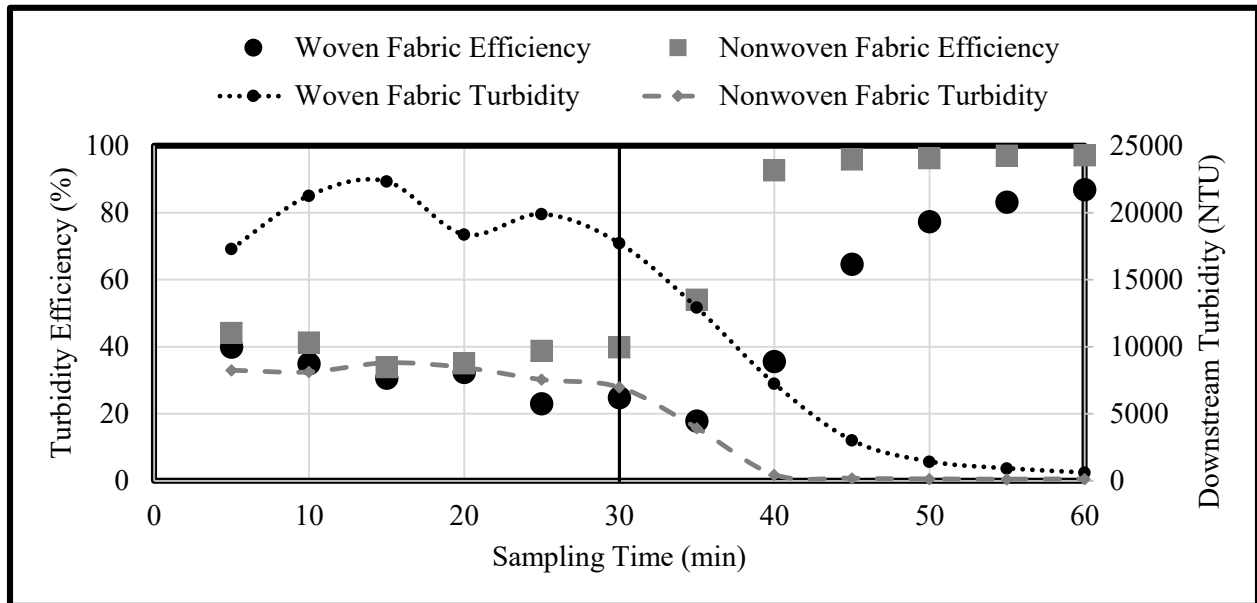


FIGURE 21 TIME DEPENDENT AVERAGE TURBIDITY PERFORMANCE EFFICIENCY AND DOWNSTREAM VALUE ON 25 PERCENT SLOPE

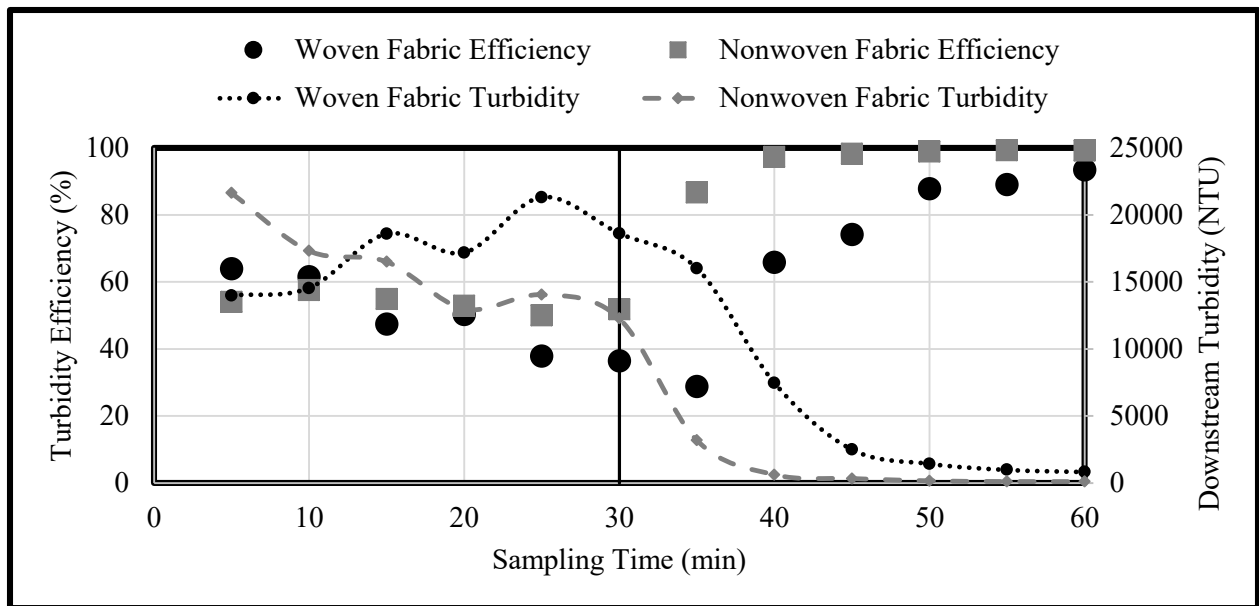


FIGURE 22 TIME DEPENDENT AVERAGE TURBIDITY PERFORMANCE EFFICIENCY AND DOWNSTREAM VALUE ON 33 PERCENT SLOPE

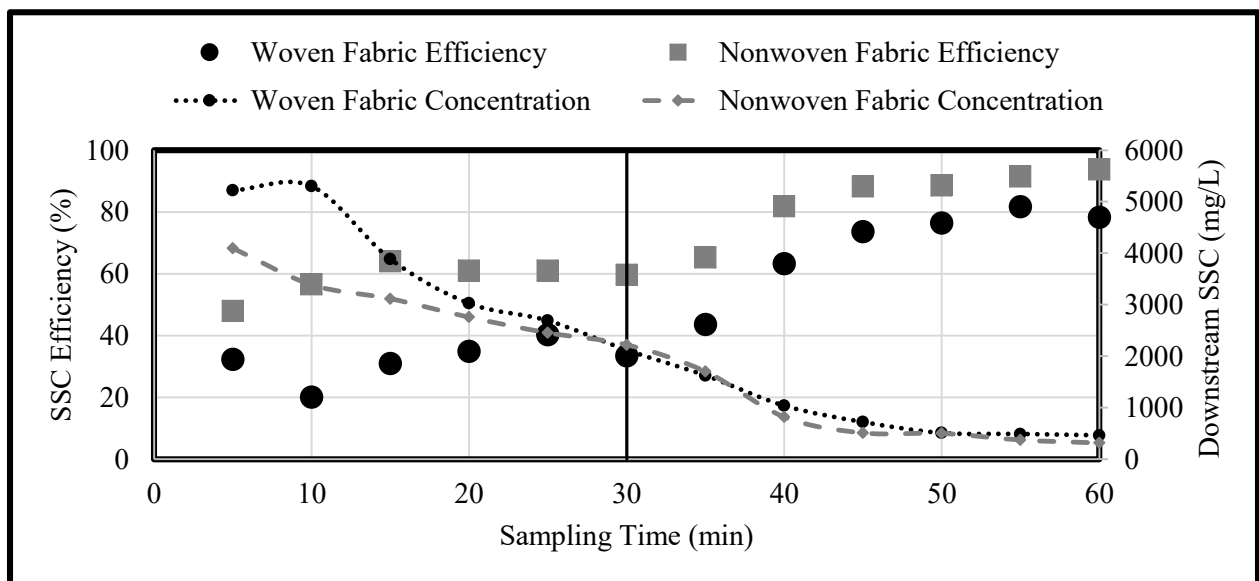


FIGURE 23 TIME DEPENDENT AVERAGE SSC PERFORMANCE EFFICIENCY AND DOWNSTREAM VALUE ON 10 PERCENT SLOPE

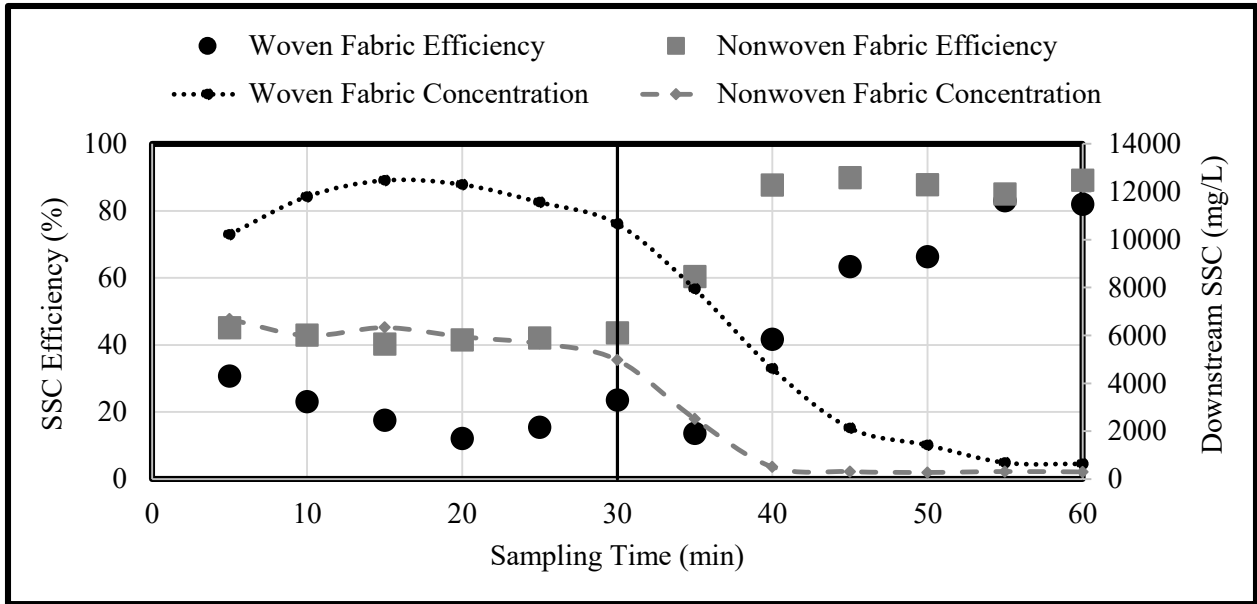


FIGURE 24 TIME DEPENDENT AVERAGE SSC PERFORMANCE EFFICIENCY AND DOWNSTREAM VALUE ON 25 PERCENT SLOPE

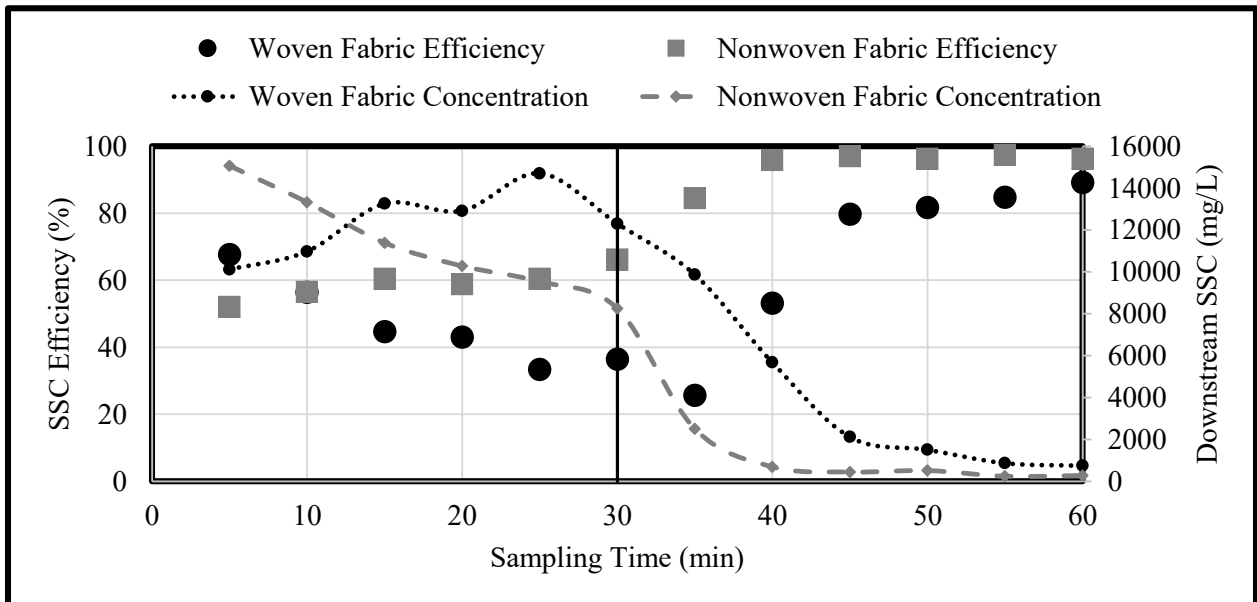


FIGURE 25 TIME DEPENDENT AVERAGE SSC PERFORMANCE EFFICIENCY AND DOWNSTREAM VALUE ON 33 PERCENT SLOPE

LIST OF REFERENCES

APHA, AWWA and WEF (2005). Standard Method for the Examination of Water and Wastewater, A.D. Eaton, Washinton D.C.

Arjunan, J., S. Yeri, E. Stevens, B. Barfield and K. Gasem (2006). Application of Polyacrylamide to Enhance Silt Fence Performance, Oklahoma State University.

ASTM (1987). D 4632-86 Standard Test Method for Breaking Load and Elongation of Geotextiles. Annual Book of ASTM Standards, American Society for Testing and Materials. **Vol. 4.08**.

ASTM C117-13 (2013). Standard Test Method for Materials Finer than 75-um (No. 200) Sieve in Mineral Aggregates by Washing. ASTM Volue 04.02 Concrete and Aggregates.

ASTM C136-06 (2013). Standard Test Method for Sieve Analysis of Fine and Coarse Aggregates. ASTM Volume 04.02 Concrete and Aggregates.

ASTM D422-63 (2013). Standard Test Method for Particle-Size Analysis of Soils. ASTM Volue 04.08 Soil and Rock (I): D420-D5876.

ASTM D2434-68 (2006). Standard Test Method for Permeability of Granular Soils (Constant Head). ASTM Volume 04.08 Soil and Rock (I): D420-D5876.

ASTM D4491 (2009). "Test Methods for Water Permeability of geotextiles by Permittivity." West Conshohocken, PA, ASTM International. 04.13.

ASTM D6461 (2007). Standard Specification for Silt Fence Materials. ASTM Volume 04.09 Soil and Rock (II): D5877-latest.

Aydilek, A. and T. Edil (2003). "Long-term filtration performance of nonwoven geotextile-sludge systems." Geosynthetics International **10**(4): 110-123.

Barrett, M. E., J. E. Kearney, T. G. McCoy, J. F. Malina, R. Charbeneau and G. Ward (1995). An evaluation of the use and effectiveness of temporary sediment controls, Center for Research in Water Resources, University of Texas at Austin.

Bilotta, G. and R. Brazier (2008). "Understanding the influence of suspended solids on water quality and aquatic biota." Water research **42**(12): 2849-2861.

Britton, S. L., K. M. Robinson, B. J. Barfield and K. Kadavy (2000). Silt fence performance testing. 2000 ASAE Annual International Meeting, Milwaukee, Wisconsin, USA, 9-12 July 2000, American Society of Agricultural Engineers.

D698-12, A. (2013). Standard Test Methods for Laboratory Compaction Characteristics of Soil Using Standard Effort. ASTM Volume 04.08 Soil and Rock (I): D420-D5876.

Dierickx, W. and P. Van Den Berghe (2004). "Natural weathering of textiles used in agricultural applications." Geotextiles and Geomembranes **22**(4): 255-272.

EPA (2007). Developing Your Stormwater Pollution Prevention Plan: A Guide for Construction Sites: 46.

European Commission. (2012). "Soil Compaction." European Soil Portal - Soil Data and Information System Retrieved January 28, 2014, from <http://eusoils.jrc.ec.europa.eu/library/themes/compaction/>.

Farias, R., E. Palmeira and J. Carvalho (2006). "Performance of geotextile silt fences in large flume tests." Geosynthetics International **13**(4): 133-144.

Faucette, L., K. Sefton, A. Sadeghi and R. Rowland (2008). "Sediment and phosphorus removal from simulated storm runoff with compost filter socks and silt fence." Journal of soil and water conservation **63**(4): 257-264.

Faure, Y.-H., A. Baudoin, P. Pierson and O. Ple (2006). "A contribution for predicting geotextile clogging during filtration of suspended solids." Geotextiles and Geomembranes **24**(1): 11-20.

FDEP (2008). "Florida Stormwater Erosion and Sedimentation Control Inspector's Manual". Tallahassee, Florida Department of Environmental Protection: 378.

Fisher, L. and A. Jarrett (1984). "Sediment retention efficiency of synthetic filter fabrics [Land management, erosion, flowing soil suspensions]." Transactions of the ASAE [American Society of Agricultural Engineers](USA).

Geotechdata.info. (2008, July 7, 2013). "Soil permeability coefficient." Retrieved January 28, 2014, from <http://www.geotechdata.info/parameter/permeability.html>.

Gogo-Abite, I. (2012). Effluent Water Quality Improvement Using Silt Fences and Stormwater Harvesting. Doctor of Philosophy, University of Central Florida.

Gogo-Abite, I. and M. Chopra (2013). "Performance evaluation of two silt fence geotextiles using a tilting test-bed with simulated rainfall." Geotextiles and Geomembranes **39**: 30-38.

Harbor, J. (1999). "Engineering geomorphology at the cutting edge of land disturbance: erosion and sediment control on construction sites." Geomorphology **31**(1): 247-263.

Hayes, S. A., R. McLaughlin and D. Osmond (2005). "Polyacrylamide use for erosion and turbidity control on construction sites." Journal of soil and water conservation **60**(4): 193-199.

Howe, K. J., D. W. Hand, J. C. Crittenden, R. R. Trussell and G. Tchobandglous (2012). Principles of Water Treatment, John Wiley & Sons, Inc.

Koerner, R. M. (2012). Designing with geosynthetics, Xlibris Corporation.

Lamy, E., L. Lassabatere, B. Bechet and H. Andrieu (2013). "Effect of a nonwoven geotextile on solute and colloid transport in porous media under both saturated and unsaturated conditions." Geotextiles and Geomembranes **36**: 55-65.

Owens, D. W., P. Jopke, D. W. Hall, J. Balousek and A. Roa (2000). "Soil erosion from two small construction sites, Dane County, Wisconsin." USGS Fact Sheet, USGS, Madison, WI.

Rawal, A. and H. Saraswat (2011). "Pore size distribution of hybrid nonwoven geotextiles." Geotextiles and Geomembranes **29**(3): 363-367.

Risse, L., S. Thompson, J. Governo and K. Harris (2008). "Testing of new silt fence materials: A case study of a belted strand retention fence." Journal of soil and water conservation **63**(5): 265-273.

Sansone, L. and R. Koerner (1992). "Fine fraction filtration test to assess geotextile filter performance." Geotextiles and Geomembranes **11**(4): 371-393.

Suits, L. D. and Y. G. Hsuan (2003). "Assessing the photo-degradation of geosynthetics by outdoor exposure and laboratory weatherometer." Geotextiles and Geomembranes **21**(2): 111-122.

USEPA. (2011). "Sediment and Erosion Control." Retrieved March 10, 2014, from <http://www.epa.gov/region6/gen/w/sw/sediment.pdf>.

USEPA. (2012). "Nonpoint Source Pollution: The Nation's Largest Water Quality Problem." Water: Outreach & Communication Retrieved March 11, 2013, from <http://water.epa.gov/polwaste/nps/outreach/point1.cfm>.

Weggel, J. R. and J. Dortch (2012). "A model for filter cake formation on geotextiles: Experiments." Geotextiles and Geomembranes **31**: 62-68.

Weggel, J. R. and N. D. Ward (2012). "A model for filter cake formation on geotextiles: Theory." Geotextiles and Geomembranes **31**: 51-61.

Wu, C.-S., Y.-S. Hong and R.-H. Wang (2008). "The influence of uniaxial tensile strain on the pore size and filtration characteristics of geotextiles." Geotextiles and Geomembranes **26**(3): 250-262.

Zhang, Y., W. Liu, W. Shao and Y. Yang (2013). "Experimental study on water permittivity of woven polypropylene geotextile under tension." Geotextiles and Geomembranes **37**: 10-15.